Cellulose Degradation Under Alkali Conditions, Representative of Cementitious Radioactive Waste Disposal Sites

A thesis submitted to the University of Manchester for the degree of PhD in the Faculty of Engineering and Physical Sciences

2015

Naji Milad Bassil

School of Earth Atmospheric and Environmental Sciences

List of Contents

List of Figures

List of Tables

List of Abbreviations and Definitions

Acetogens	Microorganisms that generate acetate from the anaerobic reduction of CO_2
Alkali conditions	High pH conditions
Alkaliphiles	Microorganisms that thrive in alkali conditions (pH>8.5)
Barophiles (Piezophile)	Organisms that thrive under high-pressure conditions (>38 MPa)
Crystallinity index	A ratio of the mass of crystalline polymer (for example cellulose) to the mass of amorphous polymer
DECC	Department of Energy and Climate Change
Degree of polymerisation	The number of monomeric units in a polymer
EDTA	Ethylinediaminetetraacetic acid
Extremophiles	Organisms that thrive under conditions that are considered to be extreme for life
GA	Gluconic acid
GDF	Geological disposal facility
HLW	High-level waste
ILW	Intermediate-level waste
ISA	Isosaccharinic acid
α-ISA	3-deoxy-2-C-(hydroxymethyl)-D-erythro-pentonic acid
β-ISA	3-deoxy-2-C-(hydroxymethyl)-D-threo-pentonic acid
Lithoautotrophs	Microorganism that derives energy from reduced inorganic compounds of mineral origin
LLW	Low-level waste
Methanogens	Archaea that produce methane from the reduction of CO_2
NDA	Nuclear Decommissioning Authority
NTA	Nitrilotriacetic acid
Thermophiles	Organisms that thrive at high temperatures (41-122^{o}C)

Thesis Abstract

The University of Manchester

Naji Milad Bassil

Doctor of Philosophy (PhD)

Cellulose Degradation Under Alkali Conditions, Representative of Cementitious Radioactive Waste Disposal Sites

2015

Deep geological disposal in a multibarrier cementitious facility is being developed by a number of countries for the safe, long-term disposal of intermediate-level radioactive wastes. Intermediate-level radioactive waste, which dominates the radioactive waste inventory in the United Kingdom on a volumetric basis, is a heterogeneous wasteform that contains organic materials including cellulosic materials, encased in concrete. Under the alkaline conditions expected in the cementitious geological disposal facility (GDF), these materials will undergo abiotic, chemical hydrolysis, and will produce degradation products including isosaccharinic acid (ISA) or gluconic acid (GA) that can form soluble complexes with radionuclides. Alkaliphilic microorganisms sampled from a hyperalkaline site contaminated with lime-kiln waste, were able to degrade cellulosic material (tissue paper) in $Ca(OH)_2$ saturated microcosms at a starting pH of 12. Enzymatic processes in these microcosms caused the production of acetate, acidification of the microcosms and a cessation of ISA production. Enrichment cultures prepared at pH 10 and inoculated with a sediment from the same hyperalkaline site were able to degrade ISA, and couple this degradation process to the reduction of electron acceptors that will dominate as the GDF progresses from an aerobic 'open phase' through nitrate- and Fe(III)-reducing conditions post closure. A strictly alkaliphilic bacterium belonging to the *Bacillus* genus was isolated from the nitrate-reducing enrichment culture, and was found to degrade a variety of organic molecules that are expected to be found in a cementitious GDF. Detailed investigation into the growth of this bacterium suggested that different mechanisms are involved in the biodegradation of ISA and GA, and that bacterial growth is coupled to a decrease in soluble U(VI) concentrations. This implies that microorganisms could have a role in attenuating the mobility of radionuclides in and around a GDF via (i) the biodegradation of cellulose and cessation of ISA production, (ii) the biodegradation of the ligands (ISA and GA) and (iii) the immobilisation of radionuclides. This should facilitate the reduction of undue pessimism in the long-term performance assessment of such facilities.

Declaration

No portion of the work referred in the thesis has been submitted in support of an application for another degree or qualification of this or any other university or other institute of learning.

Copyright Statement

i. The author of this thesis (including any appendices and/or schedules to this thesis) owns certain copyright or related rights in it (the "Copyright") and he has given the University of Manchester certain rights to use such Copyright, including for administrative purposes.

ii. Copies of this thesis, either in full or in extracts and whether in hard or electronic copy, may be made **only** in accordance with the Copyright, Designs and Patents Act 1988 (as amended) and regulations issued under it or, where appropriate, in accordance with licencing agreements which the University has from time to time. This page must form part of any such copies made.

iii. The ownership of certain Copyright, patents, designs, trade marks and other intellectual property (the "Intellectual Property") and any reproductions of copyright works in the thesis, for example graphs and tables ("Reproductions"), which may be described in this thesis, may not be owned by the author and may be owned by third parties. Such Intellectual Property and Reproductions cannot and must not be made available for use without the prior written permission of the owner(s) of the relevant Intellectual Property and/or Reproductions.

iv. Further information on the conditions under which disclosure, publication and commercialisation of this thesis, the Copyright and any Intellectual Property and/or Reproductions described in it may take place is available in the University IP Policy (see http://documents.manchester.ac.uk/DocuInfo.aspx?DocID=487), in any relevant Thesis restriction declarations deposited in the University Library, The University Library's regulations (see http://www.manchester.ac.uk/library/aboutus/regulations) and in the University's policy on Presentation of Theses.

Acknowledgements

I would like to thank everyone who assisted with or contributed to the research contained in this thesis. A special thanks to my supervisor Jon Lloyd, without his scientific creativity, persuasion skills and patience, I wouldn't have had the opportunity to do a PhD degree in the first place. I hope I have acquired some of these skills along the way. I would also like to thank my co-supervisor Nick Bryan for proposing new experiments and spending time reading transfer reports and manuscripts.

I acknowledge financial support from the CNRS-Lebanon and the BIGRAD consortium under the UK Natural Environmental Research Council (NE/H007768/1).

A very special *"thank you"* to Alastair Bewsher for analysing on the IC, the large number of samples I used to send him. Also a special *"thank you"* to Christopher Boothman for helping me settle in the lab and for helping on various occasions.

I would also like to thank all the members of the Geomicrobiology research group for their friendliness and support.

These three and a half years would have been much harder if it weren't for the support and advice of my friends and family back home. A very big "*thank you*" to my parents for every time they asked about my experiments, and for always wanting to know more about some details that I didn't even understand!

Above all, one person who I can't thank enough for all the moments we had for the past 9 years is my soulmate and the love of my life, Cécile El-Chami. Thank you Cécile for being the person you are, without you none of this would have been possible.

The Author

The author graduated from the University of Balamand with a B.Sc. in Biology in 2006. He then joined the M.Sc. programme at the same university and graduated in 2009 with a M.Sc. in Molecular Biology with distinction and won the "Professors of the Faculty of Sciences at the University of Balamand, Student Excellence Award". The author then worked as a research assistant at the Faculty of Sciences at the American University of Beirut for a year and a half, and published an article "*Pleurotus ostreatus* and *Ruscus aculeatus* extracts cause non-apoptotic Jurkat cell death" in the *Journal of Plant Studies*. The author then started an MPhil degree at the University of Manchester in 2011 and secured funding from the Conseil National de la Recherche Scientifique Libanais (National Scientific Research Council of Lebanon) to switch the MPhil to a first year of PhD. During his higher education, the author published an article "Microbial degradation of isosaccharinic acid at high pH" in the *ISME* journal, one of the highest-ranking journals in the fields of ecology and microbiology. This publication got a lot of national and international media attention, and as a result the author won the SEAES Postgraduate Research Student Best Outstanding Output Award for 2014 and the Manchester Doctoral College Best Outstanding Output Award 2015 (Faculty of Engineering and Physical Sciences).

Chapter 1

Thesis Content and Layout

1 Thesis Content and Layout

This thesis is presented in the alternative format style. It is divided into eight chapters, each of which is presented as an independent body of work. There will be some degree of repetition in each of the chapters, which is essential to enable the submission of each chapter for publication in a scientific journal. The following list describes each chapter, the contributions of the authors and its publication status.

Chapter 1

Thesis Content and Layout

Chapter 2

Introduction and Literature Review

Naji M. Bassil

Chapter 3

Methodology

Naji M. Bassil

Chapter 4

Microbial degradation of cellulosic material under intermediate-level waste simulated conditions.

Naji M. Bassil, Alastair D. Bewsher, Olivia R. Thompson, Jonathan R. Lloyd

Author contributions: N. M. Bassil - Principal author, preparation and monitoring of samples and data acquisition and analysis; A. D. Bewsher – Samples analysis on IC system; O. R. Thompson – Help in initial setup of experiments; J. R. Lloyd – Corresponding author and manuscript review.

Status: Manuscript accepted by the *Mineralogical Magazine* for a special issue on the IGD-TP conference.

Chapter 5

Microbial degradation of isosaccharinic acid at high pH.

Naji M. Bassil, N. Bryan, Jonathan R. Lloyd

Author contributions: N. M. Bassil - Principal author, preparation and monitoring of samples and data acquisition and analysis; N. Bryan – Co-author and manuscript review; J. R. Lloyd – Corresponding author and manuscript review.

Status: Published in the February 2015 issue of the *ISME Journal*

Chapter 6

Bacillus buxtonensis sp. nov., an alkaliphilic bacterium which can degrade isosaccharinic acid.

Naji M. Bassil, Jonathan R. Lloyd

Author contributions: N. M. Bassil - Principal author, preparation and monitoring of samples and data acquisition and analysis; J. R. Lloyd – Corresponding author and manuscript review.

Status: Manuscript is ready for submission to the *International Journal of Systematic and Evolutionary Microbiology*.

Chapter 7

Growth profiles of *Bacillus buxtonensis* utilising isosaccharinate or gluconate

Naji M. Bassil, Jonathan R. Lloyd

Author contributions: N. M. Bassil - Principal author, preparation and monitoring of samples and data acquisition and analysis; J. R. Lloyd – Corresponding author and manuscript review.

Status: Manuscript in preparation to *Nature Biotechnology* (awaiting complementary genomic and transcriptomic data to complete manuscript).

Chapter 8

Conclusion and Future Directions

Appendices

Chapter 2

Introduction and Literature Review

2 Introduction and Literature Review

2.1 Radioactive Waste in the UK

The radioactive waste inventory of the UK is composed of legacy waste that was produced over 6 decades, and is expanding due to the addition of waste being produced from ongoing civil and defence nuclear programmes. According to the 2013 report on the UK radioactive waste inventory (NDA, 2014), radioactive waste is classified as "material that shows radioactivity above a certain level and has no further use and is harmful to people and the environment". The total amount of existing and predicted UK radioactive waste is 4.5 million cubic meters, which corresponds to 4.9 million tonnes. This waste can be classified into four categories based on the radioactivity it contains and the heat it generates (NDA, 2014; NDA and DEFRA, 2007; DECC, 2014).

(i) Low-level waste (LLW) is classified as having a radioactive content not exceeding 4 GBq (gigabecquerels) per tonne of alpha or 12 GBq per tonne of beta/gamma activity. This wasteform contains clothing, plastic, paper, building rubble, soil and steel items like framework, pipework and reinforcement that has become contaminated during maintenance, monitoring, dismantling and demolition of nuclear power plants, nuclear fuel production facilities, spent nuclear fuel reprocessing facilities, hospitals, universities and research establishments. It can also be in the form of contaminated soil, building materials and obsolete plant and equipment that have been used to clean up decommissioned facilities and the land around them.

(ii) Intermediate-level waste (ILW) exceeds the upper radioactivity boundaries for LLW, but does not generate so much heat to be taken into account in the design of storage or disposal facilities. This wasteform constitutes the majority of the radioactive waste by volume (about 75%) and includes (1) graphite that is produced from the moderator blocks in the cores of decommissioned nuclear power plant reactors, (2) steel from plant items and equipment, fuel cladding and reactor components, (3) some building materials like cement, concrete and rubble that are produced from decommissioning of buildings, and (4) other waste materials, for example sludges and flocs from the treatment of liquid effluents and from the corrosion of fuel cladding.

(iii) High-level waste (HLW) is waste with a significantly high temperature, as a result of their radioactivity, to be taken into account in the design of storage or disposal facilities. This wasteform is produced initially as a concentrated nitric acid solution containing fission products from the primary stage of reprocessing spent nuclear fuel. Therefore it is made predominantly of a highly radioactive liquid residue that is awaiting conditioning

(for example vitrification in glass) and small quantities of contaminated scrap items, which consist mostly of metal and ceramic.

(iv) Other radioactive materials, which include radioactive materials that are not considered as waste at the moment, but their status might change if the UK government decided that they have no further use. These include (1) spent nuclear fuel, which arises in the reactors of operational nuclear power stations and consists mostly of uranium, plutonium and other fission products, most of which may be reprocessed and reused, (2) plutonium, which is the product of ^{238}U irradiation in nuclear fuel cells in the reactor and is isolated during reprocessing of spent nuclear fuel, and is currently stored pending decision on its fate, and (3) uranium, which arises from fuel manufacture, enrichment or reprocessing of spent fuel, and is also currently stored pending decision on its fate.

These wastes are being stored on an interim basis at nuclear sites in the UK, however, a more permanent solution for the passive management of these wastes (as opposed to active management, which requires the active intervention by humans to manage the waste) is being sought. A wide range of options had been considered, including propelling them into space. The Committee on Radioactive Waste Management recommended in 2008 that deep geological disposal, coupled to safe and secure interim storage was the best long-term management approach for the UK's radioactive wastes (NDA, 2010b; DECC, 2014).

2.2 Deep Geological Disposal for (Passive) Long-Term Waste Management

The deep geological disposal concept depicts that a cement based underground geological disposal facility (GDF) will be built about 600-1000 m below the surface, where packaged radioactive waste will be safely stored for hundreds of thousands of years, until their radioactivity decays and they become safe. The GDF is expected to form a multi-barrier containment system against the transport of radioactive elements from the waste packages to the biosphere, where the engineered packages and structures of the facility will provide physical and chemical (high pH and reducing conditions) hindrance to the transport of radionuclides to the biosphere (Figure 2.1).

At the time of writing this document, a site for building the GDF in the UK had not been decided, therefore the geology around the GDF is not yet known. For this reason, the Nuclear Decommissioning Authority (NDA), which is the public body responsible for managing the strategy for the safe disposal of radioactive waste in the UK, is constantly preparing and updating a generic safety case that will later be tailored to the specific site where the GDF will be built (NDA, 2010a). The safety case is required to answer any questions that may arise from the local community or from the Department of Energy and Climate Change (DECC) on the long-term safety of the GDF. For this reason, research is

being conducted in all aspects related to the GDF, and in all the possible scenarios that the facility will go through during the hundreds of thousands of years that it will be expected to function.

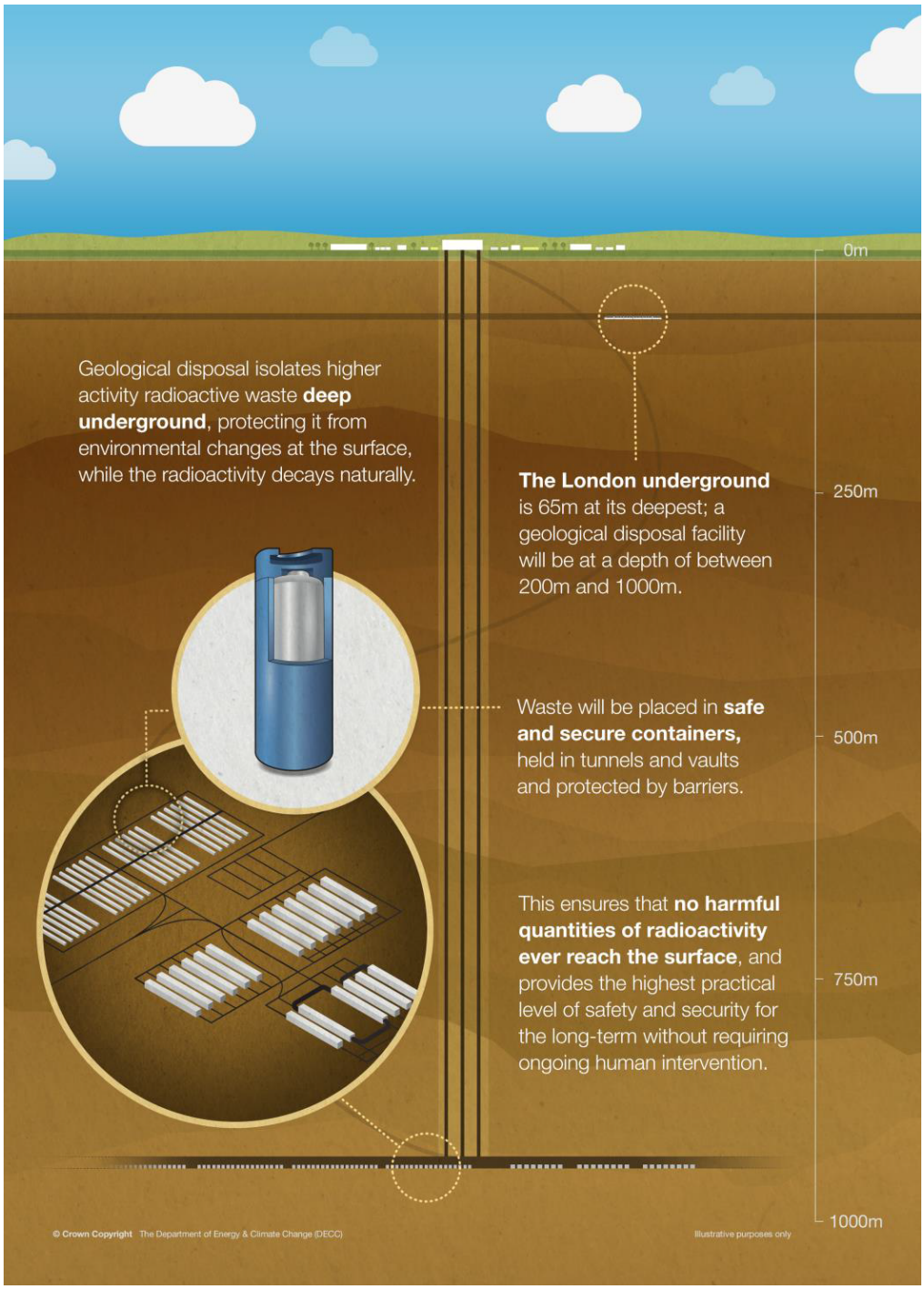

Figure 2.1: A schematic representation showing the physical separation of the wasteforms from each other and from the biosphere (adapted from DECC, 2014).

In its current state, the role that subsurface environmental microorganisms may play in the evolution of the GDF is vastly underrepresented in the generic safety case. This is understandable given that the GDF is an engineered environment, previously considered too extreme for life to survive in, where high pH, radiation and radionuclide toxicity combine. However, extremophilic microorganisms have been found in various natural and

engineered extreme environments, for example hydrothermal vents, acid mine drainage sites, soda lakes and under arctic glaciers, some of which offer analogous conditions to those expected in and around a GDF. These microorganisms have evolved to live under extreme conditions and have developed mechanisms to help them flourish under these conditions. Similar microorganisms may be able to survive and colonise the GDF, and may further affect the conditions there.

In this respect, three foreseen challenges to the view that the GDF will stay a sterile environment for a long period of time are; (1) although the conditions in the GDF will be very harsh for microorganisms at the start, the pH, heat and radiation levels will drop with time; (2) they will also drop at increasing distances from the GDF and into the surrounding host-rock; and (3) although the average conditions in the GDF can be considered extreme for life to develop, radioactive wasteforms are considered heterogeneous, and spatially separated niches may support microbial colonisation.

In this respect, the role that microorganisms may play in the biogeochemical evolution of a GDF cannot be neglected from long-term performance models, if an informed decision has to be made regarding the safety of the GDF.

2.3 Expected Conditions in the UK Geological Disposal Facility

In order to identify the conditions that are expected to be present in a GDF, it is essential to know the types of materials that will be stored and how they might affect the local conditions. As mentioned earlier, the largest volume of material in the GDF will be cement and concrete, which are used for the construction of the facility, for closure of the access tunnels, for the construction of ILW storage vaults, as well as being used as a grout in ILW. Iron will also be present in very high volumes, especially in steel canisters, rock bolts, seals for canisters and drums, and in other construction materials. In addition, a large volume of organic material, mainly cellulosic materials will be present in ILW, along with cement additives that will be present throughout the facility. Furthermore, pending decision on the fate of uranium and spent nuclear fuel and other fission products, the GDF may house uranium, plutonium and other fission products (NDA, 2014). All these materials may affect or be affected by the conditions in the GDF.

During the operational phase of the GDF (when waste is still being transported to the GDF), an aerobic dry environment is expected to dominate due to the use of water pumps and ventilation systems. During this period, the wasteforms are expected to stay intact and no chemical or biological activities are expected to take place. Although it is highly dependent on the geology and hydrogeology of the area where the GDF will be built, it is

expected that after closure, groundwater will gradually fill the repository facility, and this will introduce a number of changes to the chemistry of the GDF.

2.3.1 pH in the GDF

Movement of groundwater into the GDF will leach the cement surrounding the facility and in the backfilled access tunnels, which will form a hyperalkaline environment in and around the engineered facility, which will evolve over time (Berner, 1992). According to Berner, the cement porewater chemistry will pass through three phases, where the dominant cations and pH will change with increasing water exchange cycles. It is important to note here that a number of parameters and variables will influence the time required for the facility to fill with water; each water exchange cycle may require anywhere between 1 and 100 years to complete. Initially (1-100 water exchange cycles or 1-10,000 years), the cement porewater pH would have a value of about 13.3, with the concentrations of Na^+ and K^+ dominating the water chemistry. The second stage (100-1,000 water exchange cycles or 100-100,000 years) will show a drop in pH (to 12.5) and a drop in the concentrations of Na^+ and K^+ cations, while the concentration of Ca^{2+} cations will increase to around 20 mM. The final stage of the cement porewater evolution (>1,000 water exchange cycles or >100,000 years) will be dominated by CO_3^{2-} with a drop in Ca^{2+} concentration (to 1-5 mM) and a drop in pH to a value of about 10.

As mentioned earlier, although the near-field environment will be dominated by hyperalkaline pH, it will not be distributed uniformly throughout the repository, and some lower pH regions are expected to exist (Askarieh *et al.*, 2000). The distance from the GDF will also play an important role in defining the pH in the chemically disturbed zone (host-rock area around the GDF), where the pH is expected to drop in the far-field, and cement leachate concentrations will be diluted by the groundwater (Moyce *et al.*, 2014).

2.3.2 Eh in the GDF

Groundwater movement into the GDF will have an adverse effect on the redox potential of the environment, and this is of concern to the GDF safety case because it determines radionuclide mobility based on their redox state. Upon closure and resaturation of the GDF with groundwater, aerobic conditions will dominate for a short period of time, during which aerobic corrosion of iron and steel and the subsequent production of Fe(III) oxides and hydroxides will dominate the solution chemistry (Duro *et al.*, 2014). The system is expected to rapidly consume the initial oxygen present, for example through the aerobic corrosion of steel, and the inflowing water is expected to be anoxic since it had already been in contact with the deep subsurface host-rock. In this oxygen-free environment, Fe^0

corrosion is favoured through the reduction of water (Duro *et al.*, 2014), along with the reduction of the Fe(III) oxides that were produced during the aerobic corrosion of metals (Humphreys *et al.*, 1997), leading to the production of magnetite (Fe_3O_4) and the subsequent release of H_2 (Eq 1; Duro *et al.*, 2014).

$$3Fe(s) + 4H_2O \rightarrow Fe_3O_4(s) + 4H_2(g) \quad \text{Eq 1}$$

2.3.3 Gas production in the GDF

As mentioned earlier, H_2 is the main gas that is expected to be produced in the GDF from the anoxic corrosion of the large amounts of steel that will be present (Duro *et al.*, 2014). In addition a number of other gasses are of concern to the safety case. These include CO_2, SO_2 and CH_4, which are expected to be produced from microbial metabolism of organic matter that is released from ILW, into the chemically disturbed zone (Askarieh *et al.*, 2000). Gas production in the GDF is of concern to the safety case for a number of reasons, including increased pressure on the surfaces surrounding the GDF that may cause fracture of the cement walls; but of more concern is the rapid transport of radioactive isotopes ^{14}C and ^{3}H to the surface through cracks in the geosphere (Thorne, 2005).

2.3.4 Temperature in the GDF

It is expected that during the operational period of the GDF, localised high temperature areas will be present around HLW only, and these will be accounted for in the design of the GDF. On the other hand, ILW does not produce significant heat to be considered in the design of storage facilities for these wasteforms. After closure of the GDF and its resaturation with groundwater, and for a short period of time, temperature in parts of the GDF in short proximity from HLW could reach a short-lived maximum of 80^{o}C (Askarieh *et al.*, 2000). With time, the temperature of the GDF will become more homogeneous, with an estimated average of 50^{o}C, which will drop even further to approach the temperature of the inflowing groundwater (Askarieh *et al.*, 2000).

2.4 Microorganisms in Extreme Conditions Relevant to the GDF

The above mentioned extreme stress conditions in the GDF, which include hyperalkalinity, relatively high temperature and pressure (in the deep subsurface), radiation and heavy metal toxicity have been previously considered to play a role in limiting microbial colonisation, and therefore the GDF is expected to stay "sterile" for a long period of time. However, microorganisms are the earliest forms of life on Earth, and have been playing important roles in controlling the chemistry of Earth for several billion years (Falkowski *et al.*, 2008), for example through the continuous cycling of elements (Madsen, 2011).

Throughout Earth's history, microorganisms have survived ice ages, heavy volcanic eruptions and bombardments from outer space, and can be found today in some extremely harsh environments (Pikuta *et al.*, 2007). Extremophilic microorganisms (microorganisms that thrive under conditions that are considered to be extreme for life) have been found in a number of natural and anthropogenic places, and a number of these microorganisms show tolerance or even thrive in the presence of more than one extreme condition in the environment. Some of these environments that are colonised by microorganisms are analogues to a cement-based GDF, in particular sites containing high pH and $Ca(OH)_2$ waters (Khoury *et al.*, 1992; Alexander *et al.*, 2012; Rizoulis *et al.*, 2012) and deep underground excavated sites (Pedersen *et al.*, 1996). Although the GDF is expected to be an "extreme" environment that is challenging to life, it will contain a range of electron donors that microorganisms could use as energy sources, for example the organic materials that were mentioned earlier, along with H_2 that is produced from the anaerobic corrosion of iron-containing materials (Duro *et al.*, 2014). In addition, the GDF is also expected to contain a range of electron acceptors that microorganisms could utilise, including oxygen (for a short period after closure), nitrate (which may be found in ILW wasteforms (Albrecht *et al.*, 2013; Rafrafi *et al.*, 2015)), Fe(III) (which is produced from the oxic and anoxic oxidation of Fe^0 and Fe(II) in steel and iron bearing structures in the GDF), sulphate (that is present in groundwaters of many geological formations (Gunn *et al.*, 2006; Samborska *et al.*, 2013)), and CO_2 and other potential electron acceptors that will be present in relatively lower amounts in the different wasteforms.

Two main stressors that are linked together are high pressure and high temperature, for example in deep-sea hydrothermal vents and in very deep subsurface continental sediments (Pedersen, 2000). These stressors cause denaturation of proteins and nucleic acids, and affect the fluidity of the phospholipid bilayer to lethal levels. Thermophilic and barophilic microorganisms that belong to the domains Archaea and Bacteria are very diverse in these environments, and can be found at temperatures as high as 113^{o}C and depths of 3,000 m below the surface (Pedersen, 2000; Fry *et al.*, 2008). These microorganisms produce enzymes that show high temperature stability due to a generally higher content of α-helices and β-sheets than mesophilic proteins (Yano and Poulos, 2003; Nagi and Regan, 1997). Furthermore, they utilise a number of organic and inorganic molecules as electron donors and acceptors to support the increased energy requirement for growth under high temperature and pressure conditions (Pedersen, 1999). In this respect a number of lithoautotrophic (acetogenic and methanogenic) microorganisms have been identified in sediments sampled from such environments. These organisms are thought to utilise H_2 to produce acetate and methane, which can be utilised by other heterotrophic microorganisms

as electron donors, to reduce nitrate, Fe(III), and sulphate (Pedersen, 1999, 2000). Indeed, experiments performed on groundwater samples taken from various depths (10-600 m below ground) of the Swedish Äspö hard rock laboratory showed that (1) although the amount of viable bacteria dropped with increased depth, more than 10^5 bacteria per ml of sample were still observed at the deepest point tested, (2) with increasing depth, different bacterial genera dominated the samples, and (3) sulphate- and iron-reducing and acetogenic bacteria dominated the deepest boreholes (Pedersen *et al.*, 1996).

High pH is one of the major barriers that microorganisms should overcome in order to colonise the GDF and the surrounding chemically disturbed zone, especially considering that the pH in the GDF will stay alkaline for a very long period of time after closure. Alkaliphilic and alkalitolerant microbial species have been identified in a wide range of bacterial and archaeal genera, and in a number of environments ranging from aerobic to anaerobic conditions (Zhilina and Zavarzin, 1994). Under anaerobic conditions, alkaliphilic/haloalkaliphilic bacteria that are capable of fermentative growth (Zavarzina *et al.*, 2009; Zhilina *et al.*, 2005; Zhilina *et al.*, 1996), denitrification, Fe(III) reduction (Williamson *et al.*, 2013; Rizoulis *et al.*, 2012), sulphate reduction (Zhilina *et al.*, 1997; Zhilina *et al.*, 2005) and acetogenesis (Pikuta *et al.*, 2003) have been identified and in a number of cases isolated. Growth under alkaline conditions introduces a number of structural stresses to the microorganisms, including nucleic acid degradation, protein denaturation due to interactions with charged amino acids, changes in the fluidity of the phospholipid bilayer, and changes in the peptidoglycan cell wall. These are mainly overcome by maintaining homeostasis in the intracellular environment through the use of sodium-proton antiporters and sodium channels and the production of hydrophobic proteins that shield charged amino acids (Janto *et al.*, 2011). In addition, the high pH also disrupts the electrochemical (proton) gradient across the bacterial cell membrane, which is vital for the function of the ATP synthase and the metabolic energy production of the bacterium (Janto *et al.*, 2011; Sydow *et al.*, 2002).

Bacterial tolerance to radiation and radionuclide toxicity has not been studied thoroughly, although there have been sporadic reports of bacterial and fungal species identified in spent nuclear fuel storage ponds (Chicote *et al.*, 2004). The most pronounced damage to living organisms from ionising radiation is damage to DNA, however, the indirect damage that includes osmotic stress and the production of oxidants may be more severe. These damages resemble desiccation damage, and it is believed that the bacterial and archaeal genera that have been identified to tolerate ionising radiation (the best known is *Deinococcus radiodurans*) had developed this tolerance as a response to desiccation (Battista, 1997). A number of mechanisms have been implemented by radiotolerant

bacteria and archaea to counter these damages, and these include the production of efficient DNA damage checking and repair machinery and the presence of repeating sequences in the genome (Makarova *et al.*, 2001), along with the accumulation of reduced manganese (Mn(II)) that can act as an antioxidant (Ghosal *et al.*, 2005).

2.5 Cellulose: Major Organic Molecule in ILW

Cellulose is the major carbohydrate synthesized by plants to strengthen their cell walls, making it the most abundant polysaccharide biopolymer on Earth and a primary source of energy for life. Due to its abundance and its physical properties, cellulose is the target of many industries dealing with wood and its derivatives, clothing and biofuels. Cellulose is made of rigid, insoluble microfibrils that are oriented in parallel, with the reducing ends located at the same end. These microfibrils are a polymer of 100-14,000 glucose subunits linked by β-1,4 glycosidic bonds, oriented at an angle of 180^{o} relative to their neighbours, making up the basic repeating unit of cellobiose (Beguin and Aubert, 1994).

Cellulose forms highly ordered crystalline domains that are interspersed by more disordered amorphous regions (Leschine, 1995; Lynd *et al.*, 2002). Native cellulose (for example cotton) is highly crystalline, while treated cellulose (for example paper or tissue) is swollen and shows a higher specific surface area, a lower crystallinity index and therefore more amorphous regions than native cellulose (Mosier et al. 1999). The major constituent of organic matter in LLW and ILW that will be stored in a repository will be wood derivatives, for example paper and cardboard, and clothing and other cotton derivatives (Leschine, 1995), which are made of treated cellulose.

2.5.1 Biological Degradation of Cellulose

The ubiquity of cellulose on Earth dictates that a wide diversity of organisms have developed the ability to degrade this molecule. Cellulolytic organisms can be found in a variety of environments where cellulose accumulates, ranging from aerobic to anaerobic, mesophilic to hyperthermophilic, and acidic to alkaline environments (Lynd *et al.*, 2002). The most intensively studied cellulolytic microorganisms belong to the fungal & bacterial kingdoms. These include the aerobic cellulolytic fungi *Trichoderma reesi*, *Humicola insolens*, and *Phanerochaete chrysosporium*, and the lesser studied anaerobic fungi, which belong to the genera *Piromyces* and *Neocallimastix* (Lynd *et al.*, 2002). The anaerobic bacteria that are known for their cellulolytic activity belong to the genera *Clostridia*, *Ruminococcus*, *Fibrobacter*, *Thermotoga* and *Caldicellulosiruptor*; while the aerobic cellulolytic bacteria belong to the genera *Cellulomonas*, *Thermobifida*, *Acidothermus* and *Rhodothermus* (Lynd *et al.*, 2002).

The insoluble nature of cellulose, especially in the highly crystalline regions, necessitates that the cellulolytic enzyme system be composed of a number of proteins, each with a specific function (Leschine, 1995). Eleven different families of cellulolytic enzymes have been identified and grouped into three groups (Beguin and Aubert, 1994). (I) Cellobiohydrolases hydrolyse the reducing end (cellobiohydrolase I) or the non-reducing end (cellobiohydrolase II) of the cellulose molecule and release cellobiose as a hydrolysis product (Mosier et al. 1999). (II) Endoglucanases act on the amorphous regions and cause random mid-chain scissions in the cellulose polymer, which increases the number of free cellulose chain ends for cellobiohydrolases to hydrolyse (Mosier *et al.*, 1999). (III) β-glucosidases hydrolyse the β-1,4-glycosidic bond between the two monomers of the cellobiose and release the two glucose molecules (Mosier *et al.*, 1999). These enzymes may be secreted from bacterial cells (Figure 2.2A), or may be bound to the bacterial cell wall to form a cellulose-degrading enzyme complex called the cellulosome (Figure 2.2B). Each approach has its advantages and disadvantages. Secreted enzymes can access tighter regions of the cellulose fibres, thereby enabling the degradation of more crystalline domains. However, the cellulose hydrolysis products are free in solution and may be incorporated by any bacterium in the vicinity, thereby increasing competition (this secretory approach is mainly used by aerobic bacteria and fungi). The cell wall bound cellulosome complex contains enzymes with the same functions of the free enzymes, but they are grouped together by a scaffoldin protein and a cohesin moiety. Adhesion to the cellulose fibre is mediated by a noncatalytic domain, called the carbohydrate-binding module and a thin layer of glycoprotein called the glycocalyx. This cellulosome-mediated approach enables a more efficient degradation of the cellulose fibres since all the catalytic domains are clustered in the same vicinity, and the close proximity of the bacterial cell to the hydrolysis site ensures the incorporation of the hydrolysis products by the bacterium. On the other hand, tight regions of the cellulose molecule are rendered inaccessible for degradation due to the size of the bacterial cell (this approach is mainly used by anaerobic bacteria and fungi).

These enzymes follow a basic mechanism for breaking the glucose monomers of the cellulose polymer. It involves a nucleophilic attack by a deprotonated acidic amino acid that is found in the catalytic domain, on the β-1,4-glycosidic bond, and requires another protonated acidic amino acid on the opposite side of the catalytic domain to return the enzyme to its original state (Mosier *et al.*, 1999). Although this mechanism can describe cellulose degradation under acidic and neutral pH, it cannot describe cellulose biodegradation at high pH where all the acidic amino acids would be deprotonated if exposed to the alkaline solution (Zvereva *et al.*, 2006).

The synergism between the three enzyme groups ensures that the cellulose molecule can be fully biodegraded into glucose monomers that can be metabolised by microorganisms for energy production.

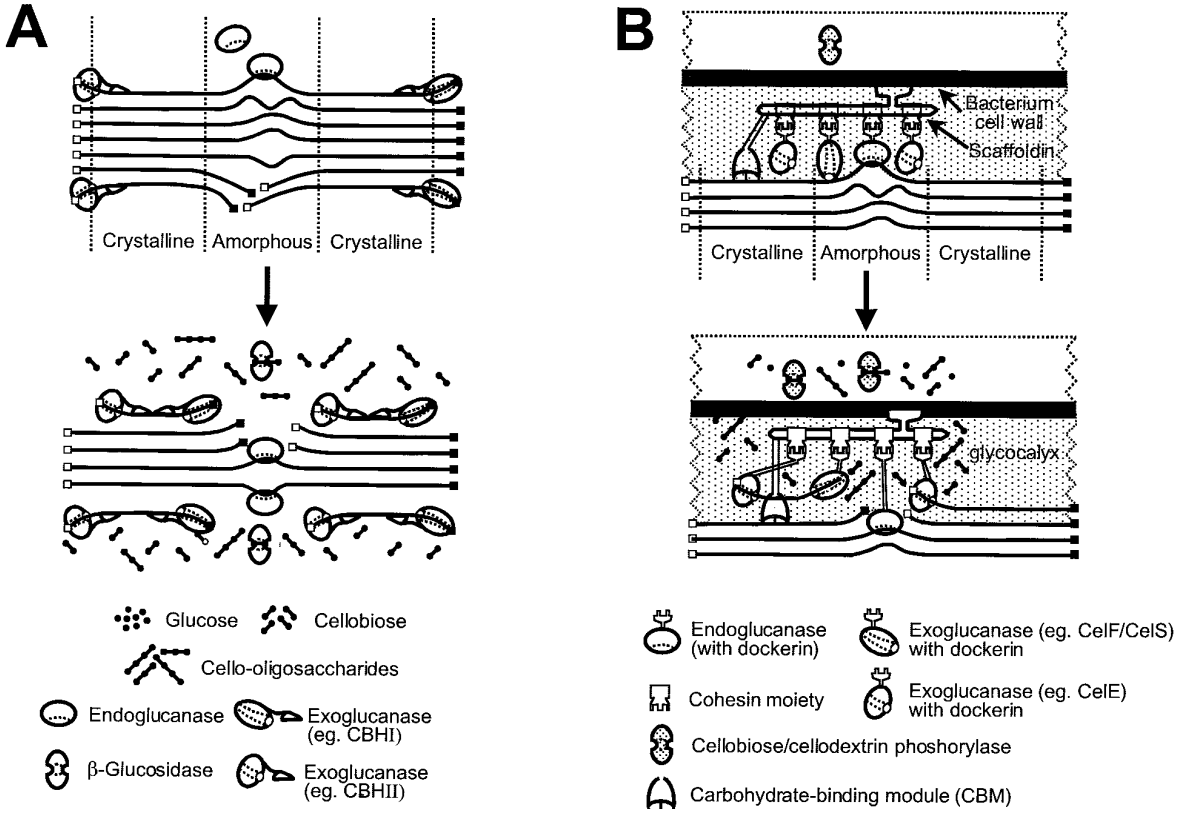

Figure 2.2: Enzymatic hydrolysis of cellulose by cellulolytic enzymes. A) Secreted enzymes. B) Cell bound enzymes (adapted from Lynd *et al.*, 2002).

2.5.2 Radiolysis of Cellulose

Radioactive molecules will be present in the GDF, and as such, radioactivity is expected to bombard cellulose fibres present in ILW (Askarieh *et al.*, 2000). Irradiation of cotton filters, hardwood and softwood with an electron beam, led to an increase in mid chain scissions and in the degree of polymerisation of cellulose fibres, along with an increase in the number of carbonyl and carboxyl groups (Bouchard *et al.*, 2006; Lawton *et al.*, 1951). Similar observations were made when cotton and wood were exposed to various doses of gamma-radiation, with an increase in the amount of depolymerisation and mid chain scissions with increasing dosage, especially in the presence of oxygen (Glegg and Kertesz, 1957; Blouin and Arthur, 1958). However, the effects of cellulose radiolysis are expected to be negligible compared to the abiotic alkali hydrolysis of cellulose in the ILW (Van Loon and Glaus, 1997; Van Loon *et al.*, 1999).

2.5.3 Abiotic Alkali Cellulose Hydrolysis

Under high pH conditions, similar to those expected in the earlier stages of the GDF (pH values between 13.3 and 12.5), cellulose-containing materials that are likely to be present in ILW have been shown to undergo chemical hydrolysis (van Loon, Glaus, Laube, *et al.*, 1999). Three reactions govern this abiotic hydrolysis of cellulose: (i) the initiation reaction, (ii) the stopping reaction and (iii) the re-initiation reaction. These reactions are illustrated in Figure 2.3.

2.5.3.1 The Initiation Reaction

The β-1,4-glycosidic linkages between the monomers of the cellulose fibbers are alkali stable, while the reducing end glucose molecules are vulnerable to attack by alkali (Knill and Kennedy, 2003), therefore alkaline cellulose hydrolysis is initiated by peeling off single glucose subunits from the reducing end of the cellulose molecule.

The peeling off mechanism starts with a keto-enol tautomerism where a OH^- nucleophile attacks the hydrogen on the α-carbon of the reducing end glucose molecule, and causes a nucleophilic elimination that creates a double bond between C1 and C2 of the glucose molecule. This breaks the carbonyl double bond on C1 and creates an enediolic ion functional group. This molecule can undergo an anion isomerisation reaction where the carbonyl O^- on C1 attacks the hydroxyl hydrogen on C2 and creates a hydroxyl group on C1, and a carbonyl group on C2. The C1 carbon acquires a H^+ from the solution and breaks the double bond and forms an alkane instead of the alkene group. These rearrangements (termed the Lobry de Bruin/Alberda van Ekenstein transformation) create a fructose molecule instead of the glucose molecule on the reducing end of cellulose.

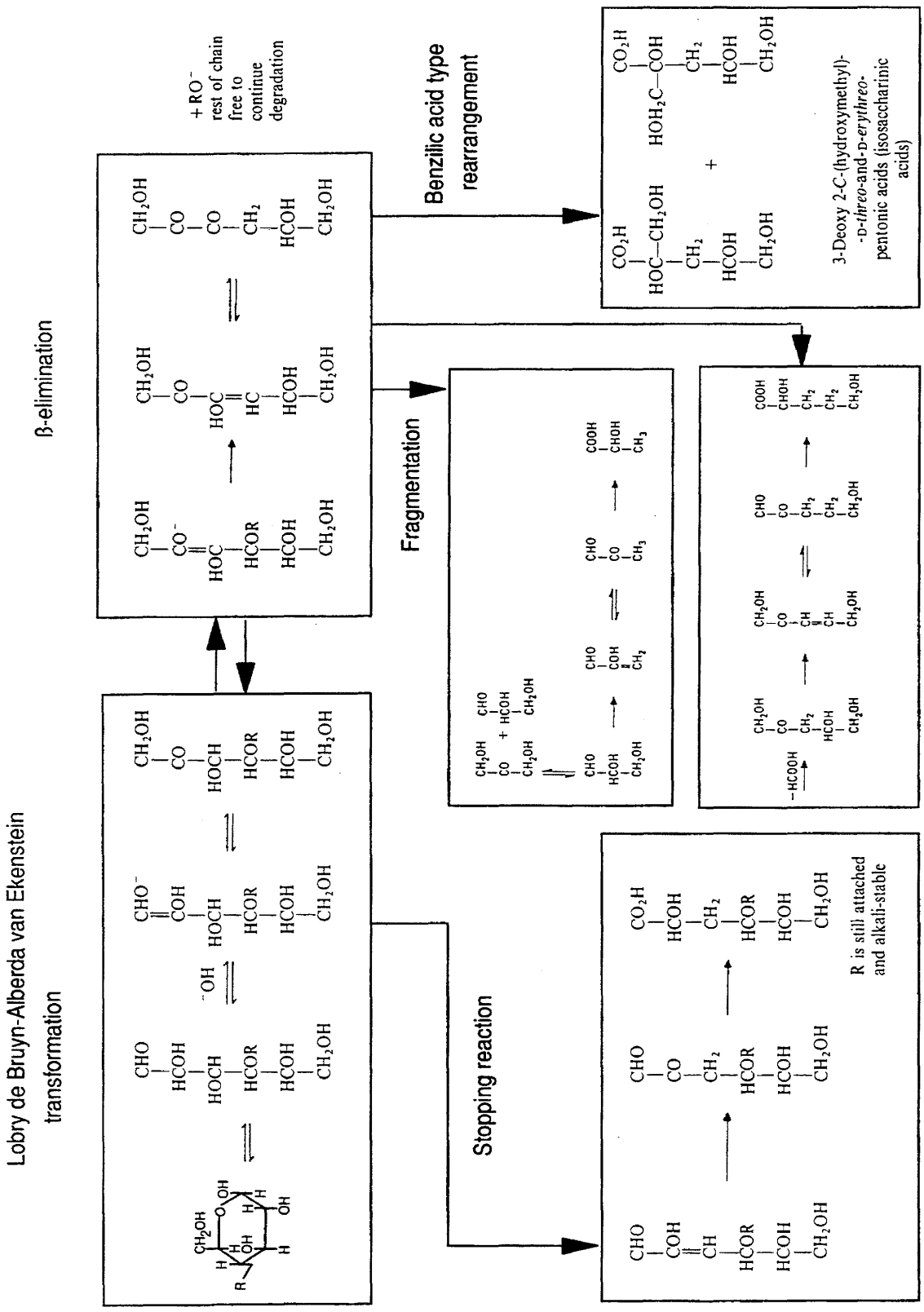

Figure 2.3: Proposed reaction mechanism for cellulose hydrolysis by alkali (adapted from van Loon and Glaus, 1998).

The fructose undergoes a β-alkoxycarbonyl elimination step, where a OH^- nucleophile attacks the hydrogen on the C3 and causes a nucleophilic elimination reaction that creates a double bond between C2 and C3 of the fructose molecule. This breaks the carbonyl

double bond on C2, and creates an enediolic ion functional group between C2 and C3. This molecule is unstable and upon the reformation of the carbonyl double bond on C2, the alkene double bond changes positions to between C3 and C4, which leads to a β-alkoxy group elimination reaction that thereby breaks the β-1,4-glycosidic bond between this molecule and the remaining polymeric chain of the cellulose molecule. This bond breakage creates a new reducing group at this end of the cellulose polymer, which can start a new cycle of peeling off reactions. The detached molecule contains an alkene group next to a hydroxyl group, which induces a keto-enol tautomerism reaction that creates a vicinal dicarbonyl compound on C2 and C3. This molecule may either fragment to produce the different acids with less than 6 carbons, or may undergo benzilic acid rearrangement. In the latter case a OH^- attempts a nucleophilic elimination on C2 and breaks the carbonyl double bond and upon the reformation of the carbonyl group on C2, the hydroxymethyl group is substituted from C2 to C3 and induces the breakage of the second carbonyl double bond. This O^- will now act as a nucleophile that can attack any H^+ molecule in the vicinity to create a hydroxyl group, thereby predominantly creating the molecules 3-deoxy-2-C-(hydroxymethyl)-D-erythro-pentonic acid (α-ISA) and 3-deoxy-2-C-(hydroxymethyl)-D-threo-pentonic acid (β-ISA) (van Loon et al. 1999a).

It has been demonstrated that reaction conditions, especially temperature and the constituents of the alkali solution used (mainly Na^+ or Ca^{2+}), greatly influence the products of the peeling off reaction. Although it has no direct role in the reaction mechanism, the presence of Ca^{2+} in solution favours benzilic acid rearrangement reactions (Isbell, 1944). On the other hand, in the presence of Na^+ ions and at higher temperature, short chain acids (less than 6 carbon molecules) are produced at the expense of ISA (Isbell, 1944). These acids have already been identified as lactic, formic, acetic, glycolic, glyceric, butyric, threonic, adipic, succinic, pyruvic, and propionic acid (Glaus *et al.*, 1999).

2.5.3.2 The Stopping Reactions

In some cases, the reducing end glucose molecule on the cellulose polymer does not undergo the Lobry de Bruin/Alberda van Ekenstein transformation (Figure 2.3). Instead it directly undergoes a β-hydroxycarbonyl elimination followed by a keto-enol tautomerism and benzilic acid rearrangement (Isbell, 1944). In this case, the hydroxyl group on C3 of the glucose molecule becomes the leaving group from the β-hydroxycarbonyl elimination reaction, instead of the alkoxy group on C4. The product of this reaction (3-deoxy-D-arabino-hexonic acid, also known as metasaccharinic acid) is alkali stable and does not detach from the cellulose polymer. The formation of metasaccharinic acid prevents further degradation of the cellulose polymer, since it produces a non-reducing group at the end of

the cellulose polymer and causes a chemical stopping of the peeling off reaction. Another stopping mechanism (termed physical stopping) occurs when the cellulose molecule has been peeled back to a crystalline region with very low solubility and hydroxide ions cannot reach the reducing end groups, thereby preventing further degradation (Haas *et al.*, 1967). The competition between the peeling off and the stopping reactions control the rate and amount of cellulose hydrolysis by alkali.

2.5.3.3 The Re-initiation Reactions

The last reaction that occurs under these conditions is the re-initiation reaction (Glaus and van Loon, 2008). As its name indicates, this reaction causes a restart in the hydrolysis of cellulose after it had been stopped by the chemical or physical stopping mechanisms. Although the mechanism governing this type of reaction is still unclear, two mechanisms have been proposed. The first mechanism suggests that alkali attack will break the glycosidic linkage between two consecutive glucose molecules in the cellulose polymer, thereby creating a new reducing end glucose unit that can reinitiate the peeling off process (van Loon and Glaus, 1997). The other mechanism proposes that reducing end glucose molecules that are hidden in the crystalline regions will temporarily be available to attack, and this will induce a slow peeling off process that continues throughout (Glaus and van Loon, 2008).

2.5.4 Kinetics of Cellulose Hydrolysis

The rate of cellulose hydrolysis depends on the chemistry of the environment where the cellulosic material will be present, which is, in turn, dependent on the evolution of the porewater in the GDF. As mentioned earlier, the expected porewater chemistry in the GDF at the time when cellulose degradation will take place will be dominated by a pH between 12 and 12.5 and a Ca^{2+} concentration of about 20 mM, under anaerobic conditions (Berner 1992). These conditions favour the β-alkoxycarbonyl elimination and benzilic acid rearrangement reactions over the β-hydroxycarbonyl elimination and fragmentation reactions, therefore favouring the production of ISA over the shorter chain aliphatic acids.

The first model to predict the rate of cellulose hydrolysis under GDF conditions was based on the observation that the rate of cellulose hydrolysis by alkali is inversely proportional to the degree of polymerisation and predicted that all the alkali degradable cellulosic material would be hydrolysed by the peeling off reaction after about 2 years of repository closure (van Loon and Glaus, 1997). The remaining cellulose will be cellulose with alkali stable end groups or with reducing end groups that are no longer accessible to alkali due to crystallinity. These will be hydrolysed by a slow process of alkali hydrolysis of the

glycosidic bonds followed by a peeling off reaction starting from the newly formed reducing end group. This model estimated the period of total cellulose degradation under GDF conditions to be anywhere between 100,000 and 1,000,000 years. It also indicates that ISA will be present in very high amounts during the first 2 years, while its production will slow down during the following years. A number of studies supported this model and showed that (i) different cellulosic materials are hydrolysed at different rates based on the degree of polymerisation and amount of reducing end groups of the cellulose tested; (ii) different cellulosic materials produce different combinations of the various organic acids, and these are in turn affected by the time of incubation; and (iii) only 10% of cellulose will be degraded during the initial 2 year period (Glaus *et al.*, 1999; van Loon, Glaus, Laube, *et al.*, 1999).

A seven years incubation study showed that during the first 3 years of incubation of different cellulosic materials a considerable amount of cellulose (up to 30%) would be hydrolysed, followed by a rapid hydrolysis of all the cellulose in 150-550 years (Pavasars *et al.*, 2003). Based on these observations, the first model was amended by factoring in the temporary exposure of the protected reducing end groups by the crystalline domains to alkali, which reinitiates a slow peeling off reaction (Glaus and van Loon, 2008). The addition of this factor greatly enhanced the rate of cellulose hydrolysis due to the high number of reducing end groups that were protected by the crystalline domains after the initial 2-3 years of incubation (hydrolysis of the amorphous regions). This revised model proposed that the complete hydrolysis of cellulose under GDF conditions would require between 1,000 and 5,000 years after closure of the GDF, and was supported by results from a 12 years incubation study of different cellulosic materials (Glaus and van Loon, 2008).

2.6 Isosaccharinic Acid and Gluconic Acid: Major Ligands in a GDF

As mentioned earlier, the major products of the abiotic alkali hydrolysis of cellulose are the two isomers of ISA, α-ISA and β-ISA, which are the products of the benzilic acid rearrangement (the final step in the ISA production mechanism from cellulose hydrolysis (Figure 2.3)). Both isomers are produced in equimolar concentrations from the alkali hydrolysis of cellulose, although it has been reported that higher concentrations of $Ca(OH)_2$ favour the production of the α-ISA isomer, while the use of NaOH favours the production of the β-ISA isomer (Shaw *et al.*, 2012). Because the β-ISA isomer is harder to produce and has a lower yield than α-ISA, most studies have focused on the latter and therefore it will be the main focus of this work.

Gluconic acid (GA) is another organic ligand that is used as a cement additive and is expected to be present in a GDF. Cement additives are organic molecules that are added to the cement mixture to give it flexibility and durability. Because the GDF will contain large quantities of cement in the walls of the facility and as backfill material in the ILW and LLW vaults, it is expected that high amounts of GA will be present in the GDF. Furthermore, ISA and GA show similar chemical properties and therefore it is logical to discuss them in the same context, especially that they are both organic ligands that are expected to be present in a GDF (although unlike ISA, GA is not a product of the abiotic alkali hydrolysis of cellulose).

The polyhydroxy carboxylic acid nature and the structures of ISA and GA enable them to be present in the protonated (ISA_H and GA_H, respectively), deprotonated (ISA^- and GA^-, respectively), or the lactone (ring) forms (ISA_L and GA_L, respectively), depending on the pH of the solution (Figures 2.4 and 2.5).

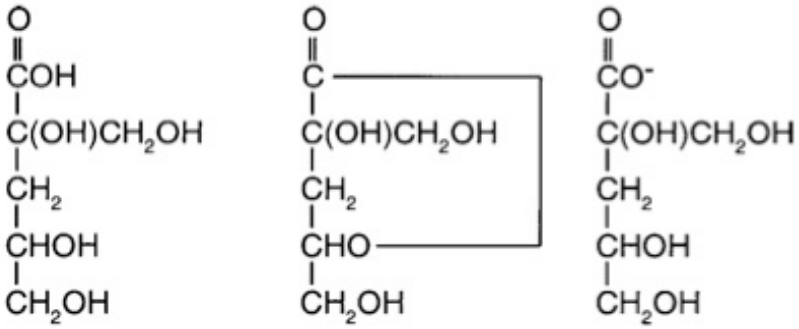

Figure 2.4: Structure of the different forms of α-ISA (adapted from Rai *et al.*, 2008). Left: the protonated form (ISA_H), middle: the lactone form (ISA_L), and right: deprotonated form (ISA^-).

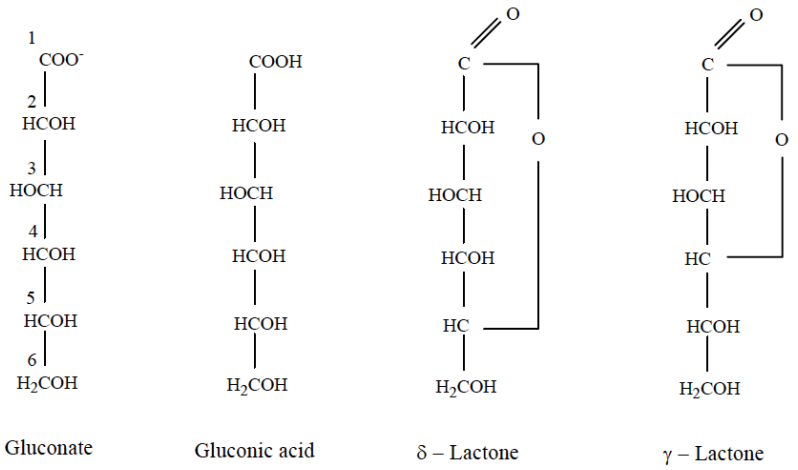

Figure 2.5: Structure of the different forms of GA (adapted from Zhang *et al.*, 2007).

Much work has been carried out to identify the acid dissociation constants for ISA, especially since the transformation reaction between the ISA_H and the ISA_L forms complicates the proton dissociation reaction. The latest study has proposed the presence of two acid dissociation constants, an intrinsic constant, which governs only the proton

dissociation of ISA_H to ISA^-, and a composite constant, which measures the sum of proton dissociation from ISA_H and ISA_L to ISA^- (Brown *et al.*, 2010). The intrinsic acid dissociation constant for ISA_H (Eq 2) was calculated to be $\log K_a^o = -4.04 \pm 0.06$, and the transformation constant from ISA_H to the lactone form ISA_L (Eq 3), was calculated to be $\log K_L^o = 0.79 \pm 0.04$; these values enabled the calculation of the composite dissociation constant $\log K_c^o = -4.90 \pm 0.07$ (Brown *et al.*, 2010; Cho *et al.*, 2003).

$$ISA_H \rightleftharpoons ISA^- + H^+ \qquad \text{Eq 2}$$

$$ISA_H \rightleftharpoons ISA_L + H_2O \qquad \text{Eq 3}$$

Work has also been done to determine the acid dissociation constant for GA, which is even more complicated than that of ISA since it has two lactone forms, $\delta\text{-}GA_L$ and $\gamma\text{-}GA_L$ (Zhang *et al.*, 2007). δ-GA forms more rapidly than γ-GA, with the latter only forming at pH less than 2. The intrinsic dissociation constant for the protonated carboxylic acid form (GA_H; Eq 4) was determined to be $\log K_a = -3.30 \pm 0.02$, while the transformation constant to the δ-lactone form ($\delta\text{-}GA_L$; Eq 5) was calculated to be $\log K_L = 0.54 \pm 0.04$ (Zhang *et al.*, 2007).

$$GA_H \rightleftharpoons GA^- + H^+ \qquad \text{Eq 4}$$

$$GA_H \rightleftharpoons \delta\text{-}GA_L + H_2O \qquad \text{Eq 5}$$

It is important to note that these dissociation constants represent the proton dissociation from the carboxylic acid moiety of ISA and GA, however, the pH in the GDF is expected to stay at a value of about 12.5 for a long period of time due to the use of cement in construction and as backfilling. Under these conditions, the ISA and GA will be in the deprotonated ion forms ISA^- and GA^-, respectively. As mentioned earlier also, groundwater intrusion into the GDF will leach cations and will be dominated by Ca^{2+} (at a concentration of about 20 mM) at pH 12.5, which will have a major effect on the behaviour of these ligands in the GDF.

Two theories for the mechanism of complex formation between polyhydroxy carboxylic acids and metals have been proposed (Gaona *et al.*, 2008), and experimental data have not resolved which is the more appropriate. The first mechanism includes the hydrolysis of the cation (for example Eq 6), and the second involves the deprotonation of alcohol groups on the polyhydroxy carboxylic acid (for example Eq 7).

$$An^{4+} + ISA^- + 4H_2O \rightleftharpoons AnISA(OH)_4^- + 4H^+ \qquad \text{Eq 6}$$

$An^{4+} + ISA^{-} \rightleftharpoons An(ISA_{-4H})^{-} + 4H^{+}$ Eq 7

Although identifying the proton dissociation constant of the hydroxyl group would seem to resolve this uncertainty, it is argued that the presence of various cations enhances the deprotonation reaction, thereby decreasing the apparent acid dissociation constant of this group. Resolving this issue is not the aim of the present work, and therefore, the complexes that were reported by the original authors are adopted here.

2.6.1 Complex Formation with Alkaline Earth Metals and Transition Metals

Both diastereomers of ISA (α-ISA and β-ISA) and GA can form stable complexes with Ca^{2+}. The complexes formed between Ca^{2+} and β-ISA are readily soluble (for this reason $Ca(\beta\text{-}ISA)_2$ is harder to isolate from the mixture during ISA synthesis in the laboratory), and no studies of the complexation between these two species have been reported previously. For this reason this work will only focus on the α-ISA isomer. The nature of the complexes formed between Ca^{2+} and ISA or GA, and their formation and solubility coefficients have been studied and re-evaluated on a number of occasions and are summarised in Table 2.1.

Table 2.1: Solubility and stability constants of Ca-ISA and Ca-GA complexes.
I (M) is the ionic strength (mol l^{-1}) of the solutions that the experiments were conducted in.

Reaction	pH	I (M)	Log *K*	Reference
$Ca(ISA)_2(cr) \rightleftharpoons Ca^{2+} + 2ISA^{-}$	6.5 - 8	0	-6.53 ± 0.02	Van Loon *et al.*,1999
	8.3	0	-6.26 ± 0.07	Rai *et al.*, 2003
	6 - 11	0	-7.62	Rai *et al.,* 1998
	6	0	-6.53 ± 0.1	Van Loon *et al.,* 2004
	10.8 - 12	0.3	-6.36 ± 0.1	Vercammen *et al.,* 1999
$Ca(GA)_2(cr) \rightleftharpoons Ca^{2+} + 2GA^{-}$	6.5 - 8	0	-3.54 ± 0.06	Van Loon *et al*., 1999
$Ca^{2+} + ISA^{-} \rightleftharpoons Ca(ISA)^{+}$	6.5 - 8	0	1.7	Van Loon *et al*., 1999
	8.3	0	1.44 ± 0.07	Rai *et al.,* 2003
	6	0	1.78 ± 0.04	Van Loon *et al.,* 2004
	6	0	1.78 ± 0.04	Van Loon *et al.,* 2004
$Ca^{2+} + GA^{-} \rightleftharpoons Ca(GA)^{+}$	6.5 - 8	0	1.7	Van Loon *et al*., 1999
$Ca^{2+} + ISA^{-} \rightleftharpoons Ca(ISA_{-H})^{o} + H^{+}$	12 - 13.3	0.3	-10.4 ± 0.2	Vercammen *et al.*, 1999
$Ca^{2+} + 2ISA^{-} \rightleftharpoons Ca(ISA)_2(aq)$	6 - 11	0	5.4	Rai *et al.*, 1998

In solution $Ca(ISA)_{2(cr)}$ dissociates into Ca^{2+} and ISA^{-}, which form $Ca(ISA)^{+}$ complex; also $Ca(GA)_{2(cr)}$ dissociates into Ca^{2+} and GA^{-}, which form $Ca(GA)^{+}$, and these reactions are independent of pH above a pH value of 5 (when all the ISA and GA are in the deprotonated forms) (van Loon, Glaus and Vercammen, 1999; Rai *et al.*, 2003; van Loon *et al.*, 2004). At higher pH values (between 12 and 12.8 expected to dominate under GDF conditions) however, an additional more stable uncharged complex is formed by the displacement of one proton from the α-hydroxyl group of ISA to form $Ca(ISA_{-H})^{o}$

(Vercammen *et al.*, 1999). At even higher pH (>12.8), most of the Ca^{2+} drops out of solution as portlandite ($Ca(OH)_2$), leaving soluble ISA^- in solution (Rai *et al.*, 1998).

As mentioned earlier, other molecules that are expected to be present in high concentrations in the GDF are Fe(III) or Fe(II), which are produced from the aerobic and anaerobic corrosion of steel and iron containing materials. These species have been shown to form stable complexes with GA in the presence and absence of Ca^{2+} in the system, at pH values between 5 and 12 (Bechtold *et al.*, 2002). No studies on complex formation between Fe(III) and ISA under alkaline conditions have been found in the open literature.

Experiments on the complexation of Ni(II) (another transition metal that is of concern to the GDF safety case since Ni-based alloys may be used in containment canisters for ILW) by ISA and GA showed that different complexes form at different pH ranges, where green soluble solutions of $Ni(ISA)^+$ and $Ni(GA)^+$ form at pH < 7, green precipitates of $Ni_2ISA(OH)_3$ and $Ni_2GA(OH)_3$ form at 7 < pH < 10, while soluble green solutions of $Ni_2ISA(OH)_4^-$ and $Ni_2GA(OH)_4^-$ form at pH > 10 (Warwick *et al.*, 2003).

2.6.2 Complex Formation with Actinides and Lanthanides

The actinide that will be present in the highest amounts in the GDF is uranium, which is used in various stages of the nuclear fuel cycle. Under high pH and reducing conditions, uranium is expected to be in its reduced form, U(IV), although recent studies have suggested that U(VI) may be stable at high pH and have shown the formation of colloidal U(VI) structures under similar conditions (Bots *et al.*, 2014; Smith *et al.*, 2015). Complex formation between U(IV) and ISA or GA were studied at the pH range between 3 and 13.8 and the stability constants of the 1:1 complexes ($UISA(OH)_4$ and $UGA(OH)_4$) are shown in Table 2.2 (Warwick *et al.*, 2004). It was noted in this study that $U(IV)ISA_2$ or $U(IV)GA_2$ complexes may also form, and that these are dependent on the availability of the ligand, and that $U(ISA_{-4H})^-$ and $U(GA_{-4H})^-$ can also form at high pH, through the deprotonation of the hydroxyl groups.

Another actinide that is expected to be present in the GDF is neptunium, which is produced by neutron irradiation of nuclear fuel in reactors, and will be present in the GDF in the reduced form, Np(IV). Studies on NpO_2(am) at various pH showed that Np(IV) is less soluble with increasing pH up to pH 7, above which the pH no longer plays a role, but increasing ISA concentrations cause higher Np(IV) solubility (Rai *et al.*, 2003). These observations were explained by the formation of $Np(OH)_4ISA^-$ and $Np(OH)_4ISA_2^{2-}$ at pH 12 and ISA concentrations ≤0.01 M and ≥0.01 M, respectively (Table 2.2).

Table 2.2: Stability constants of ISA and GA complexes with actinides and lanthanides. I (M) is the ionic strength (mol l^{-1}) of the solutions that the experiments were conducted in.

Reaction	pH	I (M)	Log *K*	Reference
$U^{4+} + ISA^- + 4OH^- \rightleftharpoons UISA_2(OH)_4^{2-}$	13.5 ± 0.06	0.3	-4.9 ± 1	Warwick et al. 2004
$U^{4+} + GA^- + 4OH^- \rightleftharpoons UGA(OH)_4^-$	13.8 ± 0.03	0.3	-5.2 ± 1	Warwick et al. 2004
$NpO_2(am) + ISA^- + 4OH^- \rightleftharpoons Np(OH)_4ISA^-$	12	0	-4.76 ± 0.37	Rai et al. 2003
$NpO_2(am) + 2ISA^- + 4OH^- \rightleftharpoons Np(OH)_4ISA_2^{2-}$	12	0	-2.9 ± 0.37	Rai et al. 2003
$Th^{4+} + ISA^- \rightleftharpoons Th(ISA_{-4H})^- + 4H^+$	10.7 – 13.3	0.3	-10.1 ± 0.2	Vercammen et al. 2001
$Th^{4+} + 2ISA^- + Ca^{2+} \rightleftharpoons Th(ISA_{-2H})_2Ca + 4H^+$	10.7 – 13.3	0.3	-3.6 ± 0.2	Vercammen et al. 2001
	13.3	0	-5.0 ± 0.3	Tits et al. 2005
$Th^{4+} + 2GA^- + Ca^{2+} \rightleftharpoons Th(GA_{-2H})_2Ca + 4H^+$	13.3	0	-2.1 ± 0.1	Tits et al. 2005
$Eu^{3+} + ISA^- \rightleftharpoons Eu(ISA_{-4H})^{2-} + 4H^+$	10.7 – 13.3	0.3	-30.6 ± 0.2	Vercammen et al. 2001
$Eu^{3+} + ISA^- \rightleftharpoons Eu(ISA_{-3H})^- + 3H^+$	13.3	0	-20.9 ± 0.2	Tits et al. 2005
$Eu^{3+} + GA^- \rightleftharpoons Eu(GA_{-3H})^- + 3H^+$	13.3	0	-18.5 ± 0.2	Tits et al. 2005
$Am^{3+} + ISA^- \rightleftharpoons Am(ISA_{-3H})^- + 3H^+$	13.3	0	-21.4 ± 1	Tits et al. 2005
$Am^{3+} + GA^- \rightleftharpoons Am(GA_{-3H})^- + 3H^+$	13.3	0	-19.6.± 1	Tits et al. 2005

The complexation of thorium and europium by ISA and GA were studied in batch sorption experiments using feldspar or BioRad 50W-X2 resin at pH values between 10.7 and 13.3 in the presence and absence of Ca^{2+} (Vercammen *et al.*, 2001). Similar experiments studied the complexation of thorium, europium and americium with these ligands in the presence of calcite at pH 13.3 (Tits et al. 2005), and also on thorium in hardened cement paste equilibrated systems (Wieland et al. 2002). The stability constants for these complexes are shown in Table 2.2. These studies showed that Th forms stable 1:1 $Th(ISA_{-4H})^-$ complexes in the absence of Ca^{2+} and 1:2:1 $Th(ISA_{-4H})_2Ca$ complexes in the presence of Ca^{2+}, through the deprotonation 4 hydroxyl groups of the ligand (Vercammen et al. 2001; Wieland et al. 2002; Tits et al. 2005). On the other hand, europium was shown to form 1:1 complexes with ISA or GA (($Eu(ISA_{-3H})^-$ and $Eu(GA_{-3H})^-$) through the deprotonation of 3 hydroxyl groups from the ligand, independent of the presence of Ca^{2+} (Vercammen et al. 2001; Tits et al. 2005). It should be noted that a 1:1 complex was reported to be formed through the deprotonation of 4 hydroxyl groups from ISA ($Eu(ISA_{-4H})^{2-}$) (Vercammen et al. 2001). Similar to europium, americium also forms 1:1 complexes with ISA and GA ($Am(ISA_{-3H})^-$ and $Am(GA_{-3H})^-$), through the deprotonation of 3 hydroxyl groups in the ligand (Tits et al. 2005).

2.6.3 Ligand sorption to cement and other mineral phases

A key factor influencing the increased transport of radionuclides from the GDF due to complexation with the ligand is the amount of free ligand available in the GDF in the first place. In the case of GA, this is primarily dependent on the amount added in the cement used for the construction of the GDF and backfill material. However, since ISA is the

product of cellulose hydrolysis by alkali, the amount of free ISA present in the GDF is dependent on a number of factors, including the amount of cellulose added, the water flow rate, the rate of cellulose hydrolysis, and the cations present in the GDF at the time of ISA production (as mentioned earlier, the presence of Ca^{2+} enhances ISA production from cellulose hydrolysis but also forms sparingly soluble salts with α-ISA). Another factor that must be considered is the interaction of the ligand with solid phases that will form in the GDF and the chemical degradation of the ligand under alkaline conditions. Batch sorption studies on hardened cement paste at pH 13.4 showed that ISA (van Loon *et al.*, 1997; Pointeau *et al.*, 2006) and GA (Pointeau *et al.*, 2006) are stable for prolonged periods in cement water and under conditions expected in the GDF. They also showed that both ligands strongly sorb to calcium-silicate-hydrate phases (although the mechanism of interaction is not yet fully understood), which decreases the concentration of soluble ligand until saturation of the solid phase is reached (van Loon *et al.*, 1997), or the formation of calcite deposits occurs (Pointeau *et al.*, 2006). Indeed the interaction of ISA and GA with calcite had no effect on the solubility of calcite at a pH value of 13.3, and suggested that the ligands do not sorb to this mineral phase (Tits *et al.*, 2005). This was also the case when hematite was used as the solid phase (Baston *et al.*, 2012).

2.6.4 Ligand Effects on Radionuclide Retention by Solid Phases

As mentioned earlier, cementitious material will dominate the GDF, in particular the ILW, and one of the most studied solid phases for a cement-based repository is hardened cement paste. Studies showed that increasing the concentration of ISA to above 1 mM in a solution in contact with hardened cement paste caused a significant increase in the concentration of Ca in solution at pH 13.3, due to the dissolution of portlandite (Wieland *et al.*, 2002). A lower concentration of ISA (0.1 mM) caused a significant decrease in the concentration of sorbed Th(IV) at pH 13.3, due to the formation of a $Th(ISA)_2Ca$ complex (Wieland *et al.*, 2002; Vercammen *et al.*, 2001).

Calcite ($CaCO_3$) may dominate the chemically disturbed zone surrounding the GDF (if the GDF is built in calcite containing geological formations) and the GDF itself, the latter being due to the carbonation of portlandite by carbonate containing groundwater (Dow and Glasser, 2003). Batch sorption experiments showed that although Eu(III) and Am(III) sorb to calcite, this sorption significantly decreases in the presence of 0.01 mM of ISA and 0.1 μM of GA at pH 13.3 (Tits *et al.*, 2005). Similarly, Th(IV) sorption to calcite was significantly reduced in the presence of 0.05 mM ISA and 1 μM of GA. Note that lower concentrations of ISA are required for the desorption of Th(IV) from calcite than from

portlandite, which is mainly due to the surface interaction of Th(IV) with the solid phase material.

It is important to note that an estimate of ISA concentration in the GDF is about 44 mM (van Loon, Glaus and Vercammen, 1999), although as mentioned earlier, this will greatly depend on the groundwater flow rate, the amount of cellulose loaded in the GDF, the rate of the chemical degradation reactions, the stability of ISA and its sorption to solid phases and the formation of sparingly soluble salts with cations.

2.6.5 Radionuclide Transport from the GDF

The rate of radionuclide transport from the GDF is dependent on a number of factors, some of which are still not established yet. These include (i) the geology and hydrogeology of the host site for the GDF, which define the rate of water movement through the facility; (ii) the rate of cellulose hydrolysis (which depends primarily on the nature of the cellulosic material), ISA production, and the release of other ligands (for example GA, EDTA and NTA) from the wasteforms (Glaus and van Loon, 2008; Haas *et al.*, 1967; Keith-Roach, 2008); (iii) the stability and solubility of the ligand-radionuclide complexes, and the affinity of the ligand to radionuclides in the presence of competing cations like Ca^{2+}, which will be present in high concentrations (approximately 20 mM) due to the extensive use of cement (Gaona *et al.*, 2008; Berner, 1992); (iv) the sorption of the ligand and the ligand-radionuclide complex to the solid phases already present or produced over time in the GDF (Tits *et al.*, 2005; Wieland *et al.*, 2002; Vercammen *et al.*, 2001; Moyce *et al.*, 2014). Another factor that is overlooked in studies on radionuclide transport from the GDF is the role of microorganisms, probably due to the fact that the GDF has been considered to be an environment that is too harsh to support microbial life. In this respect, extremophilic microorganisms that could grow under GDF-similar conditions, may play a significant role in reducing radionuclide transport to the biosphere through (i) the direct or indirect bioreduction of radionuclides, (ii) biomineralisation into insoluble solid phases, or (iii) bioaccumulation into or biosorption onto the surface of microorganisms (Newsome *et al.*, 2014). As mentioned earlier, organic ligands like ISA, GA, EDTA, and NTA can increase radionuclide mobility, and therefore it is safe to assume that the biodegradation of these organic ligands (or their precursor polymers) would favour the immobilisation of radionuclides in the GDF or surrounding chemically disturbed zone.

2.6.6 Bacterial Degradation of ISA

Information on the degradation of ISA by bacteria is somewhat lacking. Although a number of bacteria have been identified that are able to degrade GA (Janto *et al.*, 2011), only two bacterial strains have been isolated that are able to degrade ISA, both of which were aerobic Gram-negative bacteria. The first isolate was an aerobic *Ancylobacter aquaticus* species that was isolated from a pulp mill effluent pond, and was able to grow in media containing ISA (at pH values between 7.2 and 9.5), and growth was enhanced by the addition of vitamins, peptone and phosphate (Strand *et al.*, 1984). Two other bacterial species that can also utilise ISA under aerobic conditions were isolated on media at pH values between 5.1 and 7.2 (Bailey, 1986). More recent work has shown that biogeochemical redox progression from aerobic to Fe(III) reduction is possible when a sediment is incubated in the presence of ISA, although the degradation of ISA was not studied under these conditions (Maset *et al.*, 2006).

At this point, there is much uncertainty on whether microorganisms are able to degrade ISA under repository conditions, and whether this degradation will have significant impact in the geosphere surrounding a repository.

2.7 Aims

Given the uncertainty around the ability of bacteria to survive under GDF conditions and their ability to degrade ISA and other cellulose degradation products, a number of aims have been set at the start of this project to address these matters and these are presented in four articles presented in this work.

The first aim was to understand how will bacteria, found in sediment samples from a lime-kiln effluent in Harpur Hill, Buxton, UK, perform in hyperalkaline microcosms (containing $Ca(OH)_2$ at saturation) containing different cellulosic materials (tissue and cotton) as the sole carbon source, over long incubation periods under anaerobic conditions (Chapter 4). An additional aim here was to identify bacteria that survived under these GDF simulated conditions, and to understand how they impact on the added cellulosic materials (Chapter 4).

The second aim was to identify and potentially isolate bacteria that can degrade ISA under anaerobic conditions at high pH (Chapter 5). The isolated bacterium was identified to be a novel species belonging to the *Bacillus* genus (Chapter 6), and was characterised using microbiological, microscopic and molecular approaches, and was found to degrade gluconate (another organic complexant that is of concern to the GDF).

Given this new information, an additional aim was to test the ability of this bacterium to degrade both organic complexants (ISA and GA) under the same biogeochemical conditions at high pH in the presence of various electron acceptors, including U(VI) (Chapter 7). Such redox transformations coupled to biocomplexant degradation have the potential to impact significantly on uranium speciation and solubility.

2.8 References

Albrecht A, Bertron A, Libert M. (2013). Microbial catalysis of redox reactions in concrete cells of nuclear waste repositories: A review and introduction. In: *Cement-Based Materials for Nuclear Waste Storage*, Bart, F, Cau-di-Coumes, C, Frizon, F, & Lorente, S (eds), Springer New York: New York, pp. 147–159.

Alexander WR, Milodowski AE, Pitty AF, Hardie SML, Kemp SJ, Korkeakoski P, *et al.* (2012). Reaction of bentonite in low-alkali cement leachates: an overview of the Cyprus Natural Analogue Project (CNAP). *Mineral Mag* **76**:3019–3022.

Askarieh M, Chambers A, Daniel F, FitzGerald P, Holtom G, Pilkington N, *et al.* (2000). The chemical and microbial degradation of cellulose in the near field of a repository for radioactive wastes. *Waste Manag* **20**:93–106.

Bailey M. (1986). Utilization of glucoisosaccharinic acid by a bacterial isolate unable to metabolize glucose. *Appl Microbiol Biotechnol* **1206**:493–498.

Baston GMN, Cowper MM, Heath TG, Marshall TA, Swanton SW. (2012). The effect of cellulose degradation products on thorium sorption onto hematite: Studies of a model ternary system. *Mineral Mag* **76**:3381–3390.

Battista JR. (1997). Against all odds: The survival strategies of *Deinococcus radiodurans*. *Annu Rev Microbiol* **51**:203–224.

Bechtold T, Burtscher E, Turcanu A. (2002). Ca^{2+}–Fe^{3+}–D-gluconate-complexes in alkaline solution. Complex stabilities and electrochemical properties. *J Chem Soc Dalt Trans* 2683–2688.

Beguin P, Aubert JP. (1994). The biological degradation of cellulose. *FEMS Microbiol Rev* **13**:25–58.

Berner UR. (1992). Evolution of pore water chemistry during degradation of cement in a radioactive waste repository environment. *Waste Manag* **12**:201–219.

Blouin FA, Arthur JC. (1958). The effects of gamma radiation on cotton Part I: Some of the properties of purified cotton irradiated in oxygen and nitrogen atmospheres. *Text Res J* **28**:198–204.

Bots P, Morris K, Hibberd R, Law GTW, Mosselmans JFW, Brown AP, *et al*. (2014). Formation of stable uranium (VI) colloidal nanoparticles in conditions relevant to radioactive waste disposal. *Langmuir* **30**: 14396–14405.

Bouchard J, Méthot M, Jordan B. (2006). The effects of ionizing radiation on the cellulose of woodfree paper. *Cellulose* **13**:601–610.

Brown PL, Allard S, Ekberg C. (2010). Dissociation constants of α-D-isosaccharinic acid: 'Composite' and 'Intrinsic' values. *J Chem Eng* **55**:5207–5213.

Chicote E, Moreno DA, Garcia AM, Sarro MI, Lorenzo PI, Montero F. (2004). Biofouling on the walls of a spent nuclear fuel pool with radioactive ultrapure water. *Biofouling* **20**:35–42.

Cho H, Rai D, Hess NJ, Xia Y, Rao L. (2003). Acidity and structure of isosaccharinate in aqueous solution: A nuclear magnetic resonance study. *J Solution Chem* **32**:691–702.

DECC. (2014). Implementing geological disposal. Department of Energy & Climate Change. URN 14D/235 Whitehall Place, London, UK.

Dow C, Glasser FP. (2003). Calcium carbonate efflorescence on Portland cement and building materials. *Cem Concr Res* **33**:147–154.

Duro L, Domènech C, Grivé M, Roman-Ross G, Bruno J, Källström K. (2014). Assessment of the evolution of the redox conditions in a low and intermediate level nuclear waste repository (SFR1, Sweden). *Appl Geochemistry* **49**:192–205.

Falkowski PG, Fenchel T, Delong EF. (2008). The microbial engines that drive Earth 's biogeochemical cycles. *Science* **320**:1034–1039.

Fry JC, Parkes RJ, Cragg BA, Weightman AJ, Webster G. (2008). Prokaryotic biodiversity and activity in the deep subseafloor biosphere. *FEMS Microbiol Ecol* **66**:181–196.

Gaona X, Montoya V, Colàs E, Grivé M, Duro L. (2008). Review of the complexation of tetravalent actinides by ISA and gluconate under alkaline to hyperalkaline conditions. *J Contam Hydrol* **102**:217–27.

Ghosal D, Omelchenko M, Gaidamakova E, Matrosova V, Vasilenko A, Venkateswaran A, *et al.* (2005). How radiation kills cells: Survival of *Deinococcus radiodurans* and *Shewanella oneidensis* under oxidative stress. *FEMS Microbiol Rev* **29**:361–375.

Glaus MA, van Loon LR, Achatz S, Chodura A, Fischer K. (1999). Degradation of cellulosic materials under the alkaline conditions of a cementitious repository for low and intermediate level radioactive waste. Part I: Identification of degradation products. *Anal Chim Acta* **398**:111–122.

Glaus MA, van Loon LR. (2008). Degradation of cellulose under alkaline conditions: New insights from a 12 years degradation study. *Environ Sci Technol* **42**:2906–2911.

Glegg RE, Kertesz ZI. (1957). Effect of gamma-radiation on cellulose. *J Polym Sci* **26**:289–297.

Gunn J, Bottrell SH, Lowe DJ, Worthington SRH. (2006). Deep groundwater flow and geochemical processes in limestone aquifers: Evidence from thermal waters in Derbyshire, England, UK. *Hydrogeol J* **14**:868–881.

Haas DW, Hrutfiord BF, Sarkanen KV. (1967). Kinetic study on the alkaline degradation of cotton hydrocellulose. *J Appl Polym Sci* **11**:587–600.

Humphreys P, McGarry R, Hoffmann A, Binks P. (1997). DRINK: A biogeochemical source term model for low level radioactive waste disposal site. *FEMS Microbiol Rev* **20**:557–571.

Isbell HS. (1944). Interaction of some reactions in the carbohydrate field in terms of consecutive electron displacement. *J Res Natl Bur Stand (1934)* **32**:45–59.

Janto B, Ahmed A, Ito M, Liu J, Hicks DB, Pagni S, *et al.* (2011). Genome of alkaliphilic *Bacillus pseudofirmus* OF4 reveals adaptations that support the ability to grow in an external pH range from 7.5 to 11.4. *Environ Microbiol* **13**:3289–309.

Keith-Roach MJ. (2008). The speciation, stability, solubility and biodegradation of organic co-contaminant radionuclide complexes: A review. *Sci Total Environ* **396**:1–11.

Khoury HN, Salameh E, Clark ID, Fritz P, Bajjali W, Milodowski AE, *et al.* (1992). A natural analogue of high pH cement pore waters from the Maqarin area of northern Jordan. I: introduction to the site. *J Geochemical Explor* **46**:117–132.

Knill CJ, Kennedy JF. (2003). Degradation of cellulose under alkaline conditions. *Carbohydr Polym* **51**:281–300.

Lawton EJ, Bellamy WD, Hungate RE, Bryant MP, Hall E. (1951). Some effects of high velocity electrons on wood. *Science* **113**:380–382.

Leschine SB. (1995). Cellulose degradation in anaerobic environments. *Annu Rev Microbiol* **49**:399–426.

Lynd LR, Weimer PJ, van Zyl WH, Pretorius IS. (2002). Microbial cellulose utilization: Fundamentals and biotechnology. *Microbiol Mol Biol Rev* **66**:506–577.

Madsen EL. (2011). Microorganisms and their roles in fundamental biogeochemical cycles. *Curr Opin Biotechnol* **22**:456–464.

Makarova K, Aravind L, Wolf Y, Tatusov R, Minton K, Koonin E, *et al.* (2001). Genome of the extremely radiation-resistant bacterium *Deinococcus radiodurans* viewed from the perspective of comparative genomics. *Microbiol Mol Biol Rev* **65**:44–79.

Maset ER, Sidhu SH, Fisher A, Heydon A, Worsfold PJ, Cartwright AJ, *et al.* (2006). Effect of organic co-contaminants on technetium and rhenium speciation and solubility under reducing conditions. *Environ Sci Technol* **40**:5472–5477.

Mosier NS, Hall P, Ladisch CM, Ladisch MR. (1999). Reaction kinetics, molecular action, and mechanisms of cellulolytic proteins. *Adv Biochem Eng Biotechnol* **65**:23–40.

Moyce EBA, Rochelle C, Morris K, Milodowski AE, Chen X, Thornton S, *et al.* (2014). Rock alteration in alkaline cement waters over 15 years and its relevance to the geological disposal of nuclear waste. *Appl Geochemistry* **50**:91–105.

Nagi AD, Regan L. (1997). An inverse correlation between loop length and stability in a four-helix-bundle protein. *Fold Des* **2**:67–75.

NDA. (2010a). Geological disposal: An overview of the generic disposal system safety case. Nuclear Decommissioning Authority. NDA/RWMD/010 Moor Raw, Cumbria, UK.

NDA. (2010b). Geological disposal: Radioactive wastes and assessment of the disposability of waste packages. Nuclear Decommissioning Authority. NDA/RWMD/039 Moor Raw, Cumbria, UK.

NDA. (2014). Radioactive wastes in the UK : A summary of the 2013 inventory. Nuclear Decommissioning Authority. NDA/ST/STY (14) 0006, Moor Raw, Cumbria, UK.

NDA, DEFRA. (2007). UK radioactive waste inventory. Nuclear Decommissioning Authority. Defra/RAS/08.002 NDA/RWMD/004, Moor Raw, Cumbria, UK.

Newsome L, Morris K, Lloyd JR. (2014). The biogeochemistry and bioremediation of uranium and other priority radionuclides. *Chem Geol* **363**:164–184.

Pavasars I, Hagberg J, Borén H, Allard B. (2003). Alkaline degradation of cellulose: Mechanisms and kinetics. *J Polym Environ* **11**:39–47.

Pedersen K. (1999). Evidence for a hydrogen-driven, intra-terrestrial biosphere in deep granitic rock aquifers. In:*Proceedings of the 8th International Symposium on Microbial Ecology*, Bell, C, Brylinsky, M, & Johnson-Green, P (eds), Halifax, Canada.

Pedersen K. (2000). Exploration of deep intraterrestrial microbial life: Current perspectives. *FEMS Microbiol Lett* **185**:9–16.

Pedersen K, Arlinger J, Ekendahl S, Hallbeck L. (1996). 16S rRNA gene diversity of attached and unattached bacteria in boreholes along the access tunnel to the Aspo hard rock laboratory, Sweden. *FEMS Microbiol Ecol* **19**:249–262.

Pikuta EV, Hoover RB, Bej AK, Marsic D, Detkova EN, Whitman WB, *et al.* (2003). *Tindallia californiensis* sp. nov., a new anaerobic, haloalkaliphilic, spore-forming acetogen isolated from Mono Lake in California. *Extremophiles* **7**:327–334.

Pikuta EV, Hoover RB, Tang J. (2007). Microbial extremophiles at the limits of life. *Crit Rev Microbiol* **33**:183–209.

Pointeau I, Hainos D, Coreau N, Reiller P. (2006). Effect of organics on selenite uptake by cementitious materials. *Waste Manag* **26**:733–740.

Rafrafi Y, Ranaivomanana H, Bertron A, Albrecht A, Erable B. (2015). Surface and bacterial reduction of nitrate at alkaline pH: Conditions comparable to a nuclear waste repository. *Int Biodeterior Biodegradation* **101**:12–22.

Rai D, Hess NJ, Xia Y, Rao L, Cho HM, Moore RC, *et al.* (2003). Comprehensive thermodynamic model applicable to highly acidic to basic conditions for isosaccharinate reactions with Ca(II) and Np(IV). *J Solution Chem* **32**:665–689.

Rai D, Rao L, Xia Y. (1998). Solubility of crystalline calcium isosaccharinate. *J Solution Chem* **27**:1109–1122.

Rizoulis A, Steele HM, Morris K, Lloyd JR. (2012). The potential impact of anaerobic microbial metabolism during the geological disposal of intermediate-level waste. *Mineral Mag* **76**:3261–3270.

Samborska K, Halas S, Bottrell SH. (2013). Sources and impact of sulphate on groundwaters of Triassic carbonate aquifers, Upper Silesia, Poland. *J Hydrol* **486**:136–150.

Shaw PB, Robinson GF, Rice CR, Humphreys PN, Laws AP. (2012). A robust method for the synthesis and isolation of β-gluco-isosaccharinic acid ((2R,4S)-2,4,5-trihydroxy-2-(hydroxymethyl)pentanoic acid) from cellulose and measurement of its aqueous pKa. *Carbohydr Res* **349**:6–11.

Smith KF, Bryan ND, Swinburne AN, Bots P, Shaw S, Natrajan LS, *et al*. (2015). U(VI) bahaviour in hyperalkaline calcite systems. *Geochim Cosmochim Ac* **148**:343–359.

Strand S, Dykes J, Chiang V. (1984). Aerobic microbial degradation of glucoisosaccharinic acid. *Appl Environ Microbiol* **47**:268–271.

Sydow U, Wohland P, Wolke I, Cypionka H. (2002). Bioenergetics of the alkaliphilic sulfate-reducing bacterium *Desulfonatronovibrio hydrogenovorans*. *Microbiology* **148**:853–860.

Thorne MC. (2005). Development of Increased Understanding of Potential Radiological Impacts of Radioactive Gases from a Deep Geological Repository: Form of Release of C-14. Report No. MTA/P0011b/2005-4: Issue 2.

Tits J, Wieland E, Bradbury MH. (2005). The effect of isosaccharinic acid and gluconic acid on the retention of Eu(III), Am(III) and Th(IV) by calcite. *Appl Geochemistry* **20**:2082–2096.

Van Loon LR, Glaus MA. (1998). Experimental and theoretical studies on alkaline degradation of cellulose and its impact on the sorption of radionuclides. National Cooperative for the Disposal of Radioactive Waste, NAGRA NTB 97-04, Hardstrasse 73, CH-5430 Wettingen, Switzerland.

Van Loon LR, Glaus MA. (1997). Review of the kinetics of alkaline degradation of cellulose in view of its relevance for safety assessment of radioactive waste repositories. *J Environ Polym Degrad* **5**:97–109.

Van Loon LR, Glaus MA, Laube A, Stallone S. (1999). Degradation of cellulosic materials under the alkaline conditions of a cementitious repository for low- and intermediate-level radioactive waste. II. Degradation kinetics. *J Polym Environ* **7**:41–51.

Van Loon LR, Glaus MA, Stallone S, Laube A. (1997). Sorption of isosaccharinic acid, a cellulose degradation product, on cement. *Environ Sci Technol* **31**:1243–1245.

Van Loon LR, Glaus MA, Vercammen K. (1999). Solubility products of calcium isosaccharinate and calcium gluconate. *Acta Chem Scand* **53**:235–240.

Van Loon LR, Glaus MA, Vercammen K. (2004). Stability of the ion pair between Ca^{2+} and 2-(hydroxymethyl)-3-deoxy-D-erythro-pentonate (α-isosaccharinate). *J Solution Chem* **33**:1573–1583.

Vercammen K, Glaus MA, van Loon LR. (1999). Complexation of calcium by α-isosaccharinic acid under alkaline conditions. *Acta Chem Scand* **53**:241–246.

Vercammen K, Glaus MA, van Loon LR. (2001). Complexation of Th(IV) and Eu(III) by α-isosaccharinic acid under alkaline conditions. *Radiochim Acta* **89**:393–401.

Warwick P, Evans N, Hall T, Vines S. (2003). Complexation of Ni(II) by α-isosaccharinic acid and gluconic acid from pH 7 to pH 13. *Radiochim Acta* **91**:233–240.

Warwick P, Evans N, Hall T, Vines S. (2004). Stability constants of uranium(IV)-α-isosaccharinic acid and gluconic acid complexes. *Radiochim Acta* **92**:897–902.

Wieland E, Tits J, Dobler JP, Spieler P. (2002). The effect of α-isosaccharinic acid on the stability of and Th(IV) uptake by hardened cement paste. *Radiochim Acta* **90**:683–688.

Williamson AJ, Morris K, Shaw S, Byrne JM, Boothman C, Lloyd JR. (2013). Microbial reduction of Fe(III) under alkaline conditions relevant to geological disposal. *Appl Environ Microbiol* **79**:3320–3326.

Yano JK, Poulos TL. (2003). New understandings of thermostable and peizostable enzymes. *Curr Opin Biotechnol* **14**:360–365.

Zavarzina DG, Tourova TP, Kolganova TV, Boulygina ES, Zhilina TN. (2009). Description of *Anaerobacillus alkalilacustre* gen. nov., sp. nov.—Strictly anaerobic diazotrophic *Bacillus* isolated from soda lake and transfer of *Bacillus arseniciselenatis*, *Bacillus macyae*, and *Bacillus alkalidiazotrophicus* to *Anaerobacillus* as the new combinations *A. arseniciselenatis* comb. nov., *A. macyae* comb. nov., and *A. alkalidiazotrophicus* comb. nov. *Microbiology* **78**:723–731.

Zhang Z, Gibson P, Clark SB, Tian G, Zanonato PL, Rao L. (2007). Lactonization and protonation of gluconic acid: A thermodynamic and kinetic study by potentiometry, NMR and ESI-MS. *J Solution Chem* **36**:1187–1200.

Zhilina TN, Kevbrin VV, Tourova TP, Lysenko AM, Kostrikina NA, Zavarzin GA. (2005). *Clostridium alkalicellum* sp. nov., an obligately alkaliphilic cellulolytic bacterium from a soda lake in the Baikal region. *Microbiology* **74**:557–566.

Zhilina TN, Zavarzin GA, Rainey FA, Pikuta EN, Osipov GA, Kostrikina NA. (1997). *Desulfonatronovibrio hydrogenovorans* gen. nov., sp. nov., an alkaliphilic, sulfate-reducing bacterium. *Int J Syst Bacteriol* **47**:144–149.

Zhilina TN, Zavarzin GA. (1994). Alkaliphilic anaerobic community at pH 10. *Curr Microbiol* **29**:109–112.

Zhilina TN, Zavarzin GA, Rainey F, Kevbrin VV, Kostrikina NA, Lysenko AM. (1996). *Spirochaeta alkalica* sp. nov., *Spirochaeta africana* sp. nov., and *Spirochaeta asiatica* sp. nov., alkaliphilic anaerobes from the Continental Soda Lakes in Central Asia and the East African Rift. *Int J Syst Bacteriol* **46**:305–312.

Zhilina TN, Zavarzina DG, Kuever J, Lysenko AM, Zavarzin GA. (2005). *Desulfonatronum cooperativum* sp. nov., a novel hydrogenotrophic, alkaliphilic, sulfate-reducing bacterium, from a syntrophic culture growing on acetate. *Int J Syst Evol Microbiol* **55**:1001–1006.

Zvereva EA, Fedorova TV, Kevbrin VV, Zhilina TN, Rabinovich ML. (2006). Cellulase activity of a haloalkaliphilic anaerobic bacterium, strain Z-7026. *Extremophiles* **10**:53–60.

Chapter 3

Research Methods

3 Research Methods

This chapter gives descriptions of the main analytical and molecular techniques utilised throughout this research project, and the reasons for their use.

3.1 Bacterial Growth Medium

Bacterial enrichment cultures were prepared in minimal medium (modified from ATCC 1768 *Geobacter metallireducens* Medium (Lovley *et al.*, 1993; Lovley and Phillips, 1988)), supplemented with various organic molecules as electron donors (in particular isosaccharinic acid (ISA) or gluconic acid (GA)) and various inorganic electron acceptors (NO_3^-, Fe(III)-oxyhydroxide and SO_4^{2-}). The medium composition is given in Table 3.1. The use of a highly selective minimal medium was essential in this study since the aim was to enrich for bacteria that can specifically degrade ISA. If a rich medium was used, bacteria may have been selected, which could have grown on other carbon sources in the medium, and they may not have been ISA degraders per se. Also this medium contains an inorganic ($NaHCO_3$) pH buffer, which has a large buffering range and does not have a direct effect on bacterial growth.

Table 3.1: Minimal medium composition

Media Composition in 1 L dd H_2O		**Mineral Mix Composition in 1 L dd H_2O**		**Vitamin Mix Composition in 1 L dd H_2O**	
Chemical	**Amount**	**Chemical**	**Weight (g)**	**Chemical**	**Weight (mg)**
$NaHCO_3$	2.5 g	Nitrilotriacetic acid	1.5	Biotin	2
NH_4Cl	0.25 g	$MgSO_4$	3	Folic acid	2
$NaH_2PO_4.H_2O$	0.6 g	$MnSO_4.H_2O$	0.5	Pyridoxine HCl	10
KCl	0.1 g	NaCl	1	Riboflavin	5
Vitamin mix	10 ml	$FeSO_4.7H_2O$	0.1	Thiamine	5
Mineral mix	10 ml	$CaCl_2.2H_2O$	0.1	Nicotinic acid	5
		$CoCl_2.6H_2O$	0.1	Pantothenic acid	5
		$ZnCl_2$	0.13	Vitamin B-12	0.1
		$CuSO_4.5H_2O$	0.01	p-aminobenzoic acid	5
		$AlK(SO_4)_2.12H_2O$	0.01	Thioctic acid	5
		H_3BO_3	0.01		
		Na_2MoO_4	0.025		
		$NiCl_2.6H_2O$	0.024		
		$Na_2WO_4.2H_2O$	0.025		

3.2 α-ISA Preparation

The Ca salt of α-ISA was prepared (Vercammen *et al.*, 1999) and used as an electron and carbon donor in enrichment cultures and for ion chromatography analysis in Chapters 4, 5 and 6. Briefly, 500 ml of argon flushed deionized H_2O was mixed with 50 g of α-lactose monohydrate and 13.6 g of $Ca(OH)_2$ and left to react for 3 days under anaerobic conditions at room temperature to produce ISA and other cellulose degradation products. The mixture

was then boiled for 6 h, keeping the volume constant by adding H_2O. The solution was then filtered while hot through a Whatman number one filter paper in a Büchner funnel to remove unreacted lactose and $Ca(OH)_2$, while the ISA and other small chain organic acids passed through with the filtrate. The volume of the filtrate was then reduced to about 150 ml by boiling in order to concentrate the organic molecules. The remaining solution was stored overnight at 4°C and formed a white precipitate that contained Ca(α-ISA)$_2$ and other degradation products. This precipitate was filtered and then washed sequentially with water, ethanol and acetone and dried overnight at 50°C. The dry precipitate was re-dissolved at a ratio of 1.2 g in 100 ml of deionized H_2O by boiling. While still hot, the solution was filtered to remove any solid contaminants, and the volume of the filtrate was then reduced to about 10 ml by boiling. The white precipitate that formed, which contained pure Ca(α-ISA)$_2$, was washed sequentially with water, ethanol and acetone and then dried on a watchglass overnight at 50°C. The α-ISA yield from this process was about 15% of the starting weight of α-lactose monohydrate, and produced a single sharp peak by ion exchange chromatography. The Na salt of α-ISA that was used in Chapter 7 was prepared by contacting Ca(α-ISA)$_2$ with an equimolar concentration of $NaHCO_3$ and 3 M NaOH (Rai *et al.*, 2003; Vercammen *et al.*, 1999). The precipitated $Ca(OH)_2$ and $CaCO_3$ were centrifuged at 4,000 *g* for 10 min and the supernatant, which contains Na-ISA was recovered.

3.3 Ion Exchange Chromatography

Ion exchange chromatography is a technique used in analytical chemistry for the separation of ionic and polar molecules based on their ionic affinities to a charged column. The interaction between the analytes (the ions in the sample being measured), the solid or stationary phase (a column filled with a resin or gel coated with charged functional groups), and the eluent or mobile phase (an aqueous solution with a known ionic strength and that shows varying affinity to the analytes under different conditions) is the main driving force for the separation by ion exchange chromatography. The analytes (for example anions) are carried with the eluent into the column where they are retained by the stationary phase (which for example contains positively charged functional groups). Elution of the bound analytes can be achieved typically by forming a gradient of increasing salt content (which increases the concentration of similarly charged species) or decreasing pH (which changes the charge of the species through protonation) of the eluent. The speed at which an ion passes through the column depends mainly on its charge, which is directly correlated to its interaction with the solid phase functional groups (although other factors

like size may also affect the retention time). The eluent fractions can be collected and measured by various methods, however, conductivity detection is the most commonly used mode of detection. These fractions can be analysed against matched matrix standards to determine the nature and concentrations of the analytes.

Since the first use of ion exchange chromatography, various modifications have been introduced, with the most important being the use of high-pressure systems, which greatly reduced the sample volume (and therefore the waste generated) and the time required for the run. These modifications also helped in automation of the workflow, for example the use of autosamplers (to ensure proper sample injection), injection loops (provide consistent sample volume between injections), guard columns (to protect the separation column from particulates and biomass), suppressors (remove background conductivity from the eluent) and continuous flow conductivity detectors (produce peaks that indicate concentration as the eluent passes through), ensured a continuous workflow without the need for fractionation and separate measurements.

In all the research chapters, ion chromatography was used according to the following procedure. The frozen samples were thawed at room temperature, vortexed for homogenisation and then centrifuged at 13,000 *g* for 5 min at room temperature to remove bacteria and any solid material. These samples were diluted 100 times and then analysed by ion-exchange chromatography using a Dionex ICS5000 Dual Channel Ion Chromatograph with a conductivity detector (Thermo Fisher Scientific, Waltham, MA, USA). The samples were put in 2 ml glass vials with presplit septa and cooled to 15^{o}C, and then 0.4 ml was injected into the chromatograph through a Dionex AS-AP autosampler. Molecule separation was achieved by passing the samples through a 250 x 0.4 mm Dionex AS11-HC capillary column with a 4 mm pore size, operating at 30^{o}C, with a typical operating pressure of 3,400 psi and a flow rate of 0.015 ml/min. The mobile phase used was a KOH solution, prepared in high-purity water, electronically injected to produce a gradient from 1 to 60 mM over a 38 min run time, followed by a 10 min re-equilibrium before the next injection. The chromatograph was calibrated at 4 points ranging from 0.5 to 30 mg/l for nitrate, nitrite and sulphate, 0.5 to 10 mg/l for acetate, formate, lactate, propionate and butyrate and 0.01 to 0.1 mM for ISA and GA.

3.4 Ferrozine Assay for Fe(II) Determination

The ferrozine assay is a colorimetric method used for the quantification of aqueous ferrous iron using spectrophotometry (Stookey, 1970). This method relies on the formation of a magenta coloured complex formed between 3-(2-pyridyl)-5,6-bis(4-phenylsulfonic acid)-

1,2,4-triazine and specifically ferrous iron. The stable complex is formed over a large pH range (pH 4 and 10), is very soluble in water and shows a sharp peak with maximum absorbance at 562 nm (Stookey, 1970).

The microbial reduction of Fe(III) to Fe(II) in enrichment cultures was measured in this work by digesting 20 μl of sample in 980 μl of 0.5 M HCl for 1 hour (Lovley and Phillips, 1986, 1987). The digest was centrifuged at 14,000 *g* for 3 minutes before 20 μl were reacted with 980 μl of ferrozine solution (1 g/L ferrozine, buffered in 11.9 g/L of HEPES at pH 7) in a 1.5 ml cuvette and the absorbance measured after 1 minute of reaction. Total Fe was measured by digesting 40 μl of sample in 1880 μl of 0.5 N HCl in the presence of 80 μl of hydroxylamine hydrochloride (a reducing agent that reduces all Fe(III) to Fe(II)) for 24 hours, and then following the ferrozine assay procedure. Sample absorbance was compared to the absorbance of ferrous sulphate standards that were prepared following the same procedure as the samples to determine Fe(II) and total Fe concentrations.

3.5 Bromo-PADAP Method for U(VI) Determination

The compound bromo-PADAP [IUPAC name: 2-(5-bromo-2-pyridylazo)-5-diethylaminophenol] has been used for the spectrophotometric determination of U(VI) concentrations in solution (Johnson and Florence, 1971). This compound forms a rapidly decomposing, red-violet complex with U(VI) at pH 7.3, which is stabilised by the presence of fluoride that also acts as an auxiliary ligand in the complex (Johnson and Florence, 1975). Note that this complex shows maximum absorbance at 578 nm, and in the absence of U(VI) gives a yellow coloured solution. The addition of trans-1,2-cyclohexanediamine-N,N,N',N'-tetraacetic acid (CyDTA) and sulphosalicilic acid to the reaction mixture greatly reduces interferences from other metals (Johnson and Florence, 1975). Furthermore, these compounds, along with triethanolamine help buffer the pH at about 7.3, which shows highest absorbance of the complex. This method is accurate for the determination of 0.8 to 50 μg of U(VI) in solution.

This procedure was used in Chapter 7 for the determination of U(VI) in solution, according to the following procedure. All stock solutions were prepared in a chemical fume cupboard. The buffer solution was prepared by resuspending 14.9 g of triethanol amine in 80 ml of DI H_2O and adjusting the pH to 7.8 with perchloric acid, then adjusting the volume to 100 ml, using DI H_2O. The complexing solution was prepared by resuspending 2.63 g of CyDTA, 0.5 g of NaF and 6.5 g of sulphosalicilic acid in 80 ml of DI H_2O and adjusting the pH to 7.8 using 10 N NaOH, then adjusting the volume to 100 ml, using DI

H_2O. The colouring solution was prepared by resuspending 0.05 g of Bromo-PADAP in 100 ml of absolute ethanol, and storing it at 4^oC. To measure the concentration of U(VI) in solution, the samples (containing 100 ppm of U(VI)) were centrifuged for 3 min at 13,000 *g*, and 20 μl of the supernatant were diluted in 340 μl of DI H_2O, and were transferred into a cuvette where 80 μl of complexing solution, 80 μl of buffer solution, 400 μl of absolute ethanol and 80 μl of colouring solution were added sequentially. The solution was homogenised by pipetting several times and was left for 40 min to react. Calibration standards at 5 points, covering the range 1 to 25 ppm were prepared following the same procedure. The absorbance of the samples was measured at 578 nm, and was compared to the absorbance of the standards at the same wavelength.

3.6 Polymerase Chain Reaction

Polymerase chain reaction (PCR) is a technique routinely used in a molecular biology laboratory to amplify a specific stretch of DNA, producing hundreds of billions of copies, thereby enabling the analysis of a specific DNA sequence that would have been too dilute for visualisation prior to amplification (Saiki *et al.*, 1988). This technique relies on thermal cycling (repeated heating and cooling of the reaction contents) and utilises a DNA polymerase enzyme to amplify a specific sequence of template DNA (Saiki *et al.*, 1988). The DNA to be amplified is added to the reaction mixture as a double stranded molecule, and therefore the first step in a PCR is the denaturation of the double stranded DNA to two single stranded molecules (a process termed DNA melting). This is attained by increasing the temperature of the reaction to 94^oC, thereby breaking the hydrogen bonds between complementary nucleotides on the opposite strands of the double stranded DNA molecule. Most proteins are known to denature (and therefore lose their functionality) at this high temperature, however, the DNA polymerase enzyme that was isolated from the thermophilic bacterium *Thermus aquaticus* can withstand these elevated temperatures (Chien *et al.*, 1976), and therefore this enzyme is used in PCR. The DNA polymerase cannot bind directly to the single stranded DNA template to start amplification, but requires a double stranded DNA sequence. For this reason, a small stretch of DNA (about 20 nucleotides that is called a primer sequence) that is complementary to the template DNA is also added to the reaction mixture. In general, two primer sequences are added, a forward primer that binds to the 3' end of the forward template DNA, and a reverse primer that binds to the 3' end of the complementary DNA template (Figure 3.1). Annealing of these primer sequences to the single stranded DNA template at about 60^oC enables the docking of the DNA polymerase to this short double stranded DNA sequence to start the

amplification process. Amplification occurs at 72^{o}C (the optimal working temperature of the *T. aquaticus* DNA polymerase), and in this process the DNA polymerase breaks a single deoxynucleoside triphosphate (dNTP) to pyrophosphate (PPi) and a deoxynucleoside monophosphate (dNMP), and adds the latter to the free 3'-OH group of the previous nucleotide on the DNA strand that is being synthesised (the added nucleotide is complementary to the nucleotide on the template DNA). The energy released from breaking the dNTP is used to form a phosphodiester bond between the two nucleotides. Amplification will continue until the temperature is raised again to 94^{o}C and the cycle restarts. A typical PCR cycle follows the sequence: DNA melting at 94^{o}C for 4 minutes followed by 30 cycles of: DNA melting at 94^{o}C for 30 seconds, primer annealing at 60^{o}C for 30 seconds, followed by extension at 72^{o}C for 1.5 minutes, these cycles are followed by a final extension step at 72^{o}C for 5 minutes to allow closing of any gaps in the produced DNA amplicons (Figure 3.1). Each cycle of a PCR run doubles the amount of DNA and uses the newly produced sequences as templates for further amplification (the theoretical yield of DNA = $y2^{n}$, where y is the amount of starting DNA material and n is the number of cycles of the PCR run). It is important to note that during each PCR run, negative and positive controls for the PCR run must be amplified with the samples. The former contains PCR grade (DNA and RNA free) water, and should not show any amplification during the PCR run since it does not contain the DNA sequence of interest (an amplification in this sample indicates that one of the PCR mastermix components in contaminated with DNA); the latter should contain DNA that is known to contain the sequence of interest, and should always show amplification after a PCR run (the lack of amplification in this control indicates that either the PCR conditions are not correct, the primers are not correct, or the PCR mastermix is missing one or more of its components).

Genes coding for ribosomal RNA (rRNA) have been conserved in all living organisms during evolution, because they encode ribosomes that are involved in protein synthesis. The 16S and the 23S rRNA genes, respectively, code for the small and large subunits of ribosomes in bacteria and archaea (in eukaryotes these are the 18S and the 28S rRNA molecules, respectively). In addition to having highly conserved sequences, the 16S rRNA gene is also ubiquitous in bacteria and archea and contains 9 hypervariable regions that vary between species, making this gene a perfect candidate for phylogenetic analysis (Weisburg *et al.*, 1991; Case *et al.*, 2007). Amplification and visualisation of the 16S and the 18S rRNA genes enables the identification of bacteria, archea, or eukaryotes in an unknown sample (similar to work carried out in Chapter 4), and knowing the nucleotide

sequence of the 16S rRNA gene enables the identification of the species of bacteria present in a specific sample (similar to work carried out in Chapters 4, 5 and 6).

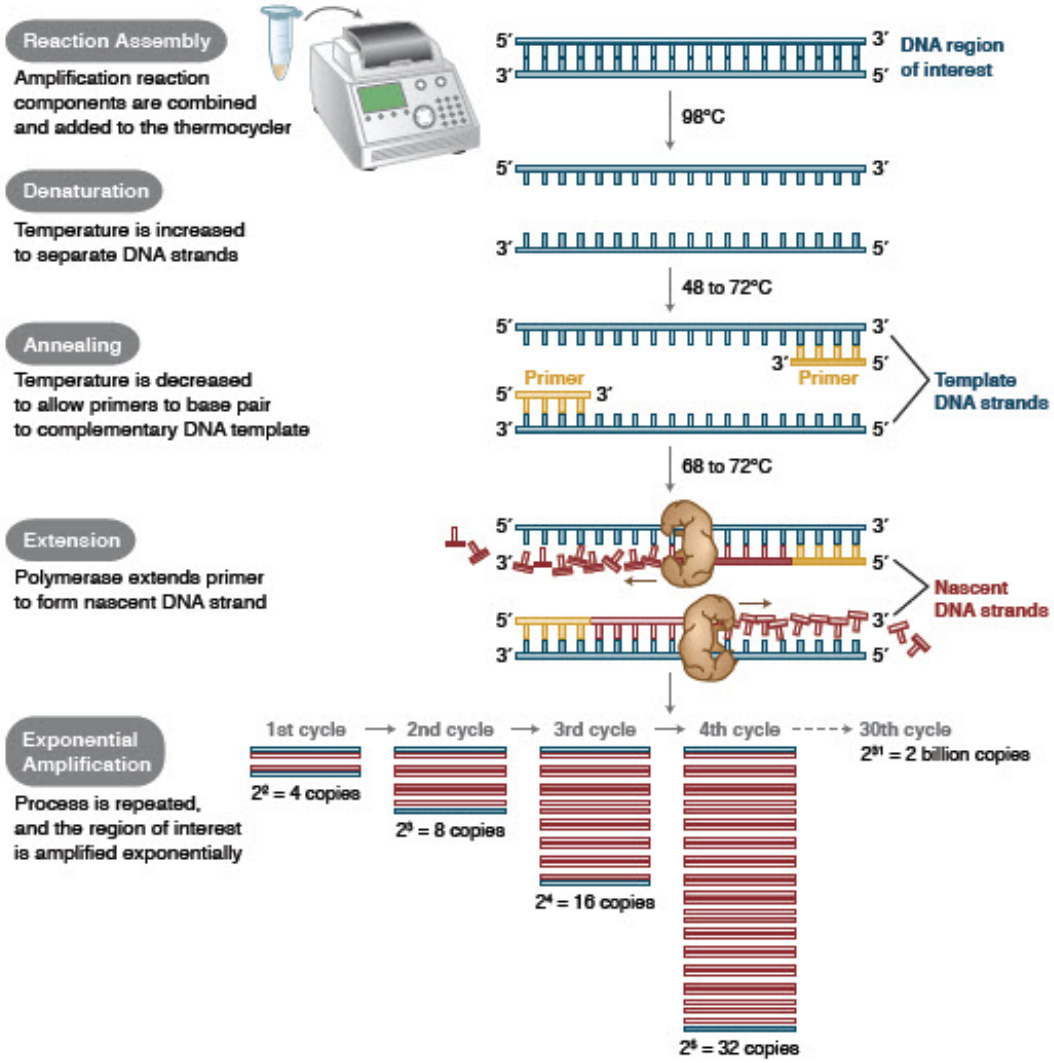

Figure 3.1: Schematic representation of a PCR run and the role of each component at different stages (adapted from www.neb.com).

3.7 Agarose Gel Electrophoresis

Agarose gel electrophoresis is a method used to separate and visualise DNA or RNA fragments. Agarose (generally at 0.8-2% (w/v)) is dissolved in an appropriate electrolyte-containing solution (typically tris-acetic acid-EDTA) by boiling, and creates a polymeric matrix that separates DNA or RNA according to the length of the fragments. DNA that is loaded into wells created in the agarose gel, and surrounded by an electrolyte-containing buffer, is exposed to an electric current that carries the negatively charged DNA fragments (due to the phosphate molecules in the DNA backbone) towards the cathode (Figure 3.2), and therefore separates them in decreasing length (smaller fragments travel further distances during the electrophoretic run). A well that is loaded with a DNA ladder, which contains DNA fragments of known lengths, is commonly included in each gel alongside

the samples for analysis. In order to visualise the DNA, the gel is commonly stained with ethidium bromide (although new stains that are less hazardous have been recently developed), which binds to the major groove of the DNA molecule and can be visualised under an ultraviolet transilluminator (similar work was carried out in Chapter 4 (in particular), and in Chapter 5 but the data were not shown).

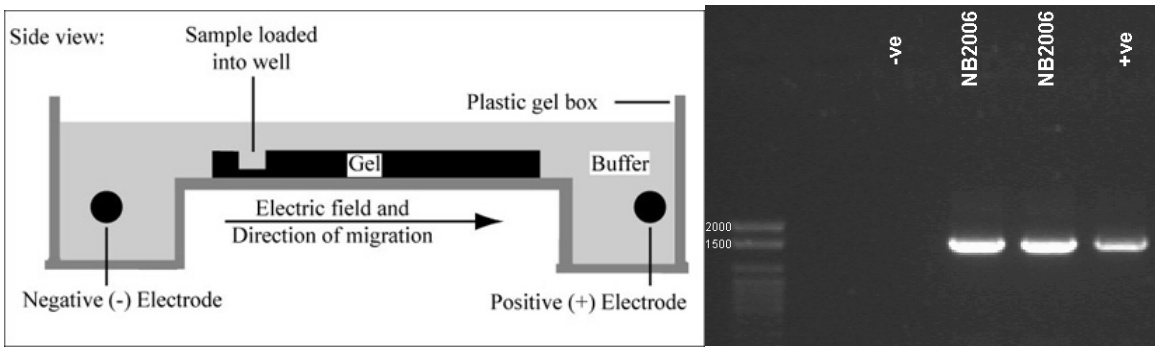

Figure 3.2: Agarose gel electrophoresis. Left: A schematic representation of an agarose gel electrophoresis setup (adapted from Massachusetts Institute of Technology Opencourseware Module 1.2: Agarose Gel Electrophoresis). Right: Image of 16S rRNA PCR products that were run on a 1.2% agarose gel in TAE buffer (right).

3.8 DNA Sequencing by the Sanger Method

DNA sequencing is the process of determining the sequence of nucleotides within a DNA fragment. The Sanger method was developed in 1977 (Sanger *et al.*, 1977) and is still widely used until the present day, primarily for obtaining long contiguous DNA sequence reads (about 1,000 bp) that are not provided by the more advanced Next-Generation Sequencing methods, especially if the number of samples required for sequencing is not too large. The Sanger method relies on the concept of chain-termination for the identification of the sequence of nucleotides in a DNA fragment. As mentioned earlier, the DNA polymerase adds nucleotides to the 3'-OH group on the growing chain of a DNA strand. The Sanger method utilises this function of the DNA polymerase and supplies the reaction with dideoxynucleosidetriphosphates (ddNTP), which lack a 3'-OH group in the ribose moiety of the nucleotide, thereby preventing the DNA polymerase from performing further additions. Since DNA is made of four different nucleotide bases, four tubes should be prepared, each containing the same reagents as a normal PCR, with one added ddNTP (tube one contains ddATP, tube two contains ddTTP, tube three contains ddCTP, tube four contains ddGTP). At the end of the reaction, the products are denatured and run on four lanes of a denaturing separation gel, and bands of increasing length (each band is 1 nucleotide larger than the previous band) can be observed and the position of each nucleotide in the DNA sequence can be identified from the lane it corresponds to (Figure 3.3). Various modifications to this method have been developed, the most important of

which is the Dye-terminator sequencing method that uses fluorescently labelled ddNTPs, each fluorescing at a different wavelength, which enables combination of all the ddNTPs in one reaction mixture and automation of analysis by capillary electrophoresis. As mentioned earlier, this method enables the identification of up to 1,000 bp per sample if only one primer is used (for example the 8f primer targeting the 16S rRNA gene, that was used in Chapter 5). This is adequate for identifying the Genus of a bacterial isolate, which was done in Chapter 5. However, in order to identify the sequence of the whole 16S rRNA gene (about 1,500 bp), 4 primers were used that cover the whole gene and produce overlapping regions (a 8f primer at the beginning of the gene, a 1492r primer at the end of the gene, and 530f and 943r as internal primers), which was done in Chapter 6.

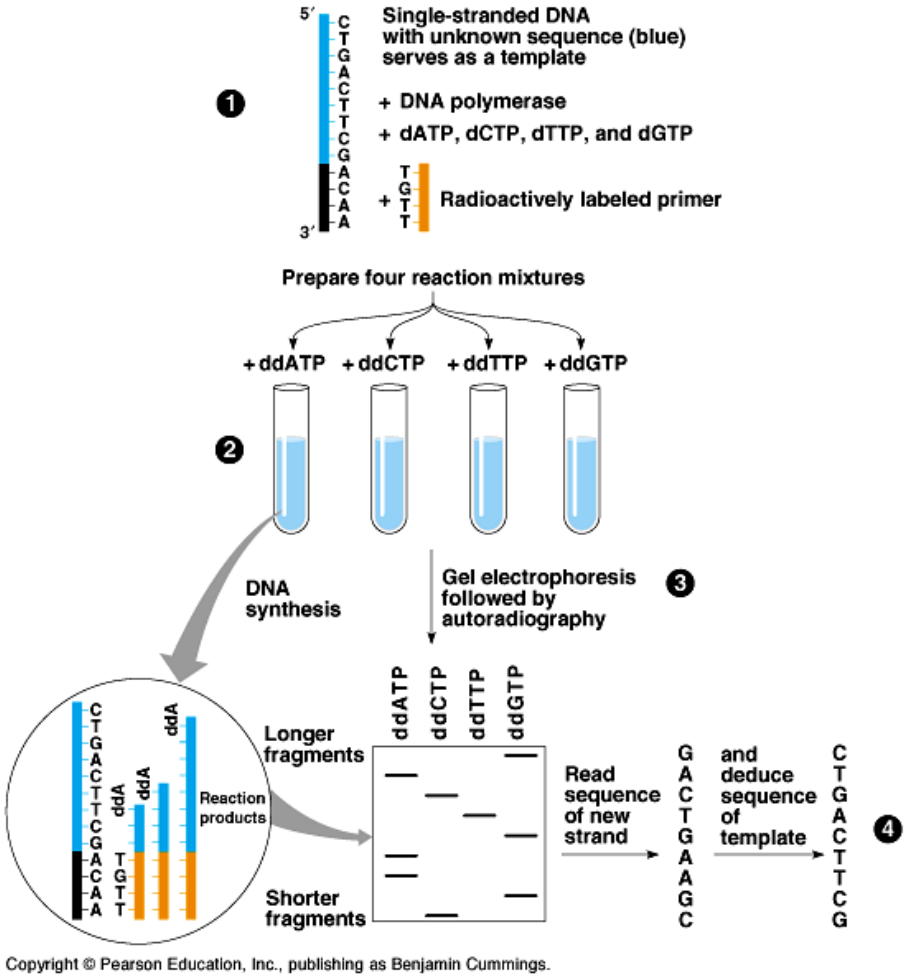

Figure 3.3: DNA sequencing following the Sanger method (adapted from University of Texas, Biol 212 course lecture: DNA Technology and Genomics-Part II). (1) Denaturation of dsDNA and annealing of sequencing primer. (2) PCR in a mixture containing one ddNTP. In the Dye-terminator modification, fluorescent ddNTPs are added into one PCR reaction mixture. (3) PCR products from each of the four tubes are run on one lane of an agarose gel. In the Dye-terminator procedure, the PCR product is run on one lane in capillary gel electrophoresis and fluorescence is detected upon exposure of the bands to a laser beam. (4) The nucleotide sequence is read one nucleotide at a time from the bottom of the gel (shortest bands travel farthest).

3.9 Pyrosequencing

Pyrosequencing is one of several next generation sequencing techniques that are appreciably less labour intensive than the older Sanger sequencing method. It has a relatively high throughput with > 100,000 sequences per run (compared to the 96 sequences of clone libraries) and the sequence length can reach up to 900 bp with the latest reagent upgrade, which is almost the same as the Sanger method. Unlike the older Sanger sequencing method, which relies on chain termination to identify the DNA sequence, pyrosequencing relies on the principle of sequencing by synthesis, which provides real-time identification of nucleotides as they are being added to the growing DNA strand through chemiluminescence detection by a CCD camera (Ronaghi *et al.*, 1996). Similar to the Sanger sequencing, this method requires single stranded DNA, DNA polymerase, primers and dNTPs as starting material, in addition to the enzymes APT sulfurylase, luciferase, and apyrase and the substrates luciferin and adenosine 5' phosphosulphate. The concept behind this technology is that each of the four dNTPs is added to the sample (which contains single stranded DNA fragments) separately and sequentially, in case the added dNTP is complementary to the template DNA, the DNA polymerase breaks the dNTP to dNMP and PPi, and forms the phosphodiester bond between the added nucleotide and the previous one in the growing DNA chain. A recombinant version of the *Saccharomyces cerevisiae* APT sulfurylase then rapidly reacts the PPi with the adenosine 5' phosphosulphate, and produces SO_4^{2-} and ATP. The latter acts as a substrate for luciferase to oxidise luciferin to oxyluciferin, which produces photons that are detected by a CCD camera (Figure 3.4). The intensity of generated light is proportional to the number of incorporated nucleotides, which allows for the detection of homopolymers (Ronaghi *et al.*, 1996). Apyrase is added at the end of each reaction, which will degrade any free nucleotides (dNTPs that were not complementary to the next nucleotide on the template strand) and remaining ATP that had not been used by lusiferase, and the reaction starts again with the next nucleotide in the sequence. The full DNA sequence can be derived from the known nucleotides that were added to the growing DNA fragment, which is complementary to the template DNA (Ronaghi *et al.*, 1998). The long sequences that are provided by this technology are advantageous over other next generation sequencing technologies (that provide shorter sequence lengths) through reducing the number of gaps in the complete sequence and facilitates computational analysis (Ronaghi *et al.*, 1998). However, this may also cause the DNA polymerase to introduce errors due to extended use.

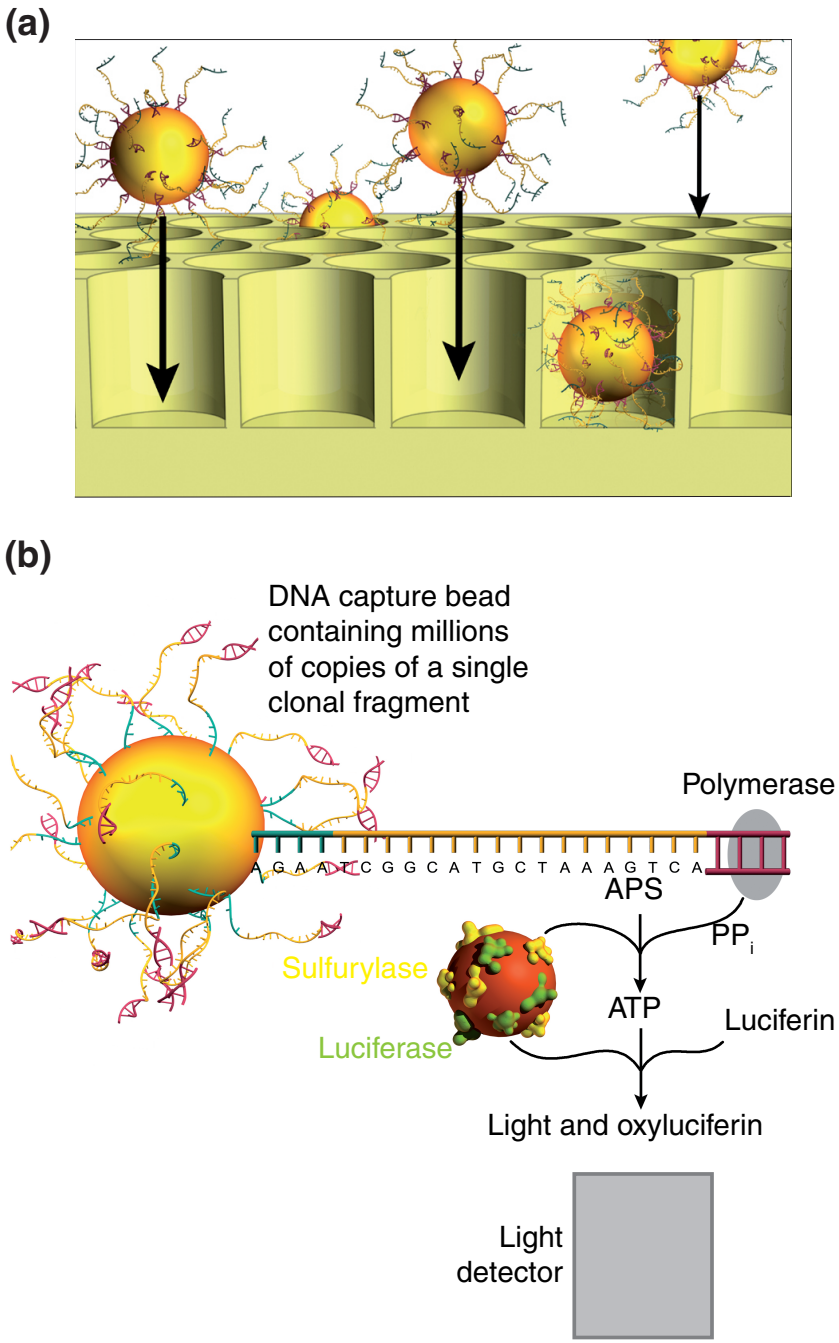

Figure 3.4: Chemical reactions leading to sequence identification during a pyrosequencing run (adapted from Owen-Hughes and Engeholm, 2007). Single stranded DNA fragments are immobilised on billions of streptavidin-coated beads, as one strand per bead. Emulsion PCR is performed on these beads, which produces beads that are coated with millions of copies of the same single stranded DNA fragment. (a) The DNA-coated beads are placed into a Picotiter plate, with each bead captured in its own microchamber (b) The wells are sequenced simultaneously by primer-initiated DNA synthesis on the single strands, using repeated cycles of each of the four nucleotides, added in turn as pyrophosphates. Incorporation of one or more bases at a time to the growing DNA strand is accompanied by the release of pyrophosphate and the consequent activation of luciferin and the release of a flash of light, which is recorded via the fiber optics (the intensity of the flash correlates with the number of bases added). The sequence of the DNA in each well is then recovered from the recorded data.

The 454-pyrosequencing, which was used in Chapters 4 and 5 for phylogenetic analysis of mixed bacterial community samples, is an array based pyrosequencing technology that can perform parallel processing of samples to produce large amounts of data (about 100 megabases) in a short period of time (about 10 hours). In this method, a specific 454 Life Sciences adaptor is ligated to the template DNA (for this work, this was done by performing PCR using the 16S rRNA gene 27f primer, attached to a 10 bp segment specific for each sample, to allow for multiplexing, which is in turn attached to the specific adaptor). This adaptor sequence complements DNA sequences bound to billions of streptavidin-coated beads that are immersed in an emulsion of water and oil, so that each bead is bound to only one adaptor ligated single stranded DNA fragment and is covered by a water droplet in an oil emulsion, thereby creating its own microreactor. Emulsion PCR is performed on this mixture to produce millions of copies of each DNA fragment on a single bead. The beads are placed in a Picotiter plate, which contains more than a million individual fiber-optic picoliter-scale wells, such that each well contains no more than one bead (Figure 3.4). The plate is then covered by the pyrosequencing enzymes and substrates mentioned earlier. At this point, the plate is placed in the sequencer and sequencing can commence.

454 Pyrosequencing was performed in Chapters 4 and 5 according to the following procedure. DNA was extracted from samples using the PowerSoil DNA isolation kit (MO BIO Laboratories, Carlsbad, CA, USA) according to the manufacturer's protocol. Pyrosequencing PCR was performed using the FastStart High Fidelity PCR System (Roche, Basel, Switzerland) and the 27F and 338R universal primers to cover the V1–V2 hypervariable regions of the 16S rRNA gene (Lane, 1991). The 338R primer with the sequence 5'-GCWGCCTCCCGTAGGAGT-3' was used for all the samples. However, each sample had a unique F primer with a different barcode sequence to distinguish between the different samples. The F primers included the 454 Life Sciences (Bradford, CT, USA) adapter region with the sequence 5'-CCATCTCATCCCTGCGTGTCTCCGACTCAG-3', followed by the 10 bp barcode sequence specific to each sample, which was followed by the universal 27F primer sequence 5'-AGAGTTTGATCMTGGCTCAG-3'. The PCR mastermix contained, per sample, 40 µl sterile purified H_2O, 5 µl of 10x PCR reaction buffer, 1 µl dNTP mix, 0.8 µl of 25 mM 338R primer and 0.4 µl High Fidelity Enzyme Blend. To perform the PCR, 47.2 µl of this mastermix was transferred into a sterile 50 µl PCR reaction tube, where 0.8 µl of one of each barcoded 27F primer and 2 µl of DNA, taken from the sample corresponding to each specific barcode, were added to separate tubes. A negative and a positive control

for the PCR reaction, which contained 2 μl sterile H_2O or DNA extracted from *Geobacter sulfurreducens*, respectively, were also prepared. The PCR conditions were: initial denaturation at 95°C for 2 min, followed by 35 cycles of denaturation at 95°C for 30 s, primer annealing at 55°C for 30 s and extension at 72°C for 45 s, followed by a final extension step at 72°C for 5 min. At the end of the PCR run, the whole PCR product was mixed with 12.5 μl of 5x gel-loading dye, and 35 μl of the mixture was loaded on a 2% Tris-Acetate-EDTA/agarose gel. A 2000 to 100 bp DNA ladder was also loaded on the gel that was run at 80 mV for 2 hours. At the end of the run, the DNA bands were observed on a Gel Doc XR system (Bio-Rad Laboratories, Hercules, CA, USA) and the band corresponding to 400 bp size for each sample was excised from the gel. DNA extraction and cleanup from the excised gel were performed using a QIAquick Gel Extraction Kit (Quiagen, Limburg, The Netherlands), according to the manufacturer's protocol. DNA was quantified on a Nanodrop ND-1000 (Thermo Scientific) and all samples were diluted to 10 ng/μl. The DNA product was then stored at 4°C prior to emulsion PCR and then sequencing was performed using a 454 GS Junior pyrosequencing system (Roche), using the facility in the Faculty of Life Sciences, University of Manchester.

Analysis of the raw 454 pyrosequencing data was done using the Quantitative Insights Into Microbial Ecology pipeline (Caporaso et al., 2010b). Sequences were first assigned to the different samples using the barcode sequences provided, and sequences outside the 300–400 bp range were removed along with the reverse primer sequence, using the split_library.py script. Chimeric sequences were identified using the usearch 6.1 programme (Edgar et al., 2011) and the identify_chimeric_seqs.py script. Chimeric sequences were filtered out of the data using the filter_fasta.py script. Operational taxonomic units (OTUs) were picked from these sequences and compared at 97% similarity with the May 2013 release of greengenes OTU reference using the usearch 6.1 programme (Edgar, 2010) through the pick_otus.py script. The most abundant OTU sequence was chosen as a representative sequence, using the pick_rep_set.py script, and assigned to taxonomy based on the greengenes reference database (McDonald et al., 2012) using the Ribosomal Database Project Naive Bayes classifier v 2.2 (Wang et al., 2007), with the confidence level set at 80% through the assign_taxonomy.py script. The sequences were then aligned to the greengenes core reference alignment (DeSantis et al., 2006) using PyNAST (Caporaso et al., 2010a) through the align_seqs.py script. Aligned sequences were then filtered using the filter_alignement.py script, and a phylogenetic tree was built through the make_phylogeny.py (Price et al., 2009). An OTU table was built through the make_otu_table.py and convert_biom.py scripts and was used to calculate and

plot the α-diversity (based on the number of OTUs) and the % 16S rRNA gene reads in each sample using the OriginPro v 9 software (OriginLab, Northampton, MA, USA).

3.10 References

Caporaso JG, Bittinger K, Bushman FD, DeSantis TZ, Andersen GL, Knight R. (2010a). PyNAST: a flexible tool for aligning sequences to a template alignment. *Bioinformatics* **26**: 266–267.

Caporaso JG, Kuczynski J, Stombaugh J, Bittinger K, Bushman FD, Costello EK et al. (2010b). QIIME allows analysis of high-throughput community sequencing data. *Nat Meth* **7**: 335–336.

Case RJ, Boucher Y, Dahllöf I, Holmström C, Doolittle WF, Kjelleberg S. (2007). Use of 16S rRNA and rpoB genes as molecular markers for microbial ecology studies. *Appl Environ Microbiol* **73**:278–288.

Chien A, Edgar DB, Trela JM. (1976). Deoxyribonucleic acid polymerase from the extreme thermophile *Thermus aquaticus*. *J Bacteriol* **127**:1550–1557.

DeSantis TZ, Hugenholtz P, Larsen N, Rojas M, Brodie EL, Keller K et al. (2006). Greengenes, a chimera-checked 16S rRNA gene database and workbench compatible with ARB. *Appl Environ Microbiol* **72**: 5069–5072.

Edgar RC. (2010). Search and clustering orders of magnitude faster than BLAST. *Bioinformatics* **26**: 2460–2461.

Edgar RC, Haas BJ, Clemente JC, Quince C, Knight R. (2011). UCHIME improves sensitivity and speed of chimera detection. *Bioinformatics* **27**: 2194–2200.

Johnson DA, Florence TM. (1975). A study of some pyridylazo dyestuffs as chromogenic reagents and the elucidation of the nature of their metal complex spectra. *Talanta* **22**:253–265.

Johnson DA, Florence TM. (1971). Spectrophotometric determination of uranium (VI) with 2-(5-bromo-2-pyridylazo)-5-diethylaminophenol. *Anal Chim Acta* **53**:73–79.

Lovley D, Phillips E. (1986). Availability of ferric iron for microbial reduction in bottom sediments of the freshwater tidal Potomac River. *Appl Environ Microbiol* **52**:751–757.

Lovley D, Phillips E. (1987). Rapid assay for microbially reducible ferric iron in aquatic sediments. *Appl Environ Microbiol* **53**:1536–1540.

Lovley DR, Giovannoni SJ, White DC, Champine JE, Phillips EJP, Gorby YA, *et al.* (1993). *Geobacter metallireducens* gen. nov. sp. nov., a microorganism capable of coupling the complete oxidation of organic compounds to the reduction of iron and other metals. *Arch Microbiol* **159**:336–344.

Lovley DR, Phillips EJ. (1988). Novel mode of microbial energy metabolism: organic carbon oxidation coupled to dissimilatory reduction of iron or manganese. *Appl Environ Microbiol* **54**:1472–1480.

McDonald D, Price MN, Goodrich J, Nawrocki EP, DeSantis TZ, Probst A et al. (2012). An improved Greengenes taxonomy with explicit ranks for ecological and evolutionary analyses of bacteria and archaea. *ISME J* **6**: 610–618.

Owen-Hughes T, Engeholm M. (2007). Pyrosequencing positions nucleosomes precisely. *Genome Biol* **8**:217.

Price MN, Dehal PS, Arkin AP. (2009). FastTree: Computing large minimum evolution trees with profiles instead of a distance matrix. *Mol Biol Evol* **26**: 1641–1650.

Rai D, Hess NJ, Xia Y, Rao L, Cho HM, Moore RC, *et al.* (2003). Comprehensive thermodynamic model applicable to highly acidic to basic conditions for isosaccharinate reactions with Ca(II) and Np(IV). *J Solution Chem* **32**:665–689.

Ronaghi M, Karamohamed S, Pettersson B, Uhlén M, Nyrén P. (1996). Real-time DNA sequencing using detection of pyrophosphate release. *Anal Biochem* **242**:84–89.

Ronaghi M, Uhlén M, Nyrén P. (1998). A sequencing method based on real-time pyrophosphate. *Science* **281**:363–365.

Saiki RK, Gelfand DH, Stoffel S, Scharf SJ, Higuchi R, Horn GT, *et al.* (1988). Primer-directed enzymatic amplification of DNA with a thermostable DNA polymerase. *Science* **239**:487–491.

Sanger F, Nicklen S, Coulson AR. (1977). DNA sequencing with chain-terminating inhibitors. *Proc Natl Acad Sci USA* **74**:5463–5467.

Stookey LL. (1970). Ferrozine-a new spectrophotometric reagent for iron. *Anal Chem* **42**:779–781.

Vercammen K, Glaus MA, van Loon LR. (1999). Complexation of calcium by α-isosaccharinic acid under alkaline conditions. *Acta Chem Scand* **53**:241–246.

Wang Q, Garrity GM, Tiedje JM, Cole JR. (2007). Naïve Bayesian classifier for rapid assignment of rRNA sequences into the new bacterial taxonomy. *Appl Environ Microbiol* **73**: 5261–5267.

Weisburg WG, Barns SM, Pelletie DA, Lane DJ. (1991). 16S ribosomal DNA amplification for phylogenetic study. *J Bacteriol* **173**:697–703.

Chapter 4

Microbial degradation of cellulosic material under intermediate-level waste simulated conditions

Paper accepted for publication in a special issue of the Mineralogical Magazine on the geological disposal of radioactive waste.

Naji M. Bassil, Alastair D. Bewsher, Olivia R. Thompson, Jonathan R. Lloyd. 2015. Microbial degradation of cellulosic material under ILW-simulated conditions. *Min Mag*

Author contributions: N. M. Bassil - Principal author, preparation and monitoring of samples and data acquisition and analysis; A. D. Bewsher – Samples analysis on IC system; O. R. Thompson – Help in initial setup of experiments; J. R. Lloyd – Corresponding author and manuscript review.

Mineralogical Magazine, October 2015, Vol. 79(6), pp. 1–9

OPEN ACCESS

Microbial degradation of cellulosic material under intermediate-level waste simulated conditions

NAJI M. BASSIL[1,2], ALASTAIR D. BEWSHER[1], OLIVIA R. THOMPSON[3] AND JONATHAN R. LLOYD[1,*]

[1] Research Centre for Radwaste Disposal & Williamson Research Centre for Molecular Environmental Science, School of Earth, Atmospheric and Environmental Sciences, The University of Manchester, Oxford Road, Manchester M13 9PL, UK
[2] National Council for Scientific Research – Lebanon (CNRS-L), Beirut, Lebanon
[3] National Nuclear Laboratory, 5th Floor, Chadwick House, Warrington Road, Birchwood Park, Warrington WA3 6AE, UK

[*Received 10 October 2014; Accepted 3 March 2015; Associate Editor: N. Evans*]

ABSTRACT

Under the alkaline conditions expected in an intermediate-level waste repository, cellulosic material will undergo chemical hydrolysis. This will produce hydrolysis products, some of which can form soluble complexes with some radionuclides. Analyses of samples containing autoclaved tissue and cotton wool incubated in a saturated solution of $Ca(OH)_2$ (pH>12) confirmed previous reports that isosaccharinic acid (ISA) is produced from these cellulose polymers at high pH. However, when inoculated with a sediment sample from a hyperalkaline site contaminated with lime-kiln waste, microbial activity was implicated in the enzymatic hydrolysis of cellulose and the subsequent production of acetate. This in turn led to acidification of the microcosms and a marked decrease in ISA production from the abiotic alkali hydrolysis of cellulose. DNA analyses of microbial communities present in the microcosms further support the hypothesis that bacterial activities can have a controlling influence on the formation of organic acids, including ISA, *via* an interplay between direct and indirect mechanisms. These and previous results imply that microorganisms could have a role in attenuating the mobility of some radionuclides in and around a geological disposal facility, *via* either the direct biodegradation of ISA or by catalysing cellulose fermentation and therefore preventing the formation of ISA.

KEYWORDS: intermediate-level waste repository, cellulose polymers, microbial degradation.

Introduction

CELLULOSE is a polymer of 100–14,000 glucose units linked by β-1,4 glycosidic bonds and is the main component of plant cell walls. As such, it is one of the most abundant polymers on Earth (Beguin and Aubert, 1994). Cellulose polymers are oriented in parallel and form highly ordered, insoluble crystalline domains interspersed by more disordered amorphous regions. Cellulose can be present in a variety of products including clothes, paper, tissue etc., which are expected to be present in intermediate-level waste (ILW) that will be disposed of in a deep geological disposal

* E-mail: jon.lloyd@manchester.ac.uk
DOI: 10.1180/minmag.2015.079.6.01

The research leading to these results has received funding from the European Union's European Atomic Energy Community's (Euratom) Seventh Framework programme FP7 (2007-2013) under grant agreements nº249396, SecIGD, and nº323260, SecIGD2.

facility (GDF) (Nuclear Decommissioning Authority, 2014).

Previous studies have shown that hyperalkaline conditions (pH 12−13) will dominate after resaturation of an ILW-GDF with groundwater, due to the extensive use of cement (Berner, 1992). Under these hyperalkaline conditions, abiotic hydrolysis of the cellulose present in ILW will take place, leading to the formation of water-soluble low molecular-weight compounds, in particular ISA (Glaus *et al.*, 1999). ISA is a particular concern as it has the potential to bind to, and mobilize, some radionuclides (Gaona *et al.*, 2008; Keith-Roach, 2008). Studies have shown that the rate and extent of cellulose hydrolysis under alkaline conditions is dependent on a number of factors, including the starting pH, temperature and the degree of polymerization of the cellulose (Van Loon and Glaus, 1997; Van Loon *et al.*, 1999; Pavasars *et al.*, 2003; Glaus and Van Loon, 2008). In this respect, native cellulose (exemplified by cotton wool) has a greater degree of polymerization and a smaller fraction of reducing end groups than treated cellulose (e.g. tissue) and therefore the rate and extent of hydrolysis of cotton wool is less than that of tissue.

In addition to abiotic hydrolysis mechanisms, microorganisms can also break down cellulose enzymatically. These cellulolytic organisms are taxonomically diverse, belonging to different genera in the Bacterial and Eukarial domains, and are found in a wide range of environments under aerobic and anaerobic conditions (Leschine, 1995; Lynd *et al.*, 2002). Furthermore, alkaliphilic and alkalitolerant cellulolytic bacteria from alkali lakes have been identified previously (Grant *et al.*, 2004; Zhilina *et al.*, 2005). They can play an important role in influencing their surrounding environment through the breakdown of cellulose and the fermentation of its component glucose monomers (Zhilina and Zavarzin, 1994).

Previous work by our group has shown that alkaliphilic bacteria present in a sediment from a legacy lime-working site, were able to utilize ISA as an electron donor for the reduction of a number of electron acceptors at pH 10 (Bassil *et al.*, 2014). The aim of this present work is to test the ability of the bacteria present in a similar sediment to survive the initial hyperalkaline pH that is expected in an ILW-GDF and then to (1) study their ability to degrade cellulosic material (tissue and cotton wool) at high pH, and hence (2) control the biogeochemical fate of cellulose degradation products under anaerobic conditions.

Materials and Methods

Sediment acquisition

Sediment samples were collected from a depth of ~20 cm from the surface of a site near Buxton, UK, which has been contaminated for decades by high pH lime-kiln workings (Rizoulis *et al.*, 2012).

Sample preparation

Samples were prepared by adding 25% (w/v) of tissue or cotton wool into 100 ml serum bottles and adding to them a 100 ml aliquot of saturated $Ca(OH)_2$ solution (1 g/l). The bottles were closed with rubber butyl stoppers, degased with N_2 for 10 min and then autoclaved. After cooling, the bottles were introduced into an anaerobic chamber where a 2.5% (w/v) inoculum of sediment was added to some of the bottles, while others were kept sterile (uninoculated). Triplicates were incubated for 30 months at 25 and 50ºC for each condition. Sampling was undertaken initially every 2 months for the first 6 months of incubation and then every 6 months. During sampling, the bottles were opened inside the anaerobic chamber after its O_2 level had dropped to zero, and 5 ml volumes of the liquid along with small sections of the cellulosic material were removed and put in sterile 15 ml tubes. A 1 ml volume was taken from the 15 ml tubes and was used for pH measurement and ion-exchange chromatography analysis, while the remaining solution was frozen at −20ºC.

Ion-exchange chromatography

The 1 ml samples were vortexed and then centrifuged at 13,000 *g* for 5 min at room temperature to remove bacteria and any solid material. The samples were diluted 50−200 times (with time, more ISA was produced and therefore the samples needed to be diluted further), then analysed by ion-exchange high-performance liquid chromatography, following the protocol reported previously (Bassil *et al.*, 2014). Preparation of the Ca salt of α-ISA was performed following the procedure reported by Vercammen *et al.* (1999) and was used as a standard for ion-exchange high-performance liquid chromatography.

Microbial community analyses

rDNA gene amplification

The frozen inoculated tissue samples from the start of the experiment (T_0) and after 30 months of incubation (T_{30}) at 25ºC were thawed and DNA was extracted from them using the PowerSoil DNA isolation kit (MO BIO Laboratories, Carlsbad, California, USA), according to the manufacturer's protocol. The presence of bacterial, archaeal and fungal DNA in these samples was assessed using an end-point polymerase chain reaction (PCR) targeting the 16S rRNA and 18S rRNA genes, using the TaKaRa Ex Taq DNA Polymerase (TaKaRa Bio Inc, Japan). Bacterial DNA was detected by using the 16S rRNA gene universal primers 8F (5′-AGAGTTTGATCCTGGCTCAG-3′) and 1492R (5′-TACGGYTACCTTGTTACGACTT-3′) (Lane, 1991), archaeal DNA was detected by using the archaeal specific 16S rRNA gene primers 21F (5′-TTCCGGTTGATCCYG CCGGA-3′) and 985R (5′-YCCGGCGTTGAMT CCAATT-3′) (DeLong, 1992), and fungal DNA was detected by using 18S rRNA gene primers nu-SSU-0817-5′ (5′-TTAGCATGGAATAA TRRAATAGGA-3′) and nu-SSU-1536-3′ (5′-ATTGCAATGCYCTATCCCCA-3′) (Borneman and Hartin, 2000). A negative control for the PCR reaction contained PCR grade water and was run under the same conditions as the test samples. DNA extracted from *Geobacter sulfurreducens*, *Methanohalophilus halophilus* and *Handkea fumosa* were used as positive controls for the PCR reaction for the detection of bacteria, archaea and fungi, respectively. The PCR products were run, along with a 2000−100 bp DNA ladder, for 45 min at 80 V on a 1% agarose gel in Tris-acetate-EDTA buffer, which was then observed on a Gel Doc XR system (Bio-Rad Laboratories, Hercules, California, USA).

454 pyrosequencing

Pyrosequencing PCR was performed on DNA extracted from samples 1 and 3 from the tissue microcosms that were incubated at 25ºC at the initial (T_0) and final (T_{30}) time-points following the procedure reported by Bassil *et al.* (2014). The PCR product was sequenced at the University of Manchester sequencing facility using a Roche 454 Life Sciences GS Junior system (Roche, Basel, Switzerland). Analysis of the raw 454 pyrosequencing data was performed according to the protocols reported by Bassil *et al.* (2014).

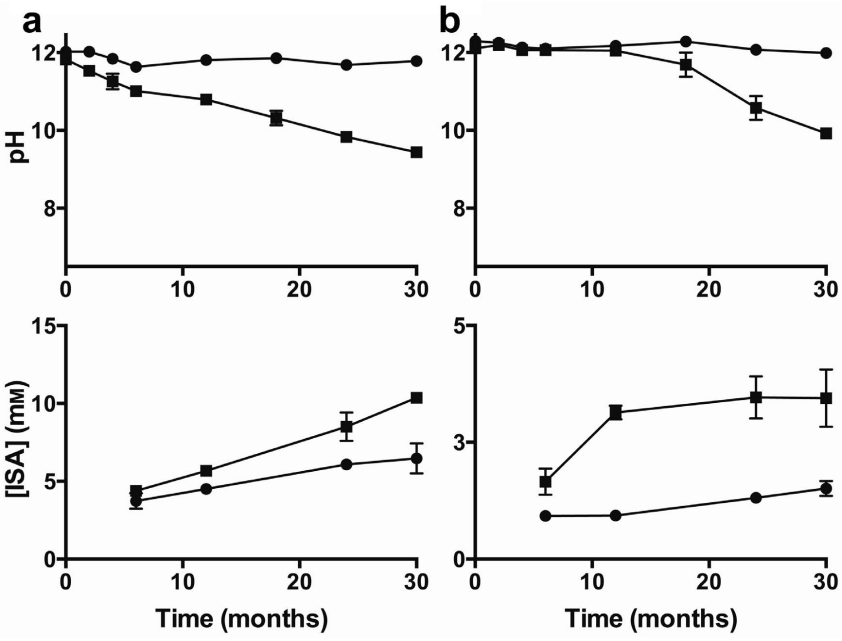

FIG. 1. Autoclaved tissue (*a*) and cotton wool (*b*) samples incubated at 25 (●) and 50ºC (■) in the presence of $Ca(OH)_2$ at saturation. The upper diagrams show the pH and the lower diagrams show the concentration of ISA in mM.

Results

The abiotic alkali hydrolysis of cellulose was demonstrated through the increase in concentrations of ISA over time in autoclaved tissue and cotton wool samples incubated at 25 and 50ºC in the presence of $Ca(OH)_2$ at saturation for 30 months (Fig. 1). At 50ºC, these samples showed a decrease in pH (from pH 11.8 to 9.4 and from 12.1 to 9.9 in the tissue and cotton wool samples, respectively) and an increase in ISA concentration (to 10.4 and 3.5 mM of ISA). At 25ºC however, they showed an almost constant pH (ranging from 12 to 11.8 and from 12.3 to 12) and a smaller production of ISA (6.5 and 1.5 mM). The microcosms that were inoculated with 2.5% (w/v) of the lime-workings sediment showed a similar pH and ISA profile to the uninoculated samples under the same conditions at 50ºC (Fig. 2). However, the tissue microcosms that were incubated at 25ºC showed a prominent fall in pH (from pH 12 to ~8.5) that was associated with an increase in acetate concentration to 17.4 mM (Fig. 2). Furthermore, one of the samples of this triplicate (sample 1) showed visibly far more cellulose degradation (Fig. 3), a significant decrease in pH and far more acetate production than noted in the other two samples of the triplicate (Fig. 4), causing an increase in the error bars with time (Fig. 2). Comparison of the

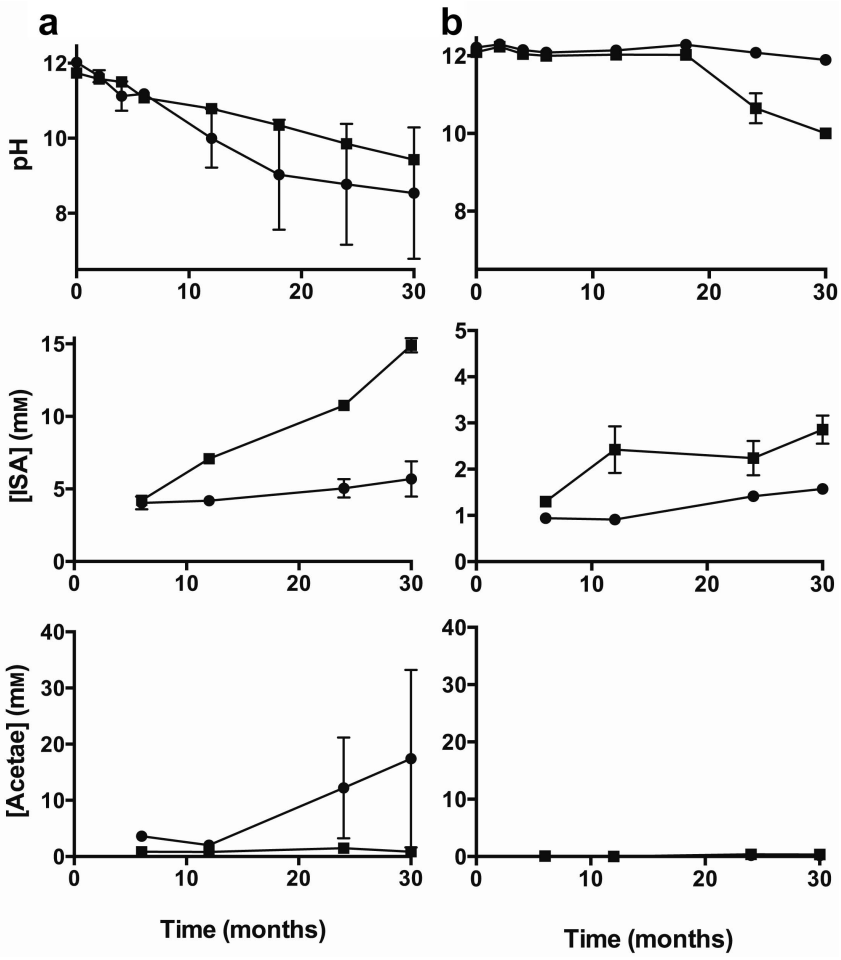

FIG. 2. Tissue (*a*) and cotton wool (*b*) microcosms (inoculated with 2.5% (w/v) of the lime-kiln sediment) incubated at 25 (●) and 50ºC (■) in the presence of $Ca(OH)_2$ at saturation. The upper diagrams show the pH, the middle diagrams show the concentration of ISA in mM and the lower diagrams show the concentration of acetate in mM.

FIG. 3. The triplicate of the tissue microcosms, incubated for 30 months at 25ºC and in the presence of $Ca(OH)_2$ at saturation. Samples 1, 2 and 3 are shown from left to right.

16S rRNA gene sequences amplified at the beginning and the end of the 25ºC incubation period for the inoculated tissue microcosms, showed an increase in the yield of amplified bacterial DNA in samples 1 and 3 over time, but not in sample 2 (which may contain very low biomass levels). Furthermore, it proved impossible to amplify archaeal or fungal rRNA genes by PCR in any of these microcosms (Fig. 5). Interestingly, samples 1 and 3 also showed an almost constant concentration of ~4.5 mM of ISA over the duration of the experiment, while sample 2 showed an increase in ISA concentration to 8.1 mM after 30 months of incubation (Fig. 4).

Identification of the bacteria present in the tissue microcosms (samples 1 and 3) by 454 pyrosequencing, showed that the overall bacterial diversity dropped in sample 1 (from 160 to 27 OTUs) but not in sample 3 after 30 months of incubation at 25ºC (Fig. 6*a*). Furthermore, there was an increase in the abundance of Firmicutes in both microcosms 1 and 3, comprising 99.6% and 44.7% of the total 16S rRNA gene sequenced after 30 months of incubation, respectively (Fig. 6*b*). Although microcosm 1 was dominated by bacteria belonging to the genera *Clostridium* and *Sporomusa*, sample 3 contained a consortium of mainly Firmicutes belonging to the genera: *Bacillus*, *Clostridium* and *Pelosinus*, along with non-Firmicutes like *Pseudomonas* and *Diaphorobacter* (Fig. 6*c*).

Discussion

Bacteria have been found flourishing in natural environments that are considered to be extreme for life on Earth, for example soda lakes (Grant *et al.*, 2004; Zhilina *et al.*, 2005), deserts (An *et al.*, 2013) and hydrothermal vents (Robidart *et al.*, 2013). An ILW-GDF is expected to be an engineered extreme environment where different factors such as hyperalkaline conditions, high-radiation levels and high concentrations of radionuclides will be present, which could restrict

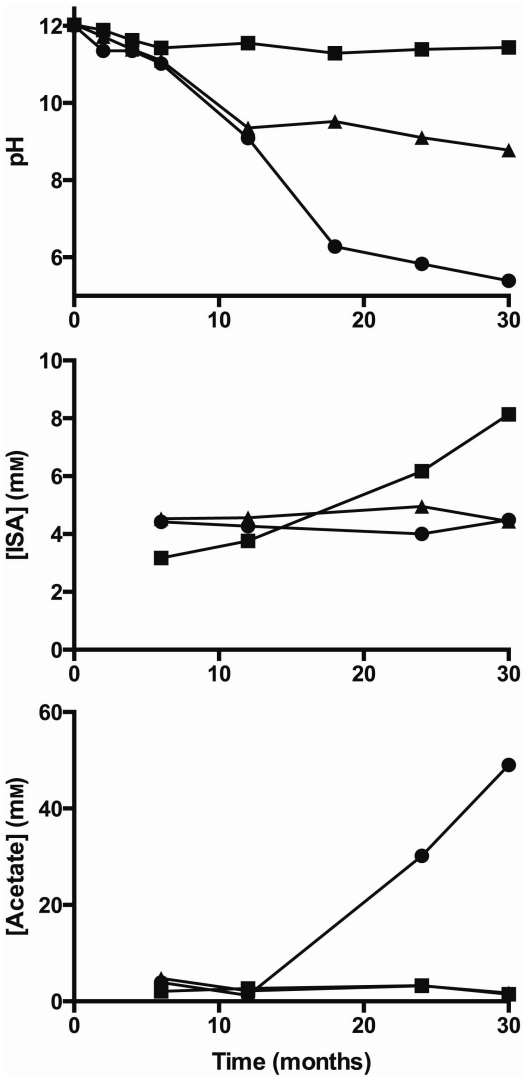

FIG. 4. The triplicate of the tissue microcosms incubated at 25ºC and in the presence of $Ca(OH)_2$ at saturation. The upper diagram shows the pH, the middle diagram shows the concentration of ISA in mM and the lower diagram shows the concentration of acetate in mM. Sample 1(●), sample 2 (▲) and sample 3 (■) are shown.

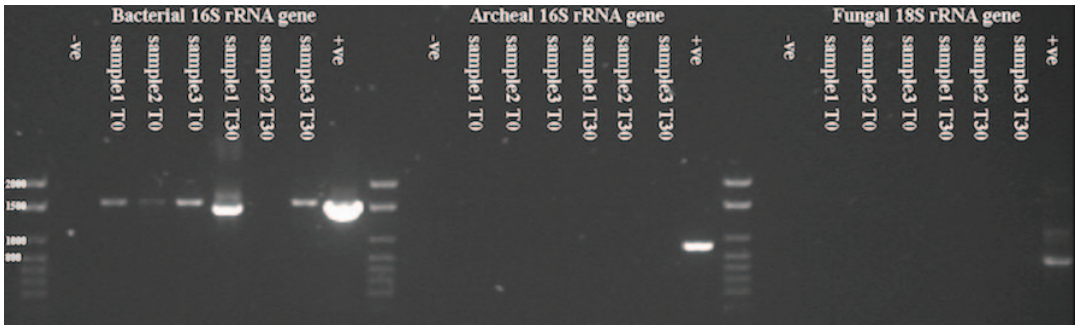

FIG. 5. Agarose gel electrophoresis of PCR products amplified using primers for the bacterial 16S rRNA gene, the archaeal 16S rRNA gene and the fungal 18S rRNA gene. In each set, from left to right, the lanes represent, the 2000−100 bp DNA ladder, the negative control (containing molecular biology grade water) for the PCR reaction, samples 1, 2 and 3 at T_0, samples 1, 2 and 3 at T_{30} and, finally, a positive control for the PCR reaction (containing DNA extracted from *Geobacter sulfurreducens*, *Methanohalophilus halophilus* and *Handkea fumosa* as representatives of bacteria, archaea and fungi, respectively).

microbial activity. Some host rocks and barrier materials may also limit water and available pore space for microbial colonization for operational periods of the GDF. However, the ILW-GDF will also contain electron donors (H_2 and organic material) and acceptors (NO_3^-, Fe(III), SO_4^{2-}, etc.) that bacteria can utilize to support growth.

Sterile tissue and cotton wool samples incubated at 25 and 50ºC for 30 months in a saturated solution of $Ca(OH)_2$ confirmed previous results that a higher temperature and lower degree of polymerization (tissue has a lower degree of polymerization than cotton wool) generate more ISA from the abiotic alkali hydrolysis of cellulosic material (Fig. 1) (Van Loon and Glaus, 1997; Van Loon *et al.*, 1999; Pavasars *et al.*, 2003; Glaus and Van Loon, 2008). Although the starting pH of the samples used in the current study were less than those tested by previous groups, due to the use of $Ca(OH)_2$ instead of NaOH and KOH, our results are representative of the more prolonged second phase of the evolution of a GDF, when Ca^{2+} will dominate the solution chemistry (Berner, 1992).

The fall in pH of the inoculated tissue microcosms that were incubated at 25ºC, the production of acetate (Fig. 2) and the visible degradation of cellulose (Fig. 3), are strong indicators of the biological degradation and fermentation of cellulose. This contrasts with the results from experiments conducted at 50ºC, where microbial activities were not implicated, presumably because inocula from the lime-workings site could not adapt to grow at elevated temperatures. Note, however, that moderate thermophiles capable of growth at such temperatures are common in hotter environments (An *et al.*, 2013). It should also be noted that microbial activity was only implicated in 2 of the 3 inoculated 25ºC triplicates (Fig. 4), possibly due to the heterogeneous distribution of active biomass in the initial sediment used for the inoculation of the microcosms (Fig. 6*c*). It may also be due to the development of lower pH niches in some of the microcosms (the samples were only shaken every 6 months during sampling), where some bacteria could have thrived by fermenting the added cellulosic material, which would have, in turn, caused a drop in the pH of the whole microcosm. Despite these differences between the triplicate samples the microcosms that showed the greatest yields of bacterial DNA (Fig. 5) also showed a cessation of ISA production (Fig. 4), which may be due to the decrease in pH associated with microbial activity, which in turn limited the abiotic production of ISA.

The increase in bacterial DNA yield (Fig. 5) and the drop in bacterial diversity (Fig. 6*a*) in the tissue microcosm (sample 1) after 30 months of incubation at 25ºC, indicates the selection of specific bacteria that are able to proliferate under ILW-GDF simulated conditions. In contrast to previous data reported on the bacterial diversity in surface low-level waste disposal sites (Field *et al.*, 2010), which were dominated by Gram-negative Proteobacteria, the tissue microcosm in this study that supported bacterial growth (sample 1), was dominated by Gram-positive Firmicutes. Members

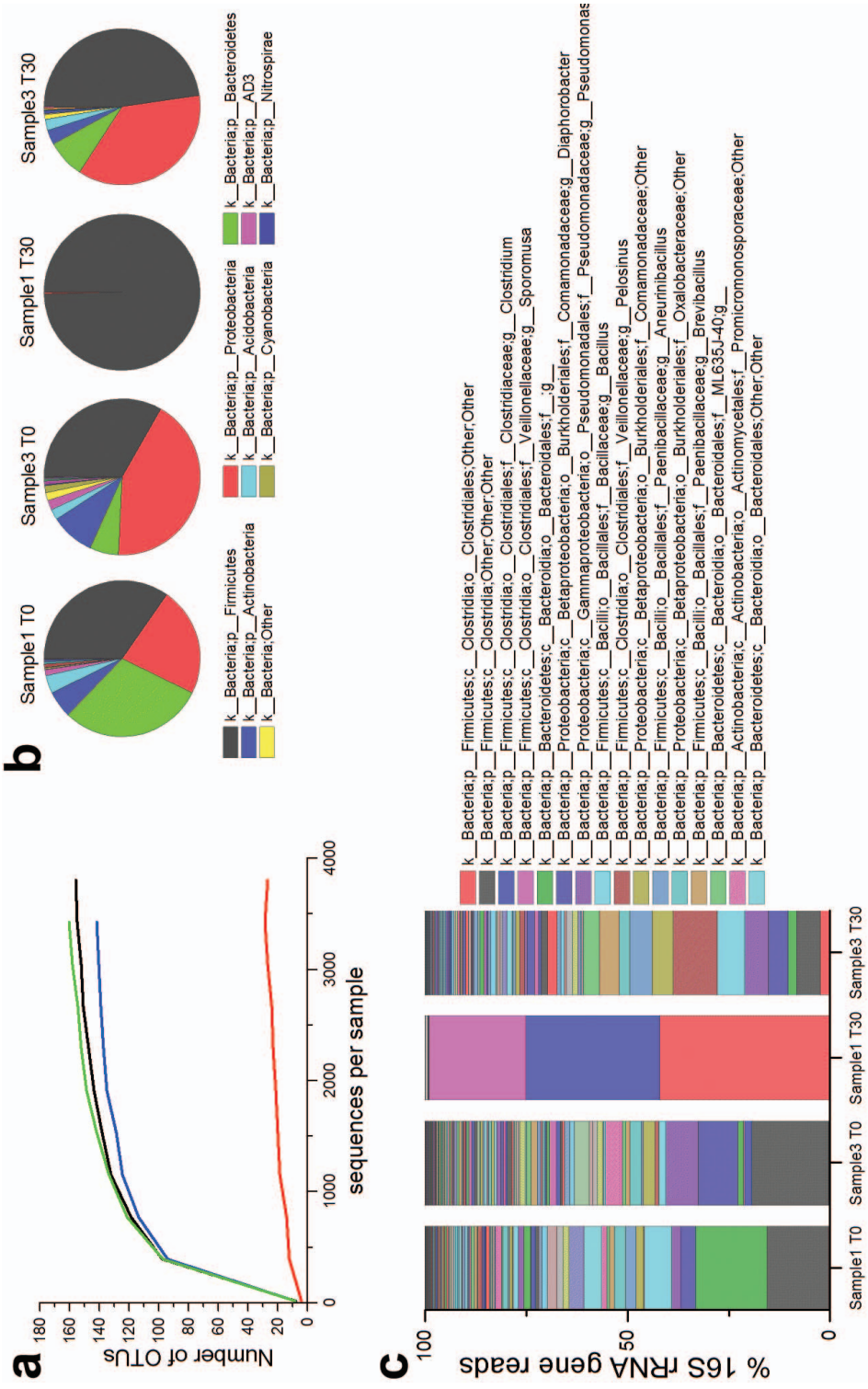

FIG. 6. Microbial diversity from 454 pyrosequencing analyses of the two tissue microcosms (samples 1 and 3), incubated at 25°C in the presence of $Ca(OH)_2$ at saturation at T_0 and T_{30}. (*a*) Alpha-diversity plot showing the number of OTUs with respect to the number of reads in sample 1 at T_0 (green), sample 3 at T_0 (black), sample 1 at T_{30} (red) and sample 3 at T_{30} (blue). (*b*) Pie charts showing the bacterial phyla present in each sample. (*c*) Bar chart showing the bacterial genera in the different samples that were analysed. All taxa that show less than 4% presence are shown in the graph, but not indicated in the legend.

of this latter group produce recalcitrant endospores that may give them the advantage needed to survive under hyperalkaline pH conditions. The dominance of *Clostridia* in this sample was expected as a number of species belonging to the *Clostridium* genus are anaerobic, spore-forming, cellulolytic bacteria (Leschine, 1995). Methane production could have a significant impact on C-14 transport and is a concern for an ILW-GDF safety case, so it is interesting to note the presence of the *Sporomusa* genus (some species of which are homoacetogenic) (Fig. 6*c*), along with the absence of methanogenic archaea (Fig. 5). These results suggest that methanogenesis is minimal in our high pH model system, but clearly warrants further research under alkaline conditions, which have been poorly studied in this context. Collectively, these results indicate that environmental microorganisms may be able to survive, as recalcitrant spores, the initial hyperalkaline pH that is expected to dominate on closure of the repository and subsequent resaturation with groundwater. It is important to note that the pH in the GDF will stay hyperalkaline for a much longer period than in our microcosm experiments, however bacterial spores are known to survive for extended periods (thousands of years) in a range of environments (O'Sullivan *et al.*, 2014). Furthermore, when the conditions become more suitable for growth, alkaliphilic, anaerobic bacteria may be able to affect the chemistry in and around the GDF through the degradation and fermentation of the cellulose present, and the subsequent production of CO_2, H_2, acetate and other fermentation products. Although it will depend largely on the amount of cement added and the amount of cellulose present, these fermentation products could have an impact on the pH buffering in zones affected by GDF processes (especially in niche areas), promoting colonization by a wider range of non-alkaliphilic microorganisms including neutrophiles.

In conclusion, these and previous results (Bassil *et al.*, 2014), suggest that microorganisms are capable of colonizing high pH environments analogous to those that will develop in an ILW-GDF. These microorganisms have the potential to play a controlling role in moderating the production (*via* fermentation processes observed in this study) and/or the subsequent degradation of radionuclide complexants, such as ISA (e.g. by coupling its oxidation to the reduction of electron acceptors such as nitrate (Bassil *et al.*, 2014)). Such activities should be considered when predicting the long-term biogeochemical evolution of ILW-GDFs.

Acknowledgements

This work was supported by the BIGRAD consortium under the UK Natural Environmental Research Council (NE/H007768/1) and The National Nuclear Laboratories Signature Research Programme. The authors thank Christopher Boothman for help with setting up the microcosms. JRL acknowledges support from the Royal Society. NMB thanks the National Council for Scientific Research-Lebanon.

References

An, S., Couteau, C., Luo, F., Neveu, J. and DuBow, M.S. (2013) Bacterial diversity of surface sand samples from the Gobi and Taklamaken deserts. *Microbial Ecology*, **66**, 850–860.

Bassil, N.M., Bryan, N. and Lloyd, J.R. (2014) Microbial degradation of isosaccharinic acid at high pH. *The ISME Journal*, doi:10.1038/ismej.2014.125.

Beguin, P. and Aubert, J.P. (1994) The biological degradation of cellulose. *FEMS Microbiology Reviews*, **13**, 25–58.

Berner, U.R. (1992) Evolution of pore water chemistry during degradation of cement in a radioactive waste repository environment. *Waste Management*, **12**, 201–219.

Borneman, J. and Hartin, R.J. (2000) PCR primers that amplify fungal rRNA genes from environmental samples. *Applied and Environmental Microbiology*, **66**, 4356–4360.

DeLong, E.F. (1992) Archaea in coastal marine environments. *Proceedings of the National Academy of Sciences*, **89**, 5685–5689.

Field, E.K., D'Imperio, S., Miller, A.R., VanEngelen, M.R., Gerlach, R., Lee, B.D., Apel, W.A. and Peyton, B.M. (2010) Application of molecular techniques to elucidate the influence of cellulosic waste on the bacterial community structure at a simulated low-level-radioactive-waste site. *Applied and Environmental Microbiology*, **76**, 3106–3115.

Gaona, X., Montoya, V., Colas, E., Grive, M. and Duro, L. (2008) Review of the complexation of tetravalent actinides by ISA and gluconate under alkaline to hyperalkaline conditions. *Journal of Contaminant Hydrology*, **102**, 217–227.

Glaus, M.A. and Van Loon, L.R. (2008) Degradation of cellulose under alkaline conditions: New insights from a 12 years degradation study. *Environmental Science & Technology*, **42**, 2906–2911.

Glaus, M.A., van Loon, L.R., Achatz, S., Chodura, A.

and Fischer, K. (1999) Degradation of cellulosic materials under the alkaline conditions of a cementitious repository for low and intermediate level radioactive waste part i: Identification of degradation products. *Analytica Chimica Acta*, **398**, 111–122.

Grant, S., Sorokin, D.Y., Grant, W.D., Jones, B.E. and Heaphy, S. (2004) A phylogenetic analysis of Wadi el Natrun soda lake cellulase enrichment cultures and identification of cellulase genes from these cultures. *Extremophiles*, **8**, 421–429.

Keith-Roach, M.J. (2008) The speciation, stability, solubility and biodegradation of organic co-contaminant radionuclide complexes: A review. *Science of the Total Environment*, **396**, 1–11.

Lane, D.J. (1991) 16S/23S rRNA sequencing. Pp. 115–174 in: *Nucleic Acid Techniques in Bacterial Systematics* (E. Stackebrandt and M. Goodfellow, editors). John Wiley & Sons Ltd., London.

Leschine, S.B. (1995) Cellulose degradation in anaerobic environments. *Annual Review of Microbiology*, **49**, 399–426.

Lynd, L.R., Weimer, P.J., van Zyl, W.H. and Pretorius, I.S. (2002) Microbial cellulose utilization: Fundamentals and biotechnology. *Microbiology and Molecular Biology Reviews*, **66**, 739–739.

Nuclear Decommissioning Authority (2014) *The 2013 UK Radioactive Waste Inventory: Radioactive Waste Composition*. Nuclear Decommissioning Authority, Moor Raw, Cumbria, UK.

O'Sullivan, L.A., Roussel, E.G., Weightman, A.J., Webster, G., Hubert, C.R.J., Bell, E., Head, I., Sass, H. and Parkes, R.J. (2014) Survival of *Desulfotomaculum* spores from estuarine sediments after serial autoclaving and high-temperature exposure. *The ISME Journal*, doi:10.1038/ismej.2014.190.

Pavasars, I., Hagberg, J., Boren, H. and Allard, B. (2003) Alkaline degradation of cellulose: Mechanisms and kinetics. *Journal of Polymers and the Environment*, **11**, 39–47.

Rizoulis, A., Steele, H.M., Morris, K. and Lloyd, J.R. (2012). The potential impact of anaerobic microbial metabolism during the geological disposal of intermediate-level waste. *Mineralogical Magazine*, **76**, 3261–3270.

Robidart, J., Callister, S.J., Song, P., Nicora, C.D., Wheat, C.G. and Girguis, P.R. (2013) Characterizing microbial community and geochemical dynamics at hydrothermal vents using osmotically driven continuous fluid samplers. *Environmental Science and Technology*, **47**, 4399–4407.

Van Loon, L.R. and Glaus, M.A. (1997) Review of the kinetics of alkaline degradation of cellulose in view of its relevance for safety assessment of radioactive waste repositories. *Journal of Environmental Polymer Degradation*, **5**, 97–109.

Van Loon, L.R., Glaus, M.A., Laube, A. and Stallone, S. (1999) Degradation of cellulosic materials under the alkaline conditions of a cementitious repository for low- and intermediate-level radioactive waste. II. Degradation kinetics. *Journal of Environmental Polymer Degradation*, **7**, 41–51.

Vercammen, K., Glaus, M.A. and Van Loon, L.R. (1999) Complexation of calcium by alpha-isosaccharinic acid under alkaline conditions. *Acta Chemica Scandinavica*, **53**, 241–246.

Zhilina, T.N. and Zavarzin, G.A. (1994) Alkaliphilic anaerobic community at pH 10. *Current Microbiology*, **29**, 109–112.

Zhilina, T.N., Kevbrin, V.V., Tourova, T.P., Lysenko, A.M., Kostrikina, N.A. and Zavarzin, G.A. (2005) *Clostridium alkalicellum* sp. nov., an obligately alkaliphilic cellulolytic bacterium from a soda lake in the Baikal region. *Microbiology*, **74**, 557–566.

Chapter 5

Microbial degradation of isosaccharinic acid at high pH

Paper published in The ISME Journal

Naji M. Bassil, Nicholas Bryan, Jonathan R. Lloyd. 2014. Microbial degradation of isosaccharinic acid at high pH. The ISME Journal 9: 310-320.

Author contributions: N. M. Bassil - Principal author, preparation and monitoring of samples and data acquisition and analysis; N. Bryan – Co-author and manuscript review; J. R. Lloyd – Corresponding author and manuscript review.

The ISME Journal (2015) 9, 310–320

www.nature.com/ismej

OPEN

ORIGINAL ARTICLE

Microbial degradation of isosaccharinic acid at high pH

Naji M Bassil[1,2], Nicholas Bryan[3] and Jonathan R Lloyd[1]
[1]*Research Centre for Radwaste and Decommissioning and Williamson Research Centre for Molecular Environmental Science, School of Earth, Atmospheric and Environmental Sciences, University of Manchester, Manchester, UK;* [2]*National Council for Scientific Research–Lebanon (CNRS-L), Beirut, Lebanon and* [3]*National Nuclear Laboratory, Birchwood Park, Warrington WA3 6AE, UK*

Intermediate-level radioactive waste (ILW), which dominates the radioactive waste inventory in the United Kingdom on a volumetric basis, is proposed to be disposed of via a multibarrier deep geological disposal facility (GDF). ILW is a heterogeneous wasteform that contains substantial amounts of cellulosic material encased in concrete. Upon resaturation of the facility with groundwater, alkali conditions will dominate and will lead to the chemical degradation of cellulose, producing a substantial amount of organic co-contaminants, particularly isosaccharinic acid (ISA). ISA can form soluble complexes with radionuclides, thereby mobilising them and posing a potential threat to the surrounding environment or 'far field'. Alkaliphilic microorganisms sampled from a legacy lime working site, which is an analogue for an ILW-GDF, were able to degrade ISA and couple this degradation to the reduction of electron acceptors that will dominate as the GDF progresses from an aerobic 'open phase' through nitrate- and Fe(III)-reducing conditions post closure. Furthermore, pyrosequencing analyses showed that bacterial diversity declined as the reduction potential of the electron acceptor decreased and that more specialised organisms dominated under anaerobic conditions. These results imply that the microbial attenuation of ISA and comparable organic complexants, initially present or formed *in situ*, may play a role in reducing the mobility of radionuclides from an ILW-GDF, facilitating the reduction of undue pessimism in the long-term performance assessment of such facilities.
The ISME Journal (2015) **9,** 310–320; doi:10.1038/ismej.2014.125; published online 25 July 2014

Introduction

High pH environments are present on Earth. They can be natural, for example, some geothermal springs and soda lakes, or man-made, for example, effluent ponds from paper pulping industries, lime working sites and closed structures made of cement. One such engineered structure is the deep geological disposal facility (GDF) that is being proposed for the safe disposal of radioactive waste. The largest volume of waste deposited into a GDF will be intermediate-level waste (ILW), which will be immobilised in steel containers backfilled with cementitious material to form a physical barrier in the form of a cement matrix (Nuclear Decommissioning Authority, 2014). The chemical and biological processes in and around this facility remain poorly understood, and therefore the impact of this facility on its surrounding environment remains uncertain. ILW contains substantial amounts of cellulosic material (Nuclear Decommissioning Authority, 2014), surrounded by hyperalkaline porewaters (Berner, 1992), and during disposal under these conditions, cellulose is known to be unstable (Van Loon and Glaus, 1997), and degrades chemically to short-chain organic acids (Glaus *et al.*, 1999), especially in the presence of radiation (Bouchard *et al.*, 2006). Although the nature and concentrations of the different products are influenced by temperature and the nature of the cellulose present (Haas *et al.*, 1967; Van Loon *et al.*, 1999), one of the main products of these degradation reactions is isosaccharinic acid (ISA) (IUPAC: 2,4,5-Trihydroxy-2-(hydroxymethyl)pentanoic acid) (Glaus *et al.*, 1999). At high pH, this molecule was found to sorb to cement in small amounts (Van Loon *et al.*, 1997), and is able to complex with a number of metals and radionuclides, particularly Ni(II) (Warwick *et al.*, 2003), Ca(II) (Vercammen *et al.*, 1999), Th(IV) (Vercammen *et al.*, 2001; Tits *et al.*, 2005), U(IV) (Warwick *et al.*, 2004), Eu(III) (Vercammen *et al.*, 2001; Tits *et al.*, 2005), Am(III) (Tits *et al.*, 2005) and Np(IV) (Rai *et al.*, 2003; Gaona *et al.*, 2008), making them potentially more mobile (Wieland *et al.*, 2002) and more likely to reach the biosphere.

Correspondence: JR Lloyd, Williamson Research Centre for Molecular Environmental Science, School of Earth, Atmospheric and Environmental Sciences, University of Manchester, Oxford Road, Manchester M13 9PL, UK.
E-mail: jon.lloyd@manchester.ac.uk
Received 16 March 2014; revised 5 June 2014; accepted 11 June 2014; published online 25 July 2014

The GDF has previously been considered to be an extreme environment where stresses including hyperalkalinity, radiation and radionuclide toxicity may play a role in limiting microbial colonisation. However, it is becoming clear that microbes may tolerate such extreme conditions (Chicote *et al.*, 2004; Rizoulis *et al.*, 2012); and as ILW will contain substantial amounts of organic molecules including cellulose and its alkali degradation products and other organic chelating agents like EDTA and nitrilotriacetic acid, used in remediation and decontamination processes, microbial colonisation should not be discounted. These organic molecules could be used as electron donors by microorganisms that respire a broad range of electron acceptors, including oxygen, nitrate, Fe(III) and sulphate. Given that natural alkaline environments harbour a wide diversity of microorganisms, it is safe to assume that the 'evolved' GDF, resaturated with groundwater, might be a potential niche for a variety of specialist microorganisms including ISA-degrading organisms that can help reduce the transport of radionuclides from the GDF.

To date, only a few publications have addressed the microbial degradation of ISA, and these have focussed on aerobic conditions in paper pulping wastes. Strand *et al.* (1984) showed that *Ancylobacter aquaticus* is able to degrade ISA at pH values between 7.2 and 9.5 under aerobic conditions. Bailey (1986) identified two strains of aerobic bacteria that are able to degrade ISA at pH values between 5.1 and 7.2. On the other hand, Maset *et al.* (2006) have shown recently that biogeochemical redox progression from aerobic to Fe(III) reduction is possible when a sediment is incubated in the presence of ISA, although the degradation of ISA was not studied under these conditions. Therefore, the aim of this work is to study the microbial degradation of ISA under a number of biogeochemical conditions at high pH. This study will better inform GDF safety case assessments, and more specifically highlight the potential of microbial metabolism to decrease radionuclide mobility through the degradation of the complexant ISA.

Materials and methods

Sediment acquisition
Sediment samples were collected from a depth of ~20 cm from the surface of a site, at Harpur Hill, Buxton, UK, that had been contaminated for decades by high pH legacy lime works. The sediments at the site generally have a pH between 11 and 12 and contain high calcium and silicate concentrations, analogous to a cementitious radioactive waste repository (Rizoulis *et al.*, 2012).

Ca(α-ISA)$_2$ preparation
Preparation of the Ca salt of α-ISA was performed following the procedure reported by Vercammen *et al.* (1999). Briefly, 500 ml of argon flushed double-distilled (dd) H_2O was mixed with 50 g of α-lactose monohydrate and 13.6 g of $Ca(OH)_2$ and left to react for 3 days under anaerobic conditions and at room temperature. The mixture was then boiled for 6 h, keeping the volume constant by adding dd H_2O. The solution was then filtered while hot, and the volume of the filtrate reduced to ~100 ml by boiling. The remaining solution was stored overnight at 4 °C. The white precipitate that formed was filtered and then washed sequentially with water, ethanol and acetone and dried overnight at 50 °C. The dry precipitate was redissolved at a ratio of 1.2 g in 100 ml of dd H_2O by boiling. While still hot, the solution was filtered and the volume of the filtrate was reduced to ~10 ml by boiling. The white precipitate that formed was washed sequentially with water, ethanol and acetone and then dried overnight at 50 °C.

Aerobic cultures
Aerobic cultures were prepared in 100 ml serum bottles where 19.5 ml of minimal medium, containing 30 mM $NaHCO_3$, 4.7 mM NH_4Cl, 4.4 mM $NaH_2PO_4.H_2O$, 1.4 mM KCl and 2 ml of mineral and vitamin solutions (Lovley *et al.*, 1984), was mixed with 200 µl of an inoculum of slightly turbid water overlaying the sediment samples from the Buxton site, and 2 mM $Ca(ISA)_2$. The bottles were closed with a foam bung before autoclaving to allow the passage of air in and out of the bottles while preventing contamination from the surrounding environment. A 'sterile' control along with a 'no electron donor' control that did not contain any added carbon source were also prepared. All samples were prepared in triplicate and the pH was adjusted to 10 using 10 M NaOH before autoclaving. The cultures were left in a 20 °C incubator for the period of the experiment (until the stationary phase (assessed by turbidity) of the enrichment culture was reached). Samples (1 ml) were removed inside a laminar flow cabinet and the pH and absorbance at 600 nm were measured. The samples were frozen at −20 °C until the end of the experiment, when they were analysed by ion-exchange chromatography for ISA and a range of geochemical indicators. The test cultures were subcultured 4 times by taking 200 µl of the culture and adding it to freshly prepared medium under the same conditions. The data from the last subculture are shown.

Nitrate-reducing cultures
Nitrate-reducing cultures were prepared following the same procedure as used with the aerobic cultures. However, 24 mM $NaNO_3$, as the terminal electron acceptor (TEA), was added to the culture medium and the bottles were stoppered with rubber butyl stoppers and then degassed with N_2 for 30 min before being autoclaved and the inoculum added. The same controls were used as in the aerobic

culture experiments, in addition to a 'no electron acceptor' control that contained 2 mM $Ca(ISA)_2$ without $NaNO_3$ added as the electron acceptor. Samples were taken with a 1 ml syringe and the pH and absorbance at 600 nm measured, and then they were frozen at −20 °C until they were analysed using ion-exchange chromatography. The test cultures were subcultured 3 times and the data from the last subculture are shown.

Isolation of nitrate-reducing bacteria
The same minimal medium that was used for growth of the planktonic nitrate-reducing cultures was supplemented with 1% agar, pH adjusted to 10, flushed with N_2 for 30 min, autoclaved and poured into petri dishes inside a laminar flow cabinet. After solidification of the agar, the plates were transferred into an anaerobic chamber and left upside down for 4 days. A subsample from the last subculture of the nitrate-reducing culture (the same one that was used for pyrosequencing studies) was spread onto the plates with a sterile disposable plastic spreader. The inoculated plate and a control plate were put in a sealed GasPak jar (Becton Dickinson, Franklin Lakes, NJ, USA), closed and incubated at 20 °C under anaerobic conditions. After 3 days, small transparent colonies were observed and five representative colonies were isolated using a sterile 5 µl microbiology loop and transferred to 20 ml of sterile minimal medium supplemented with 2 mM $Ca(ISA)_2$ and 24 mM $NaNO_3$. These bottles were incubated at 20 °C for 10 days, during which they were monitored for bacterial growth, pH change, ISA degradation and nitrate reduction. After the stationary growth phase was reached, 10 ml of the liquid culture was centrifuged at 4000 *g* for 10 min and the pellet was used for DNA extraction and microbial identification using Sanger sequencing of PCR amplified 16S rRNA gene.

Fe(III)-reducing cultures
Fe(III)-reducing cultures were prepared and sampled in the same way as the nitrate-reducing cultures, except that 30 mmol l^{-1} of insoluble Fe(III) oxyhydroxide (ferrihydrite) (Lovley and Phillips, 1986) was added instead of $NaNO_3$ as the TEA. The concentration of Fe(II) was determined spectrophotometrically after reaction with ferrozine (Lovley and Phillips, 1987). The test cultures were subcultured twice and data from the last subculture are shown.

Sulphate-reducing cultures
Sulphate-reducing cultures were prepared and sampled following the same procedure as the nitrate-reducing culture, but the $NaNO_3$ was replaced with 6 mM Na_2SO_4. These samples were not subcultured because, after 60 days of incubation of the primary enrichment culture, no reduction of sulphate or degradation of ISA was observed under the conditions imposed.

Ion-exchange chromatography
The frozen samples were thawed at room temperature, vortexed for homogenisation and then centrifuged at 13 000 *g* for 5 min at room temperature to remove bacteria and any solid material. These samples were diluted 50 times and then analysed by ion-exchange high-performance liquid chromatography using a Dionex ICS5000 Dual Channel Ion Chromatograph with a conductivity detector (Thermo Fisher Scientific, Waltham, MA, USA). The samples were put in 2 ml glass vials with pre-split septa and cooled to 15 °C, and then 0.4 µl was injected into the chromatograph through a Dionex AS-AP autosampler. Molecule separation was achieved by passing the samples through a 250 × 0.4 mm Dionex AS11-HC capillary column with a 4 µm pore size, operating at 30 °C, with a typical operating pressure of 3400 psi and a flow rate of 0.015 ml min^{-1}. The mobile phase used was a KOH solution, prepared in high-purity water, electronically injected to produce a gradient from 1 to 60 mM over a 38 min run time, followed by a 10 min re-equilibrium before the next injection. The chromatograph was calibrated at 4 points ranging from 0.5 to 30 mg l^{-1} for nitrate, nitrite and sulphate, 0.5–10 mg l^{-1} for acetate, formate, lactate, propionate and butyrate and 0.01–0.1 mM for ISA.

454 pyrosequencing
DNA was extracted from samples of aerobic, nitrate-reducing and Fe(III)-reducing cultures and the background sediment using the PowerSoil DNA isolation kit (MO BIO Laboratories, Carlsbad, CA, USA) according to the manufacturer's protocol. Pyrosequencing PCR was performed using the FastStart High Fidelity PCR System (Roche, Basel, Switzerland) and the 27F and 338R universal primers to cover the V1–V2 hypervariable regions of the 16S rRNA gene (Lane, 1991). The 338R primer with the sequence 5′-GCWGCCTCCCGTAGGAGT-3′ was used for all the samples. However, each sample had a unique F primer with a different barcode sequence to distinguish between the different samples. The F primers included the 454 Life Sciences (Bradford, CT, USA) adapter region with the sequence 5′-**CCATCTCATCCCTGCGTGTCTCCGACTCAG**-3′, followed by the 10 bp barcode sequence specific to each sample, where the background sediment had the sequence 5′-CTCGCGTGTC-3′, the aerobic sample 5′-CGTGTCTCTA-3′, the nitrate-reducing sample 5′-ATATCGCGAG-3′ and finally the Fe(III)-reducing sample had the sequence 5′-TCTCTATGCG-3′. The bold and underlines differentiate between the 454 Life Sciences adapter sequence and the barcode sequence in the forward

primers we used for each sample. The barcode sequence was followed by the universal 27F primer sequence 5′-AGAGTTTGATCMTGGCTCAG-3′. The PCR mastermix contained, per sample, 40 μl sterile purified H_2O, 5 μl of 10 × PCR reaction buffer, 1 μl dNTP mix, 0.8 μl of 25 μM 338R primer and 0.4 μl High Fidelity Enzyme Blend. To perform the PCR, 47.2 μl of this mastermix was transferred into a sterile 50 μl PCR reaction tube, where 0.8 μl of one of each barcoded 27F primer and 2 μl of DNA, taken from the sample corresponding to each specific barcode, were added to separate tubes. A negative and a positive control for the PCR reaction, which contained 2 μl sterile H_2O or DNA extracted from *Geobacter sulfurreducens*, respectively, were also prepared. The PCR conditions were: initial denaturation at 95 °C for 2 min, followed by 35 cycles of denaturation at 95 °C for 30 s, primer annealing at 55 °C for 30 s and extension at 72 °C for 45 s, followed by a final extension step at 72 °C for 5 min. At the end of the PCR run, the whole PCR product was mixed with 12.5 μl of 5 × gel-loading dye, and 35 μl of the mixture was loaded on a 2% Tris-Acetate-EDTA/agarose gel. A 2000–100 bp ladder was also loaded on the gel that was run at 80 mV for ~2 h. At the end of the run, the DNA bands were observed on a Gel Doc XR system (Bio-Rad Laboratories, Hercules, CA, USA) and the band corresponding to 400 bp size for each sample was excised from the gel. DNA extraction and cleanup from the excised gel were performed using a QIAquick Gel Extraction Kit (Quiagen, Limburg, The Netherlands), according to the manufacturer's protocol. DNA was quantified on a Nanodrop ND-1000 (Thermo Scientific) and all samples were diluted to 10 ng μl^{-1}. The DNA product was then stored at 4 °C until it was sequenced using a 454 GS Junior pyrosequencing system (Roche), using the facility in the Faculty of Life Sciences, University of Manchester.

Pyrosequencing data analysis

Analysis of the raw 454 pyrosequencing data was done using the Quantitative Insights Into Microbial Ecology pipeline (Caporaso *et al.*, 2010b). Sequences were first assigned to the different samples by using the barcode sequences provided, and sequences outside the 300–400 bp range were removed along with the reverse primer sequence, using the split_library.py script. Chimeric sequences were identified using the usearch 6.1 programme (Edgar *et al.*, 2011) and the identify_chimeric_seqs.py script. Chimeric sequences were filtered out of the data using the filter_fasta.py script. Operational taxonomic units (OTUs) were picked from these sequences and compared at 97% similarity with the May 2013 release of greengenes OTU reference using the usearch 6.1 programme (Edgar, 2010) through the pick_otus.py script. The most abundant OTU sequence was chosen as a representative sequence, using the pick_rep_set.py script, and assigned to taxonomy based on the greengenes reference database (McDonald *et al.*, 2012) using the Ribosomal Database Project Naive Bayes classifier v 2.2 (Wang *et al.*, 2007), with the confidence level set at 80% through the assign_taxonomy.py script. The sequences were then aligned to the greengenes core reference alignment (DeSantis *et al.*, 2006) using PyNAST (Caporaso *et al.*, 2010a) through the align_seqs.py script. Aligned sequences were then filtered using the filter_alignement.py script, and a phylogenetic tree was built through the make_phylogeny.py (Price *et al.*, 2009). An OTU table was built through the make_otu_table.py and convert_biom.py scripts and was used to calculate and plot the α-diversity (based on the number of OTUs) and the % 16S rRNA gene reads in each sample using the OriginPro v 9 software (OriginLab, Northampton, MA, USA) .

Sanger sequencing of 16S rRNA genes from pure cultures

DNA was extracted from the pellets of the five isolates of the nitrate-reducing culture using the PowerSoil DNA isolation kit (MO BIO Laboratories) according to the manufacturer's protocol. The 16S rRNA gene was amplified by PCR using the TaKaRa Ex Taq Polymerase (EMD Millipore, Billerica, MA, USA) and universal primers 8F (with the sequence 5′-AGAGTTTGATCCTGGCTCAG-3′) and 1492R (with the sequence 5′-TACGGYTACCTTGTTAC GACTT-3′) for the whole 16S rRNA gene (Turner *et al.*, 1999). The PCR mastermix contained, per sample, 36.7 μl sterile purified H_2O, 5 μl of 10 × Ex buffer, 4 μl dNTP mix, 1 μl of 25 μM 8F and 1492R primers and 0.3 μl Ex TaKaRa Taq polymerase. To perform the PCR, 48 μl of this mastermix was transferred into a sterile 50 μl PCR reaction tube and 2 μl of the extracted DNA was added. A negative and a positive control for the PCR reaction, which contained 2 μl sterile H_2O or DNA extracted from *Geobacter sulfurreducens*, respectively, were also prepared. The PCR conditions were: initial denaturation at 94 °C for 4 min, followed by 30 cycles of denaturation at 94 °C for 30 s, primer annealing at 55 °C for 30 s and extension at 72 °C for 1.5 min, followed by a final extension step at 72 °C for 5 min. The purity of the amplified product was determined by running 8 μl of the PCR product with 2 μl of 5 × gel loading dye on a 1% Tris-Acetate-EDTA/agarose gel against a 2000 bp DNA ladder. The PCR product (~1500 bp) was cleaned from the PCR salts using the ExoSap (Affimetrix, Santa Clara, CA, USA) protocol, where 0.08 μl Exonuclease I (20 U μl^{-1}; New England Biolabs, Ipswich, MA, USA), 1.5 μl rAPid Alkaline Phosphatase (1 U μl^{-1}; Roche) and 1.42 μl dd H_2O were mixed with 3 μl of the PCR product, incubated at 37 °C for 30 min and then at 80 °C for 15 min. Nucleotide sequences were determined by the dideoxynucleotide method by cycle sequencing using an ABI Prism 377 DNA sequencer

(Applied Biosystems, Carlsbad, CA, USA). A pre-sequencing PCR step was performed using the ABI Prism BigDye Terminator Cycle Sequencing Kit v 3.1 (Applied Biosystems) and the 16S gene universal 8F primer. The PCR mastermix contained 0.75 µl Terminator BigDye, 3.65 µl 5 × buffer, 0.15 µl 8F primer and 14.95 µl dd H_2O. The DNA template from the cleanup step was quantified on a Nanodrop ND-1000 (Thermo Scientific) and diluted to get 40 ng of DNA per PCR reaction. The PCR conditions were: initial denaturation at 96 °C for 2 min, followed by 30 cycles of denaturation at 96 °C for 40 s, primer annealing at 55 °C for 15 s and 60 °C for 3 min, followed by a final extension step at 72 °C for 5 min. The PCR product was then precipitated following the ethanol/EDTA precipitation protocol supplied with the kit. The data produced were analysed against the NCBI database, using the Basic Local Alignment Search Tool (megaBLAST) programme package and matched to known 16S rRNA gene sequences.

Results

To determine whether alkaliphilic or alkalitolerant microbial communities, capable of ISA degradation, are present in a high pH analogue site for concrete-based ILW, samples from the Harpur Hill (Buxton, Derbyshire, UK) historic lime workings were inoculated into defined minimal medium containing ISA as the sole electron donor and either oxygen (as air), nitrate, Fe(III) or sulphate as an electron acceptor. Under aerobic conditions (Figure 1), all the added ISA was degraded within 9 days of incubation. This ISA degradation was accompanied by an increase in turbidity and a drop in pH indicating bacterial growth and the production of CO_2 as a product of ISA degradation (the latter linked to acidification of the medium via the formation of bicarbonate). Under nitrate-reducing conditions (Figure 2), a broadly similar rate of degradation of ISA was recorded; however, complete removal of the substrate was noted within only 6 days of incubation that was coupled to the reduction of ~71% of the added nitrate to nitrite. Concomitant with the ISA degradation, substantial amounts of acetate (~3 mM) were produced between the initial time point and day 6 of incubation. The produced acetate was then degraded between days 6 and 15 of incubation, and part of the remaining nitrate was reduced to nitrite. Similar to the aerobic samples, the turbidity increased under nitrate-reducing conditions whereas the pH dropped, confirming bacterial growth and metabolism. Furthermore, bacteria in the nitrate-reducing cultures were also able to grow and cause a drop in the pH of the medium at a range of temperatures (10, 20 and 30 °C) in cultures incubated at starting pH values of 10 and 11 (Supplementary Figure S1), whereas no growth was observed at a starting pH of 12 even after 27 days of incubation. Under Fe(III)-reducing

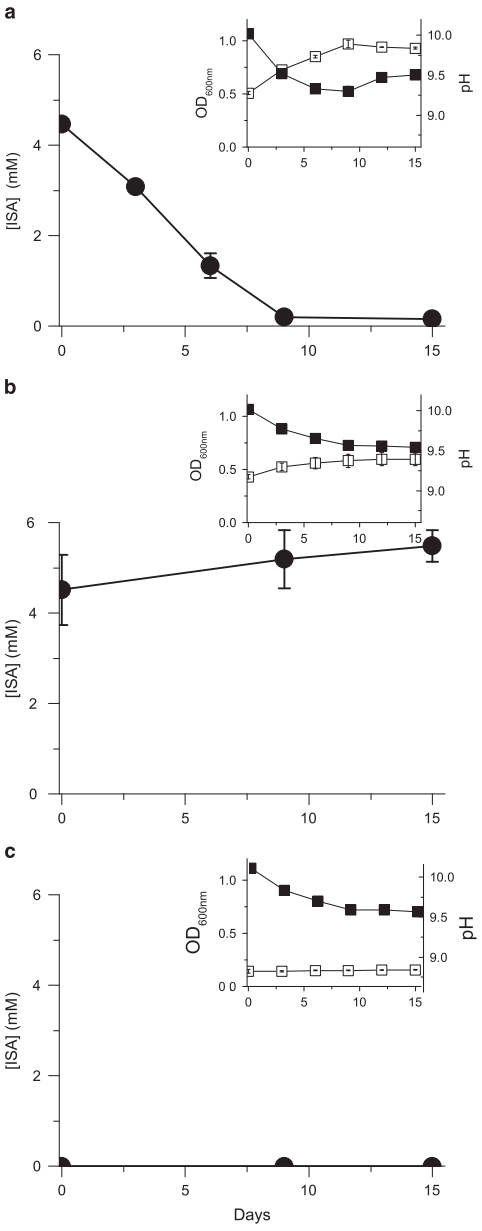

Figure 1 ISA biodegradation by aerobic microbial cultures at a starting pH of 10. (**a**) Test sample containing active microbial cells, (**b**) sterile (autoclaved) control and (**c**) a control containing an active inoculum but no added ISA as the sole carbon source and electron donor. Upper panels show bacterial growth ($OD_{600\,nm}$) (□) and pH (■). The lower panels show the concentration of ISA (●) in mM.

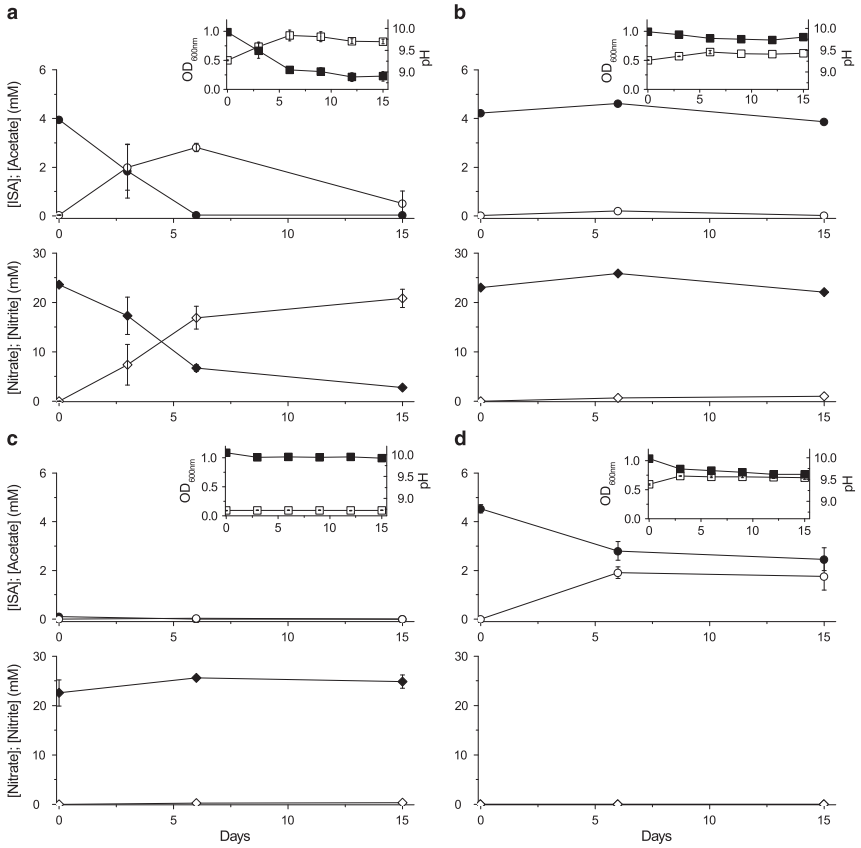

Figure 2 ISA biodegradation by nitrate-reducing microbial cultures at a starting pH of 10. (**a**) Test sample containing active microbial cells, (**b**) sterile (autoclaved) control, (**c**) a control containing an active inoculum but no added ISA as the sole carbon source and electron donor and (**d**) a control containing an active inoculum but no added nitrate as the electron acceptor. Upper panels show bacterial growth ($OD_{600\,nm}$) (□) and pH (■). The middle panels show concentrations of ISA (●) and acetate (○) in mM. The lower panels show concentrations of nitrate (♦) and nitrite (◇) in mM.

conditions (Figure 3), only ~36% of the added ISA was degraded, even after 90 days of incubation. This was accompanied by the reduction of ~21% of the added Fe(III) to Fe(II) and the production of acetate as a breakdown product. As expected, the pH dropped only slightly because of the small amount of ISA that was degraded by microbial activity. The sulphate-reducing cultures (Supplementary Figure S2) did not show any signs of bacterial growth, ISA degradation or sulphate reduction even after 60 days of incubation under the same conditions as used in the previous cultures. These results are consistent with previous data, generated using similar high pH microcosms prepared from similar sediments from the Buxton field site, that did not support sulphate reduction when lactate and acetate were supplied as electron donors, even after 20 weeks of incubation (Rizoulis *et al.*, 2012). Therefore, these enrichment cultures showed a sequential degradation of ISA, where the rate and extent of ISA biodegradation generally decreased as the reduction potential of the TEA decreased (in the order aerobic ≈ nitrate > Fe(III), with no reduction of sulphate detected at pH 10).

PCR-based 16S rRNA gene analyses of the microbial communities in these enrichment cultures using 454 pyrosequencing showed that the sediment used for the starting inoculum contained a very complex bacterial community that became far less diverse under the highly selective growth conditions employed (Figure 4). This was evident in the α-diversity plot (Figure 4a) that showed a complex bacterial community in the background sediment (with 3060 OTUs) that declined sequentially as the

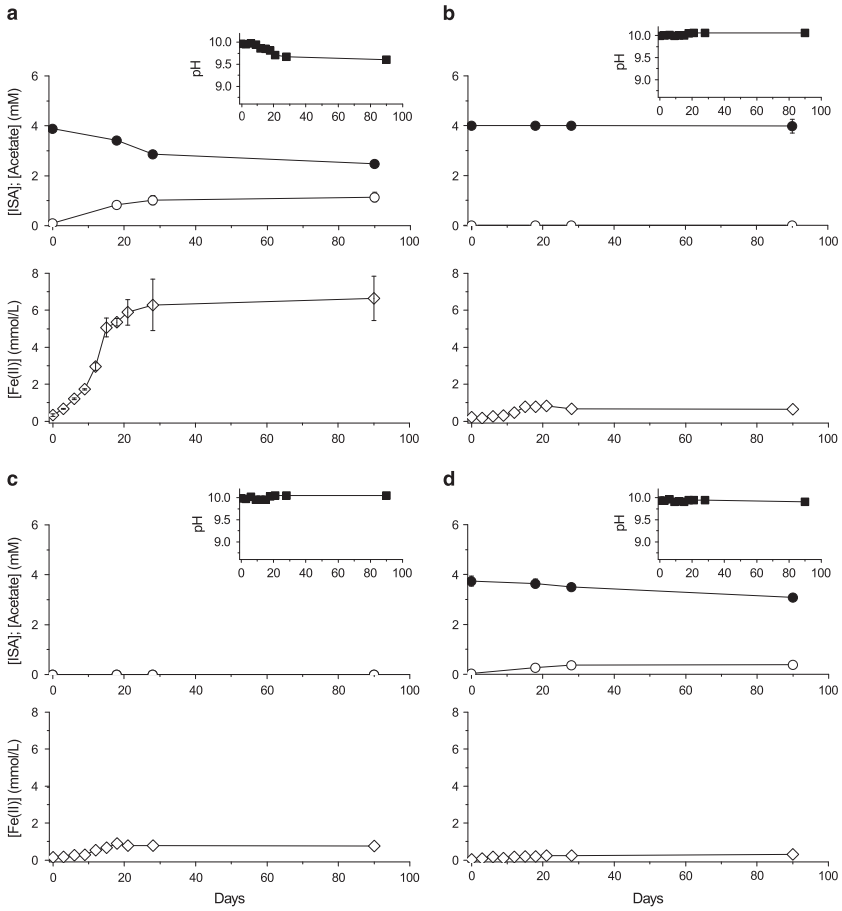

Figure 3 ISA biodegradation by Fe(III)-reducing microbial cultures at a starting pH of 10. (**a**) Test sample containing active microbial cells, (**b**) sterile (autoclaved) control, (**c**) a control containing an active inoculum but no added ISA as the sole carbon source and electron donor and (**d**) a control containing an active inoculum but no added Fe(III) as the electron acceptor. Upper panels show pH (■) change with time. The middle panels show concentrations of ISA (●) and acetate (○) in mM. The lower panels show concentrations of Fe(II) (◇) in mmol l^{-1}.

enrichment cultures progressed through a series of biogeochemical processes in the order aerobic (101 OTUs) > nitrate-reducing (64 OTUs) > Fe(III)-reducing conditions (33 OTUs). At the phylum level (Figure 4b), the background sediment and the aerobic cultures were dominated by Gram-negative bacteria, in particular Proteobacteria (44% and 81% of the 16S rRNA gene reads detected, respectively) and Bacteroidetes (24% and 13%, respectively), with a very low number of Gram-positive Firmicutes detected (6% and 3%, respectively). However, under anaerobic conditions, there was a dramatic shift in the dominant community structure, with the nitrate-reducing cultures containing an increased proportion (24%) of Gram-positive Firmicutes, and these also dominated the Fe(III)-reducing cultures (comprising almost 100% of the bacterial community). At the genus level (Figure 4c), the high microbial diversity in the background sediment and the aerobic cultures masked dominance of any particular bacterial genus in these samples; furthermore, very few OTUs were identified down to the genus level; however, these samples contained common soil bacteria such as *Aquimonas*. The bacterial genera that dominated the nitrate-reducing cultures were the facultative anaerobic denitrifiers *Azoarcus* (65%), and the obligate anaerobes *Paludibacter* (12%) and *Anaerobacillus* (21%), with the latter almost completely dominating the Fe(III)-reducing enrichment cultures (99.5%). Further

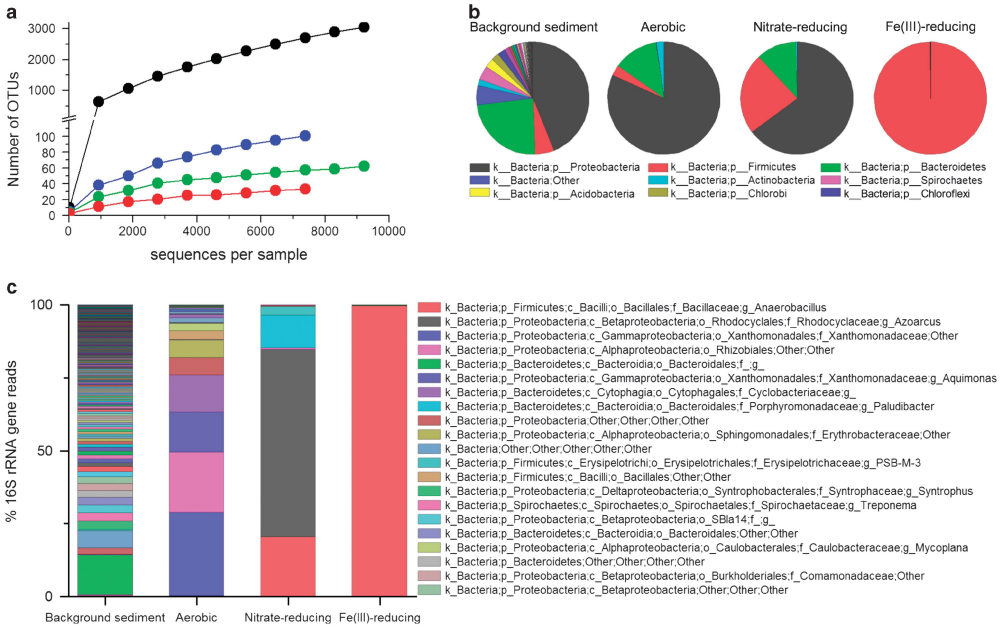

Figure 4 Microbial diversity from 454 pyrosequencing analyses of the starting inoculum, aerobic, nitrate- and Fe(III)-reducing ISA degrading cultures. (**a**) The α-diversity plot showing the number of OTUs in the background sediment (black), aerobic cultures (blue), nitrate-reducing cultures (green) and the Fe(III)-reducing cultures (red) with respect to the number of reads. (**b**) Pie charts showing the bacterial phyla present in each sample. (**c**) Bar chart showing the bacterial genera in the different samples that were tested. All taxa that show <2% expression are shown in the graph, but not indicated in the legend.

analysis was carried out using the megaBLAST programme package that matched the pyrosequencing data to known 16S rRNA gene sequences to find the closest known relatives to the OTUs identified in the nitrate- and Fe(III)-reducing enrichment cultures. This analysis showed that the OTU that dominated the nitrate-reducing cultures (65%) was a close relative (at 97% identity) of the facultative denitrifying bacterium *Aromatoleum aromaticum* (which belongs to the *Azoarcus* cluster) (Kuhner *et al.*, 2005), and the close relative *Azoarcus buckelii* (Mechichi *et al.*, 2002). The second most dominant OTU in the nitrate-reducing cultures (21%), which dominated the Fe(III)-reducing cultures with almost 100% coverage, was a close relative (at 94% identity) to the bacteria *Anaerobacillus macyae* (previously known as *Bacillus macyae*) (Santini *et al.*, 2004) and *Anaerobacillus alkalidiazotrophicus* (previously known as *Bacillus alkalidiazotrophicus*) (Sorokin *et al.*, 2008). The last OTU in this sample was most closely related to *Paludibacter propionicigenes* (Ueki *et al.*, 2006) (at 96% identity), a strictly anaerobic propionate and acetate producer.

Single colonies were isolated from agar plates prepared under nitrate-reducing conditions and all five isolates were able to degrade ISA and reduce nitrate at a similar rate to the mixed cultures under nitrate-reducing conditions (data not shown). Furthermore, analysis of the partial 16S rRNA gene sequence (1050 bp) of the isolates showed that all the isolates showed 98% similarity to the bacterium *A. alkalidiazotrophicus* and the related bacterium *A. macyae*. The former is an alkaliphilic strictly fermentative bacterium with no respiratory chain that can fix dinitrogen (Sorokin *et al.*, 2008), whereas the latter is an arsenate and nitrate respiring bacterium that is known to utilise acetate as an electron donor (Santini *et al.*, 2004). Interestingly, these bacteria were not the most dominant in the nitrate-reducing samples based on 454 pyrosequencing results; however, they dominated in the Fe(III)-reducing enrichments.

Discussion

This study shows for the first time that bacteria are able to degrade ISA (as a sole carbon and energy source in minimal media) at high pH (~10) under a wide range of biogeochemical conditions, and can couple ISA metabolism to the bioreduction of a number of TEAs relevant to an evolving ILW-GDF. Furthermore, the rates of ISA biodegradation, TEA

reduction and the bacterial diversity of the cultures were proportional to the reduction potential of the TEA, in the order aerobic ≈ nitrate > Fe(III), with no reduction of sulphate detected at pH 10. Collectively, these results are consistent with the observation that a range of anaerobic processes can support ISA oxidation, and that decreasing the reduction potential of the respiratory process redox couple results in progressively more streamlined microbial communities dominated by more specialist microorganisms, as noted previously in high pH environments (Burke *et al.,* 2012). In this case, we noted the enrichment of nitrate- or Fe(III)-reducing Gram-positive Firmicutes that may have a competitive advantage under strongly reducing conditions at high pH.

During the operational phase of the GDF, a dry oxygen-rich environment will dominate in the cementitious wasteform and a substantial amount of cellulosic material will be deposited in the ILW. After closure, the GDF will be resaturated with groundwater and anoxic conditions will develop. The pH of the GDF is expected to start at around 13.3 because of the dominance of the cementitious chemistry (Berner, 1992). Under these high pH conditions, substantial amounts of ISA will be formed from the alkali hydrolysis of the deposited cellulose (Askarieh *et al*., 2000). Although the pH inside the GDF is expected to start at much higher values than those that we tested, these starting hyperalkaline pH values will drop to ~10 over prolonged periods of time (Berner, 1992), well within the range of pH values shown to support ISA degradation in our study. Furthermore, at shorter times, even when the pH is still very high inside the GDF, there will be a pH gradient surrounding it that will result in regions of decreasing pH from hyperalkaline to ambient with increasing distance from the GDF. Therefore, any ISA produced within the ILW would pass through regions of pH similar to those tested in this study as it migrates to the geosphere.

Very few previous studies have dealt with the biological degradation of ISA, and they have exclusively targeted ISA biodegradation under aerobic conditions (Strand *et al.,* 1984; Bailey, 1986). In this respect, and to our knowledge, this is the first study that deals with the bacterial degradation of ISA at high pH and under anaerobic conditions when maximal rates of ISA formation are expected to occur because of the wasteforms becoming saturated with hyperalkaline groundwater post closure. Furthermore, ISA degradation in the presence of nitrate, which can be present in some wasteforms in the GDF, took place at a similar rate to that recorded in aerobic systems (Figures 1 and 2). Furthermore, Fe(III), which can form in the GDF by corrosion of iron associated with the wasteforms or iron-containing engineering structures like rock bolts and steel canisters, also supported ISA oxidation by bacteria (Figure 3). The lack of evidence for bacterial degradation of ISA under sulphate-reducing conditions does not negate the ability of sulphate-reducing bacteria to degrade ISA and couple this degradation to the reduction of sulphate. It is possible that such processes could take place very slowly over longer periods of time within the GDF, or in the surrounding geosphere (after diffusion of the ISA) where a lower pH groundwater dominates. Here, the ΔG for the sulphate reduction reaction will be lower than at pH 10 (Rizoulis *et al*., 2012) and active sulphate-reducing bacteria may be present. This is important as many deep groundwaters in the United Kingdom and other countries considering GDF options can contain appreciable concentrations of sulphate.

It is probable that microbial metabolism of ISA will become more pronounced as the pH drops with time and distance from the GDF, and as the extant geosphere microbial communities adapt to the high pH conditions in and around the GDF over prolonged periods of time. Furthermore, in these scenarios potential ISA degraders could be sourced from the deep geosphere, or could survive in the initial hyperalkaline pH as recalcitrant spores, and then germinate when the conditions are more suitable for growth. It should be noted that Gram-positive Bacilli, well known to sporulate as a survival mechanism (Madigan *et al*., 2010), dominated many of our experiments. As ISA-metabolising bacteria have the potential to decrease radionuclide mobility, via the degradation of soluble radionuclide-ISA complexes, such microbial processes should be included in performance assessments focussing on ILW-GDFs. This work, and follow-on studies, can help address significant gaps in our current understanding of the long-term evolution of these unusual engineered subsurface environments. Of particular interest could be investigations of microbial ISA degradation under more realistic subsurface conditions *in situ* (for example, using underground laboratory facilities) and potentially using cellulose-bearing ILW under prolonged incubation. Collectively, these studies can play an important role in removing unnecessary pessimism in performance assessment evaluations for GDFs.

Conflict of Interest

The authors declare no conflict of interest.

Acknowledgements

We thank Alastair Bewsher for his help with the IC data. This work was supported by the BIGRAD consortium under the UK Natural Environmental Research Council, (NE/H007768/1). JRL acknowledges support from the Royal Society. NMB thanks the National Council for Scientific Research-Lebanon for their financial support.

References

Askarieh MM, Chambers AV, Daniel FBD, FitzGerald PL, Holtom GJ, Pilkington NJ *et al.* (2000). The chemical and microbial degradation of cellulose in the near field of a repository for radioactive wastes. *Waste Manag* **20**: 93–106.

Bailey MJ. (1986). Utilization of glucoisosaccharinic acid by a bacterial isolate unable to metabolize glucose. *Appl Microbiol Biotechnol* **24**: 493–498.

Berner UR. (1992). Evolution of pore water chemistry during degradation of cement in a radioactive waste repository environment. *Waste Manag* **12**: 201–219.

Bouchard J, Methot M, Jordan B. (2006). The effects of ionizing radiation on the cellulose of woodfree paper. *Cellulose* **13**: 601–610.

Burke IT, Mortimer RJG, Palaniyandi S, Whittleston RA, Lockwood CL, Ashley DJ, Stewart DI. (2012). Biogeochemical reduction processes in a hyper-alkaline leachate affected soil profile. *Geomicrobiol J* **29**: 760–779.

Caporaso JG, Bittinger K, Bushman FD, DeSantis TZ, Andersen GL, Knight R. (2010a). PyNAST: a flexible tool for aligning sequences to a template alignment. *Bioinformatics* **26**: 266–267.

Caporaso JG, Kuczynski J, Stombaugh J, Bittinger K, Bushman FD, Costello EK *et al.* (2010b). QIIME allows analysis of high-throughput community sequencing data. *Nat Meth* **7**: 335–336.

Chicote E, Moreno D, Garcia A, Sarro I, Lorenzo P, Montero F. (2004). Biofouling on the walls of a spent nuclear fuel pool with radioactive ultrapure water. *Biofouling* **20**: 35–42.

DeSantis TZ, Hugenholtz P, Larsen N, Rojas M, Brodie EL, Keller K *et al.* (2006). Greengenes, a chimera-checked 16S rRNA gene database and workbench compatible with ARB. *Appl Environ Microbiol* **72**: 5069–5072.

Edgar RC. (2010). Search and clustering orders of magnitude faster than BLAST. *Bioinformatics* **26**: 2460–2461.

Edgar RC, Haas BJ, Clemente JC, Quince C, Knight R. (2011). UCHIME improves sensitivity and speed of chimera detection. *Bioinformatics* **27**: 2194–2200.

Gaona X, Montoya V, Colas E, Grive M, Duro L. (2008). Review of the complexation of tetravalent actinides by ISA and gluconate under alkaline to hyperalkaline conditions. *J Contam Hydrol* **102**: 217–227.

Glaus MA, Van Loon LR, Achatz S, Chodura A, Fischer K. (1999). Degradation of cellulosic materials under the alkaline conditions of a cementitious repository for low and intermediate level radioactive waste. Part I: Identification of degradation products. *Anal Chim Acta* **398**: 111–122.

Haas DW, Hrutfiord BF, Sarkanen KV. (1967). Kinetic study on alkaline degradation of cotton hydrocellulose. *J Appl Poly Sci* **11**: 587–600.

Kuhner S, Wohlbrand L, Fritz I, Wruck W, Hultschig C, Hufnagel P *et al.* (2005). Substrate-dependent regulation of anaerobic degradation pathways for toluene and ethylbenzene in a denitrifying bacterium, strain EbN1. *J Bacteriol* **187**: 1493–1503.

Lane DJ. (1991). 16S/23S rRNA sequencing. In: Stackebrandt E, Goodfellow M (eds) *Nucleic Acid Techniques in Bacterial Systematics*. John Wiley & Sons Ltd.: London, pp 115–174.

Lovley DR, Greening RC, Ferry JG. (1984). Rapidly growing rumen methanogenic organism that synthesizes CoenzymeM and has a high affinity for formate. *Appl Environ Microbiol* **48**: 81–87.

Lovley DR, Phillips EJP. (1986). Availability of ferric iron for microbial reduction in bottom sediments of the fresh-water tidal Potomac river. *Appl Environ Microbiol* **52**: 751–757.

Lovley DR, Phillips EJP. (1987). Rapid assay for microbially reducible ferric iron in aquatic sediments. *Appl Environ Microbiol* **53**: 1536–1540.

Madigan MT, Clark DP, Stahl D, Martinko JM. (2010). *Brock Biology of Microorganisms*, 13th edn. Benjamin Cummings: San Francisco.

Maset ER, Sidhu SH, Fisher A, Heydon A, Worsfold PJ, Cartwright AJ *et al.* (2006). Effect of organic co-contaminants on technetium and rhenium speciation and solubility under reducing conditions. *Environ Sci Technol* **40**: 5472–5477.

McDonald D, Price MN, Goodrich J, Nawrocki EP, DeSantis TZ, Probst A *et al.* (2012). An improved Greengenes taxonomy with explicit ranks for ecological and evolutionary analyses of bacteria and archaea. *ISME J* **6**: 610–618.

Mechichi T, Stackebrandt E, Gad'on N, Fuchs G. (2002). Phylogenetic and metabolic diversity of bacteria degrading aromatic compounds under denitrifying conditions, and description of *Thauera phenylacetica* sp. nov., *Thauera aminoaromatica* sp. nov., and *Azoarcus buckelii* sp. nov. *Arch Microbiol* **178**: 26–35.

Nuclear Decommissioning Authority (2014). *2013 UK Radioactive Waste Inventory: Radioactive Waste Composition: Nuclear Decommissioning Authority*. Moor Raw, Cumbria: UK.

Price MN, Dehal PS, Arkin AP. (2009). FastTree: Computing large minimum evolution trees with profiles instead of a distance matrix. *Mol Biol Evol* **26**: 1641–1650.

Rai D, Hess NJ, Xia YX, Rao LF, Cho HM, Moore RC *et al.* (2003). Comprehensive thermodynamic model applicable to highly acidic to basic conditions for isosaccharinate reactions with Ca(II) and Np(IV). *J Solution Chem* **32**: 665–689.

Rizoulis A, Steele HM, Morris K, Lloyd JR. (2012). The potential impact of anaerobic microbial metabolism during the geological disposal of intermediate-level waste. *Mineral Mag* **76**: 3261–3270.

Santini JM, Streimann ICA, Hoven RNV. (2004). *Bacillus macyae* sp. nov., an arsenate-respiring bacterium isolated from an Australian gold mine. *Int J Syst Evol Microbiol* **54**: 2241–2244.

Sorokin ID, Kravchenko IK, Tourova TP, Kolganova TV, Boulygina ES, Sorokin DY. (2008). *Bacillus alkalidiazotrophicus* sp. nov., a diazotrophic, low salt-tolerant alkallphile isolated from Mongolian soda soil. *Int J Syst Evol Microbiol* **58**: 2459–2464.

Strand SE, Dykes J, Ciang V. (1984). Aerobic microbial degradation of glucoisosaccharinic acid. *Appl Environ Microbiol* **47**: 268–271.

Tits J, Wieland E, Bradbury MH. (2005). The effect of isosaccharinic acid and gluconic acid on the retention of Eu(III), Am(III) and Th(IV) by calcite. *Appl Geochem* **20**: 2082–2096.

Turner S, Pryer KM, Miao VPW, Palmer JD. (1999). Investigating deep phylogenetic relationships among cyanobacteria and plastids by small submit rRNA sequence analysis. *J Eukaryot Microbiol* **46**: 327–338.

Ueki A, Akasaka H, Suzuki D, Ueki K. (2006). *Plaudibacter propionicigenes* gen. nov., sp. nov., a novel strictly anaerobic, Gram-negative, propionate-producing bacterium isolated from plant residue in irrigated rice-field soil in Japan. *Int J Syst Evol Microbiol* **56**: 39–44.

Van Loon LR, Glaus MA. (1997). Review of the kinetics of alkaline degradation of cellulose in view of its relevance for safety assessment of radioactive waste repositories. *J Environ Polym Degr* **5**: 97–109.

Van Loon LR, Glaus MA, Laube A, Stallone S. (1999). Degradation of cellulosic materials under the alkaline conditions of a cementitious repository for low- and intermediate-level radioactive waste. II. Degradation kinetics. *J Environ Polym Degr* **7**: 41–51.

Van Loon LR, Glaus MA, Stallone S, Laube A. (1997). Sorption of isosaccharinic acid, a cellulose degradation product on cement. *Environ Sci Technol* **31**: 1243–1245.

Vercammen K, Glaus MA, Van Loon LR. (1999). Complexation of calcium by alpha-isosaccharinic acid under alkaline conditions. *Acta Chem Scand* **53**: 241–246.

Vercammen K, Glaus MA, Van Loon LR. (2001). Complexation of Th(IV) and Eu(III) by alpha-isosaccharinic acid under alkaline conditions. *Radiochim Acta* **89**: 393–401.

Wang Q, Garrity GM, Tiedje JM, Cole JR. (2007). Naive Bayesian classifier for rapid assignment of rRNA sequences into the new bacterial taxonomy. *Appl Environ Microbiol* **73**: 5261–5267.

Warwick P, Evans N, Hall T, Vines S. (2003). Complexation of Ni(II) by alpha-isosaccharinic acid and gluconic acid from pH 7 to pH 13. *Radiochim Acta* **91**: 233–240.

Warwick P, Evans N, Hall T, Vines S. (2004). Stability constants of uranium(IV)-alpha-isosaccharinic acid and gluconic acid complexes. *Radiochim Acta* **92**: 897–902.

Wieland E, Tits J, Dobler JP, Spieler P. (2002). The effect of alpha-isosaccharinic acid on the stability of and Th(IV) uptake by hardened cement paste. *Radiochim Acta* **90**: 683–688.

Supplementary Information accompanies this paper on The ISME Journal website (http://www.nature.com/ismej)

Supplementary Figures

Microbial degradation of isosaccharinic acid at high pH

Naji M. Bassil, Nicholas Bryan, Jonathan R. Lloyd. 2014.

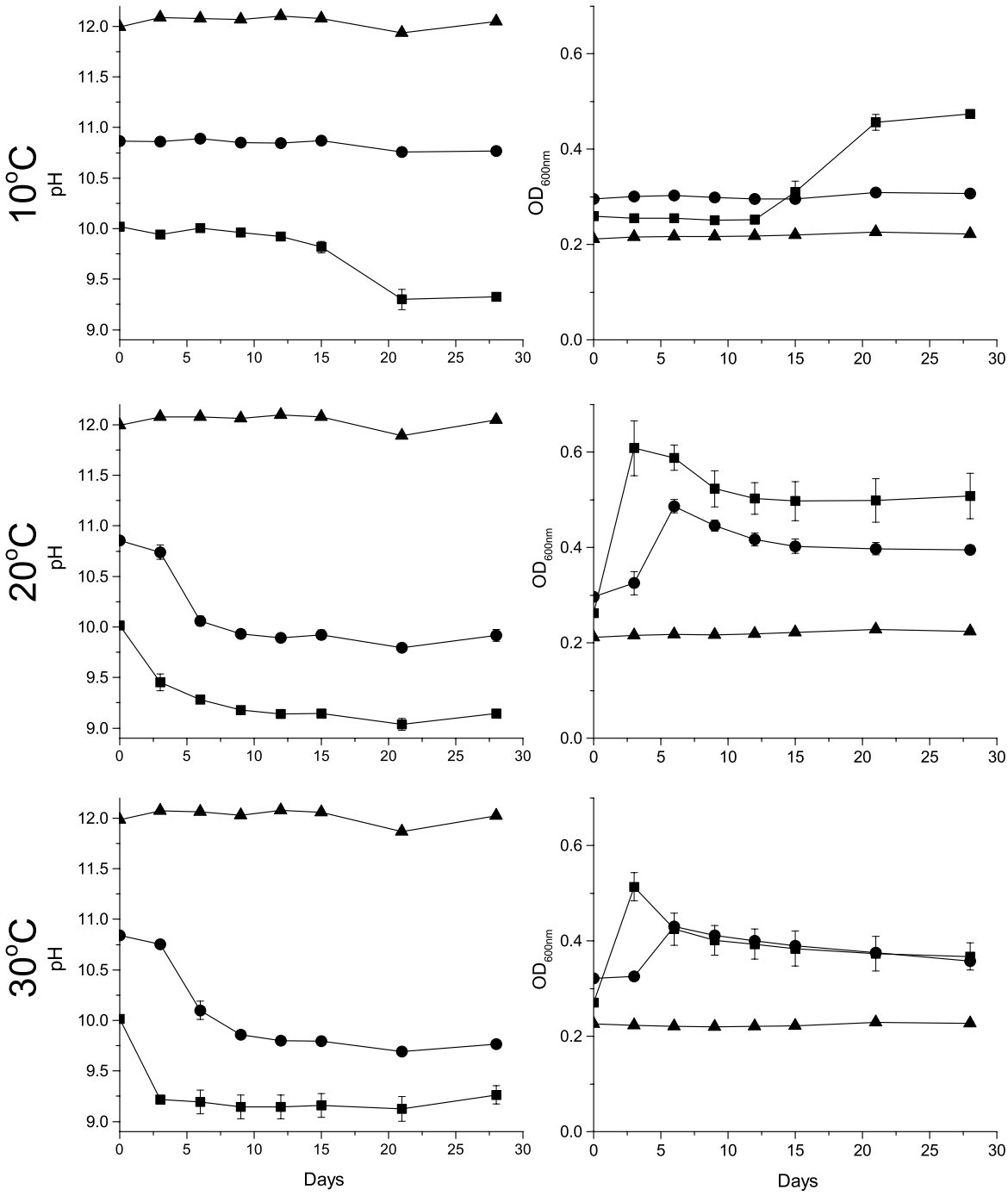

Supplementary Figure S5.1: Nitrate-reducing culture bacteria, grown at pH 10, 11 and 12 at different temperatures 10, 20 and 30°C. (A) represents pH and OD_{600} change over time at 10°C. (B) represents pH and OD_{600} change over time at 20°C. (C) represents pH and OD_{600} change over time at 30°C. ■ represents the samples prepared at a starting pH of 10, ● represents the samples prepared at a starting pH of 11, and ▲ represents the samples prepared at a starting pH of 12.

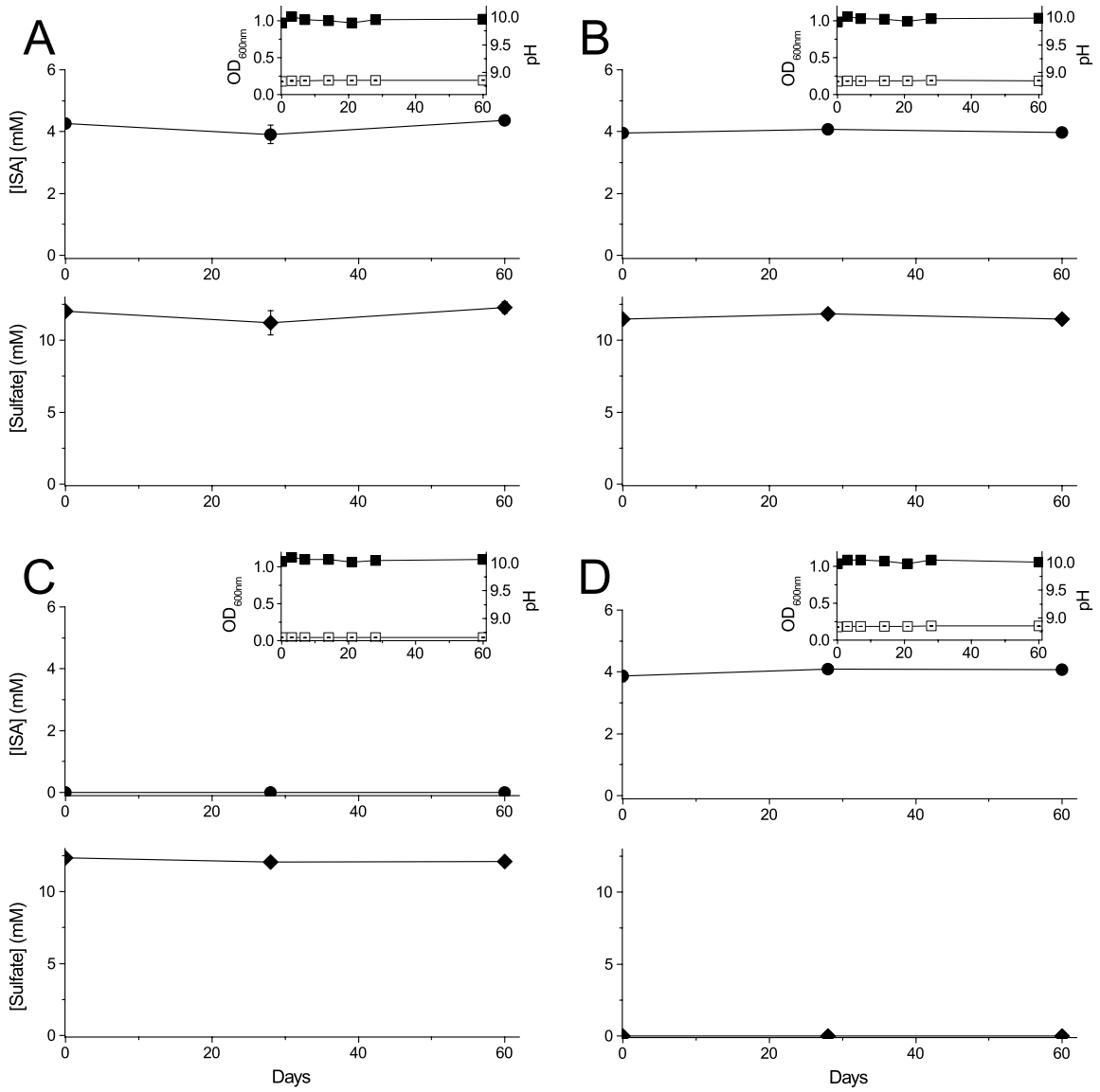

Supplementary Figure S5.2: ISA biodegradation by sulfate-reducing microbial cultures at a starting pH of 10. (A) Test sample containing active microbial cells, (B) sterile (autoclaved) control, (C) a control containing an active inoculum but no added ISA as the sole carbon source and electron donor and (D) a control containing an active inoculum but no added sulfate as the electron acceptor. Upper panels show bacterial growth (OD_{600nm}) (□) and pH (■) change with time. The middle panels show concentration of ISA (●) in mM. The lower panels show the concentration of sulfate (◆) in mM.

Chapter 6

Bacillus buxtonensis sp. nov., an alkaliphilic bacterium which can degrade isosaccharinic acid

Paper ready for submission to the International Journal of Systematic and Evolutionary Microbiology

Author contributions: N. M. Bassil - Principal author, preparation and monitoring of samples and data acquisition and analysis; J. R. Lloyd – Corresponding author and manuscript review.

6 *Bacillus buxtonensis* sp. nov., an alkaliphilic bacterium which can degrade isosaccharinic acid

Contents category: New Taxon (Firmicutes and Related Organisms)

Naji M. Bassil and Jonathan R. Lloyd

Research Centre for Radwaste and Decommissioning & Williamson Research Centre for Molecular Environmental Science, School of Earth, Atmospheric and Environmental Sciences, The University of Manchester, Oxford Road, Manchester M13 9PL, UK

Correspondence: Jonathan R. Lloyd. E-mail: jon.lloyd@manchester.ac.uk Phone: +44(0)161 275 7155. Fax: +44(0) 161 306 9361

6.1 Abstract

An alkaliphilic bacterium belonging to the *Bacillus* genus was isolated from a legacy lime-working site in Harpur Hill, Buxton, UK. Strain NB2006 is a motile (flagellated), spore-forming, Gram-positive rod. The optimal pH for growth is 9.8 and the optimal temperature is 20^{o}C. Strain NB2006 is able to utilise a number of organic acids as electron donors, including gluconate, pyruvate, isosaccharinate, succinate, glutamate and acetate. NB2006 is able to grow under aerobic as well as anaerobic conditions, the latter through fermentation or the reduction of electron acceptors including fumarate, nitrate and insoluble Fe(III) oxyhydroxide. The DNA G+C content of strain NB2006 is 37.7 mol% and analysis of its 16S rRNA gene sequence showed that strain NB2006 is most closely related to the obligate anaerobes *Anaerobacillus macyae* (97.6%) and *Anaerobacillus alkalidiazotrophicus* (97.4%). We suggest that strain NB2006 represents a novel species within the genus *Bacillus* (given its ability to grow aerobically and anaerobically), for which the name *Bacillus buxtonensis* sp. nov. is proposed. The type strain is NB2006.

6.2 Introduction

There is considerable interest in the environmental fate of isosaccharinic and gluconic acids, as they are produced during the long-term storage of cementitious intermediate-level nuclear waste, via alkaline hyrodrolysis of cellulosic materials in the wasteforms. Both

molecules are polyhydroxy carboxylic acids that can chelate metals and radionuclides, thereby increasing their solubility, potentially enhancing their transport out of the facility and into the surrounding environment (Gaona *et al.*, 2008). Although a number of bacteria have been identified that are able to degrade gluconic acid, only two bacterial strains have been isolated that are able to degrade isosaccharinic acid, both of which were aerobic Gram-negative bacteria (Strand *et al.*, 1984; Bailey, 1986). Here we describe an alkaliphilic, Gram-positive species belonging to the genus *Bacillus* that is able to utilise gluconate and isosaccharinate under a variety of biogeochemical conditions (aerobic, nitrate-reducing and Fe(III)-reducing), under the high pH conditions associated with cementitious nuclear waste.

6.3 Results

Strain NB2006 was isolated from the fourth subculture of an anaerobic, isosaccharinate-utilizing enrichment culture supplied with nitrate as the terminal electron acceptor (Bassil *et al.*, 2014). The bacterium was maintained in a minimal medium at pH 10 and incubated at 20^{o}C (Bassil *et al.*, 2014). Strain NB2006 was one of 5 isolates selected on agar plates prepared using the same defined medium but solidified with 1% (w/v) agar (Bassil *et al.*, 2014). Isolates formed protruding, small, round and transparent colonies after 3 days of incubation under anaerobic conditions at 20^{o}C.

Strain NB2006 was able to grow in minimal medium containing sodium isosaccharinate and sodium nitrate at starting pH values between 9 and 11 (no growth was detected at pH 7, 8 and 12), and caused a drop in pH during the bacterial growth phase, probably due to the production of CO_2 that caused the acidification of the culture media. Optimal growth was observed at pH 9.8, making this strain an obligate alkaliphile. Furthermore, it was able to grow between 10 and 30^{o}C, with optimal growth at 20^{o}C, and no growth at 4 or 50^{o}C (after 28 days of incubation).

The pure bacterial culture was grown at pH 10 and 20^{o}C for 6 days (to reach the late-log phase of bacterial growth) and then used to test for the presence of catalase and oxidase enzymes. Catalase activity was assessed by adding 3% H_2O_2 solution to 4 ml of bacterial culture and checking for bubble formation. Oxidase activity was assessed by adding 1% α-naphthol (Acros) and 1% N,N-dimethyl-p-phenylenediamine sulfate (Sigma) to 2 ml of the bacterial culture, and observing a change in the colour of the solution. Negative controls containing autoclaved samples were also assessed for catalase and oxidase activity and showed negative results.

The same bacterial culture was also used to check for bacterial motility in wet mounts, Gram and endospore staining of heat-fixed slides, and for the presence of flagella by staining of air-dried slides, using light microscopy. The ability of this bacterium to form endospores was observed by staining heat-fixed slides with malachite green (Pro-Lab) over steam for 5 min and then counterstaining with Safranin T solution (Fluka) for 1 min. Gram staining was done on heat-fixed slides using a Gram staining kit (Sigma). Flagella were stained on air-dried slides using Flagella Stain Droppers (BD). From these observations we note that strain NB2006 is a Gram-positive motile rod with 2-4 peritrichous flagella. It can live singly or in chains of up to 6 connected rods and can form circular, subterminal spores.

A range of potential organic electron donors were tested with nitrate as the sole electron acceptor under anaerobic conditions at pH 10 and 20 ^{o}C. Strain NB2006 showed significant growth in the presence of 5.5 mM gluconate > 8.5 mM pyruvate > 4 mM isosaccharinate > 5.9 mM succinate > 5 mM glutamate > 12 mM acetate (increase in OD_{600nm} values of between 0.9 and 0.1 for these substrates). No increase in turbidity was detected when the bacteria were incubated with 4.2 mM citrate, 2.6 mM EDTA, 4.3 mM nitrilotriacetic acid, 4 mM glucose and 9.6 mM ethanol.

In order to assess the range of electron acceptors used by this organism, growth was assessed in cultures using 4 mM isosaccharinate as the electron donor and either 48 mM of fumarate, 5 mmol/L of insoluble Fe(III) oxyhydroxide (Lovley and Phillips, 1986) or 50 mM of nitrate as terminal electron acceptors, under anaerobic conditions. Another sample that did not contain any terminal electron acceptor was also prepared to test for fermentation of the isosaccharinate and gluconate. Growth under aerobic conditions was also assessed using shake-flask cultures. The production of organic acids and the reduction of nitrate to nitrite were assessed using ion exchange chromatography (Bassil *et al.*, 2014). Fe(II) production from the reduction of Fe(III) was assessed using the ferrozine assay (Lovley & Phillips, 1986), and in these cultures growth was assessed by microscopic analysis. Optimal growth for this bacterium was observed under nitrate-reducing conditions (OD_{600nm} increase of 0.9 units), followed by the aerobic cultures (0.3 units). The fumarate containing samples and the no electron acceptor samples showed a similar change in optical density (0.115 and 0.105 OD_{600nm} units, respectively). Furthermore, this bacterium was able to reduce half of the added nitrate to nitrite (about 25 mM) coupled to the oxidation of all the isosaccharinate or gluconate, leading to the formation of acetate and potentially carbon dioxide. In addition, NB2006 was also able to reduce about 20% of the

added Fe(III) to Fe(II) under these conditions. Table 6.1 shows the full range of conditions that this novel bacterium can grow in.

Table 6.1: Comparison between strain NB2006 and related species of the genus *Anaerobacillus*

Species		**Strain NB2006**	**Strain JMM-4**	**Strain MS6**
Colony morphology		Small, circular, transparent	White, circular	ND
Cell size		0.5-0.7x2.5-4.5 μm	0.6x2.5-3 μm	0.6-1.2x3-8 μm
Cell morphology		rods	rods	rods
Gram staining		+	+	+
Clustering		single or chains of 6	single	ND
Motility		+	+	+
Flagellum		+ (peritrichous)	+ (peritrichous)	+ (peritrichous)
Spore formation		+	+	+
Spore shape		Subterminal, circular	Subterminal, ellipsoidal	Terminal, ellipsoidal
Growth temp		10-30	28-37	15-43
Growth pH		9-11	7-8.4	7.8-10.6
e- acceptor	**Fermentation**	+ (very little)	-	+
	Fumarate	+ (very little)	-	ND
	Fe(III)	+ (20%)	-	ND
	Oxygen	+	-	- (tolerant)
	Nitrate	+	+	-
e- donor	**Acetate**	+ (very little)	+	ND
	Lactate	+ (very little)	+	-
	Pyruvate	+	+	ND
	Succinate	+	+	ND
	Citrate	-	-	ND
	Isosaccharinate	+	ND	ND
	Glutamate	+	+	ND
	Gluconate	+	ND	ND
	EDTA	-	ND	ND
	NTA	-	ND	ND
	Glucose	-	ND	+
	Ethanol	-	ND	ND
Catalase		+	+	+
Oxidase		+	-	-
G+C content		37.7 mol%	37 mol%	37.1 mol%

A bacterial culture that was incubated for 4 days in the presence of isosaccharinate as the electron donor and nitrate as the electron acceptor was used for DNA extraction using the Powersoil DNA extraction kit (MO BIO Laboratories). The 16S rRNA gene was amplified by PCR, using the bacterial universal primers 8f (5'-AGAGTTTGATCCTGGCTCA-3') and 1492r (5'-TACGGYTACCTTACGACTT-3') (Lane, 1991), as described previously (Bassil *et al.*, 2014). The PCR product was then cleaned using the ExoSap DNA purification procedure and sequenced using the same universal primers 8f and 1492r, and

internal primers 530f (5'-GTGCCAGCMGCCGCGG-3') and 943r (5'-ACCGCTTGTGCGGGCCC-3') (Handley *et al.*, 2009) and an ABI Prism BigDye Terminator v3.1 cycle sequencing kit, to get the almost complete (1502 bp) 16S rRNA gene sequence. DNA sequencing was performed with an ABI Prism 3100 Genetic Analyzer (Perkin Elmer Applied Biosystems). The sequences were checked for errors, aligned and a consensus sequence was submitted for BLAST analysis (Altschul *et al.*, 1990) against NCBI rRNA reference sequences using the MEGA 6.0 software (Tamura *et al.*, 2013). This analysis showed that this bacterium was 97.6% similar to the bacterium *Anaerobacillus macyae* (Santini *et al.*, 2002, 2004) and 97.4% similar to *Anaerobacillus alkalidiazotrophicus* (Sorokin *et al.*, 2008). A maximum likelihood phylogenetic tree with Jukes-Cantor corrections (Figure 6.1) and a neighbour-joining phylogenetic tree (Figure 6.2) were constructed using the MEGA 6.0 software (Tamura *et al.*, 2013). Phylogenetic analysis of the almost complete16S rRNA gene sequence showed that this bacterium formed a separate branch between two groups; (i) the strictly anaerobic alkaliphilic *Bacilli*, *A. macyae*, *A. alkalidiazotrophicus*, *Anaerobacillus alkalilacustris* (Zavarzina *et al.*, 2009) and *Anaerobacillus arseniciselenatis* (Blum *et al.*, 1998), and (ii) the strictly aerobic alkaliphiles *Bacillus alkalinitrilicus* (Sorokin *et al.*, 2008) and *Bacillus pseudofirmus* (Janto *et al.*, 2011).

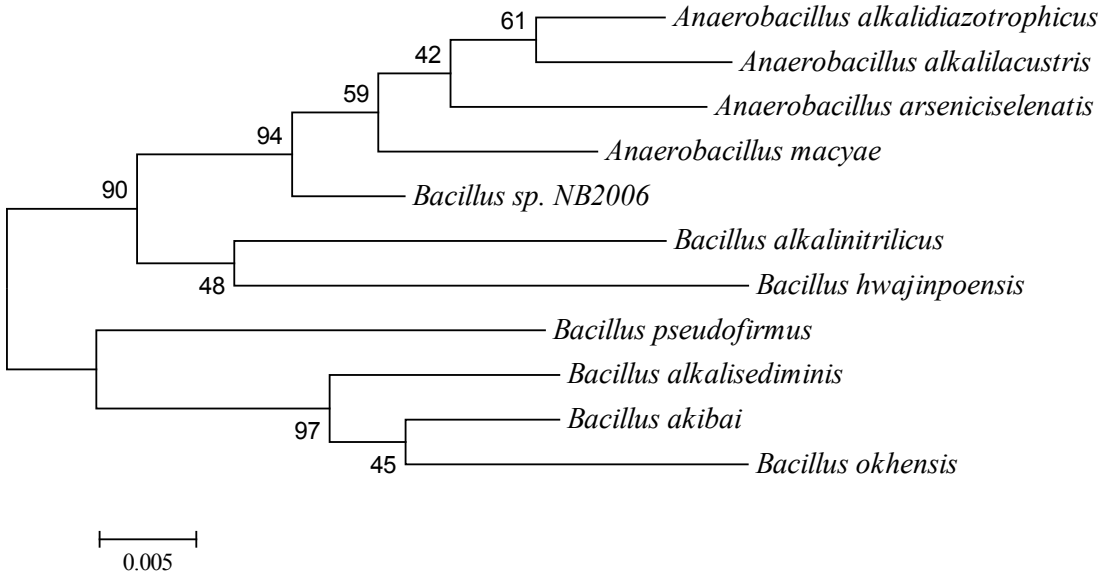

Figure 6.1: The evolutionary history was inferred by using the Maximum Likelihood method, based on the Jukes-Cantor model (Jukes and Cantor, 1969). The percentage of trees in which the associated taxa clustered together is shown next to the branches. The tree is drawn to scale, with branch lengths measured in the number of substitutions per site. All positions with less than 95% site coverage were eliminated, and a total of 1424 positions were in the final dataset.

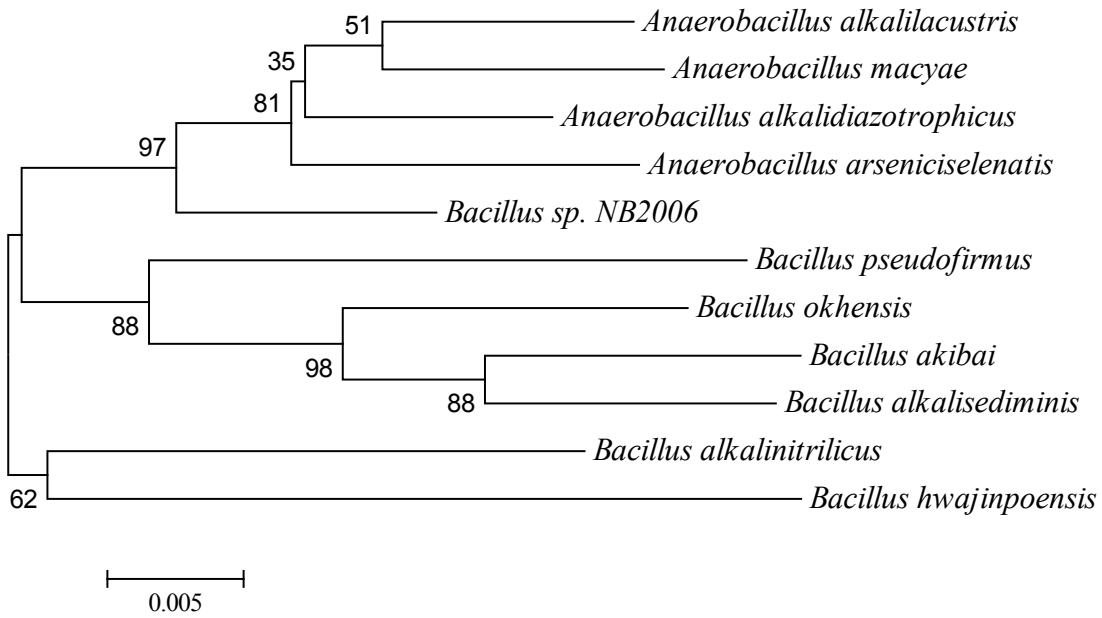

Figure 6.2: The evolutionary history was inferred using the Neighbor-Joining method (Saitou and Nei, 1987), based on the Jukes-Cantor model (Jukes and Cantor, 1969). The percentage of replicate trees in which the associated taxa clustered together in the bootstrap test (1000 replicates) are shown next to the branches (Felsenstein, 1985). The tree is drawn to scale, with branch lengths measured in the number of substitutions per site. All ambiguous positions were removed for each sequence pair, and a total of 1570 positions were in the final dataset.

The G+C content of strain NB2006 was analysed by the DSMZ Identification Service (Germany), by disrupting the cells by French pressing and purifying the DNA on hydroxyapatite (Cashion and Holder-Franklin, 1977). The DNA was hydrolysed with P1 nuclease and the nucleotides were dephosphorylated with bovine alkaline phosphatase (Mesbah *et al.*, 1989). The resulting deoxyribonucleosides were analysed by HPLC (Tamaoka and Komagata, 1984). Lambda-DNA and DNA from three bacteria with published genome sequences representing a G+C range of 43-72 mol% were used as standards. G+C mol% values were calculated from the ratio of deoxyguanosine and thymidine (Mesbah *et al.*, 1989).

Given that the 16S rRNA gene analysis showed that strain NB2006 showed 97.6% identity with its closest relative, below the 98.2% threshold above which DNA-DNA hybridisation should be considered for new species characterisation (Meier-Kolthoff *et al.*, 2013), and that this novel bacterium can grow under aerobic conditions, this indicates that this is a new species belonging to the genus *Bacillus* (rather than the genus *Anaerobacillus*, which is associated with obligate anaerobes*)* .

The ability to utilise isosaccharinic acid has not been demonstrated previously for this genus, and indeed has not been demonstrated under anaerobic conditions for any isolate in pure culture before.

6.4 Description of *Bacillus buxtonensis* sp. nov.

Bacillus buxtonensis [bux.ton.en'sis. N.L. masc. adj. *buxtonensis* from the Buxton area in the UK, where the type strain was isolated].

Cells are spore-forming, Gram-positive rods (3-5 μm) that are motile through the use of 2-4 peritrichous flagella. Colonies are protruding, circular and transparent. They are strictly alkaliphilic, with growth occurring in the range pH 9-11. They can grow at a temperature between 10 and 30^{o}C, and under aerobic or anaerobic conditions. Under anaerobic conditions they can grow in the absence of an electron acceptor by fermentation, or in the presence of fumarate, nitrate or Fe(III) as alternative electron acceptors (in the latter cases reducing nitrate to nitrite or Fe(III) oxyhydroxide to Fe(II)). They can utilise gluconate, pyruvate, isosaccharinate, succinate, glutamate and acetate as carbon substrates under anaerobic conditions, in the presence of nitrate as the terminal electron acceptor. The DNA G+C content of this type strain is 37.7 mol%.

The type strain, NB2006 was isolated from a sediment collected from a lime workings site in Harpur hill, Buxton, UK.

6.5 Acknowledgements

NMB would like to thank the CNRS-Lebanon for their financial support of this work. This work was supported by the BIGRAD consortium under the UK Natural Environmental Research Council, (NE/H007768/1). JRL acknowledges support from the Royal Society.

6.6 References

Altschul S, Gish W, Miller W, Myers E, Lipman D. (1990). Basic local alignment search tool. *J Mol Biol* **215**:403–410.

Bailey M. (1986). Utilization of glucoisosaccharinic acid by a bacterial isolate unable to metabolize glucose. *Appl Microbiol Biotechnol* **1206**:493–498.

Bassil NM, Bryan N, Lloyd JR. (2014). Microbial degradation of isosaccharinic acid at high pH. *ISME J* **9**:310–320.

Blum J, Bindi A, Buzzelli J, Stolz J, Oremland R. (1998). *Bacillus arsenicoselenatis*, sp. nov., and *Bacillus selenitireducens*, sp. nov.: Two haloalkaliphiles from Mono Lake, California that respire oxyanions of selenium and arsenic. *Arch Microbiol* **171**:19–30.

Cashion P, Holder-Franklin M. (1977). A rapid method for the base ratio determination of bacterial DNA. *Anal Biochem* **81**:461–466.

Felsenstein J. (1985). Confidence limits on phylogenies: An approach using the bootstrap. *Evolution* **39**:783-791.

Gaona X, Montoya V, Colàs E, Grivé M, Duro L. (2008). Review of the complexation of tetravalent actinides by ISA and gluconate under alkaline to hyperalkaline conditions. *J Contam Hydrol* **102**:217–27.

Handley KM, Héry M, Lloyd JR. (2009). *Marinobacter santoriniensis* sp. nov., an arsenate-respiring and arsenite-oxidizing bacterium isolated from hydrothermal sediment. *Int J Syst Evol Microbiol* **59**:886–92.

Janto B, Ahmed A, Ito M, Liu J, Hicks DB, Pagni S, *et al.* (2011). Genome of alkaliphilic *Bacillus pseudofirmus* OF4 reveals adaptations that support the ability to grow in an external pH range from 7.5 to 11.4. *Environ Microbiol* **13**:3289–309.

Jukes T.H. and Cantor C.R. (1969). Evolution of protein molecules. In: *Munro HN, editor, Mammalian Protein Metabolism*, Academic Press: New York, pp. 21-132.

Lane DJ. (1991). 16S/23S rRNA sequencing. In: *Nucleic acid techniques in bacterial systematics*, Stackebrandt, E & Goodfellow, M (eds), John Wiley & Sons Ltd.: London, pp. 115–174.

Lovley D, Greening R, Ferry J. (1984). Rapidly growing rumen methanogenic organism that synthesizes coenzyme M and has a high affinity for formate. *Appl Environ Microbiol* **48**:81–87.

Lovley D, Phillips E. (1986). Availability of ferric iron for microbial reduction in bottom sediments of the freshwater tidal Potomac River. *Appl Environ Microbiol* **52**:751–757.

Lovley D, Phillips E. (1987). Rapid assay for microbially reducible ferric iron in aquatic sediments. *Appl Environ Microbiol* **53**:1536–1540.

Meier-Kolthoff JP, Göker M, Spröer C, Klenk H-P. (2013). When should a DDH experiment be mandatory in microbial taxonomy? *Arch Microbiol* **195**:413–8.

Mesbah M, Premachandran U, Whitman WB. (1989). Precise measurement of the G+C content of deoxyribonucleic acid by high-performance liquid chromatography. *Int J Syst Bacteriol* **39**:159–167.

Saitou N, Nei M. (1987). The neighbor-joining method: A new method for reconstructing phylogenetic trees. *Mol Biol Evol* **4**:406-425.

Santini JM, Stolz JF, Macy JM. (2002). Isolation of a new arsenate-respiring bacterium-physiological and phylogenetic studies. *Geomicrobiol J* **19**:41–52.

Santini JM, Streimann ICA, vanden Hoven RN. (2004). *Bacillus macyae* sp. nov., an arsenate-respiring bacterium isolated from an Australian gold mine. *Int J Syst Evol Microbiol* **54**:2241–4.

Sorokin DY, van Pelt S, Tourova TP. (2008). Utilization of aliphatic nitriles under haloalkaline conditions by *Bacillus alkalinitrilicus* sp. nov. isolated from soda solonchak soil. *FEMS Microbiol Lett* **288**:235–40.

Sorokin ID, Kravchenko IK, Tourova TP, Kolganova TV, Boulygina ES, Sorokin DY. (2008). *Bacillus alkalidiazotrophicus* sp. nov., a diazotrophic, low salt-tolerant alkaliphile isolated from Mongolian soda soil. *Int J Syst Evol Microbiol* **58**:2459–64.

Strand S, Dykes J, Chiang V. (1984). Aerobic microbial degradation of glucoisosaccharinic acid. *Appl Environ Microbiol* **47**:268–271.

Takami H, Nakasone K, Takaki Y. (2000). Complete genome sequence of the alkaliphilic bacterium *Bacillus halodurans* and genomic sequence comparison with *Bacillus subtilis*. *Nucleic Acids* **28**:4317–4331.

Tamaoka J, Komagata K. (1984). Determination of DNA base composition by reversed-phase high-performance liquid chromatography. *FEMS Microbiol Lett* **25**:125–128.

Tamura K, Stecher G, Peterson D, Filipski A, Kumar S. (2013). MEGA6: Molecular Evolutionary Genetics Analysis version 6.0. *Mol Biol Evol* **30**:2725–9.

Zavarzina DG, Tourova TP, Kolganova TV, Boulygina ES, Zhilina TN. (2009). Description of *Anaerobacillus alkalilacustre* gen. nov., sp. nov.—Strictly anaerobic diazotrophic *Bacillus* isolated from soda lake and transfer of *Bacillus arseniciselenatis*, *Bacillus macyae*, and *Bacillus alkalidiazotrophicus* to *Anaerobacillus* as the new combinations *A. arseniciselenatis* comb. nov., *A. macyae* comb. nov., and *A. alkalidiazotrophicus* comb. nov. *Microbiology* **78**:723–731.

Chapter 7

Growth profiles of *Bacillus buxtonensis* utilising isosaccharinate or gluconate

Paper being prepared for submission to the *Nature Biotechnology* journal, awaiting complementary genomic and transcriptomic data to complete manuscript

N. M. Bassil - Principal author, preparation and monitoring of samples and data acquisition and analysis; J. R. Lloyd – Corresponding author and manuscript review.

7 Growth profiles of *Bacillus buxtonensis* utilising isosaccharinate or gluconate

Naji M Bassil[1] and Jonathan R Lloyd[1]

[1]Research Centre for Radwaste and Decommissioning and Williamson Research Centre for Molecular Environmental Science, School of Earth, Atmospheric and Environmental Sciences, University of Manchester, Manchester, UK

7.1 Abstract

Deep geological disposal in a cementitious facility is being sought by a number of countries for the safe, long-term disposal of radioactive wastes. Intermediate-level wastes contain organic co-contaminants that include gluconic acid (GA; a cement additive), and cellulose, which may be hydrolysed under the alkaline conditions of an evolving GDF to isosaccharinic acid (ISA; the major product of the abiotic alkali hydrolysis of cellulose). These can form stable, soluble complexes with a number of radionuclides. Recent studies by our group showed that *Bacillus buxtonensis* strain NB2006 was able to degrade these molecules under various biogeochemical conditions including aerobic, nitrate- and Fe(III)-reducing conditions. Although GA and ISA are both polyhydroxy carboxylic acids, with the same number of carbons, *B. buxtonensis* showed variable growth profiles when added to minimal media at pH 10, in the presence of different electron acceptors. Under aerobic conditions, turbidity was higher in the GA containing cultures, while it was similar in the nitrate-reducing cultures, and in both conditions, complete degradation of the added electron donor was observed. Under Fe(III)-reducing conditions, ISA and GA degradation was coupled to the reduction of about 30% of the added Fe(III), although the ISA was not completely degraded. Under fermentative and U(VI)-reducing conditions, only slight increase in turbidity and minimal ISA degradation were observed, which contrasted with the GA containing cultures. The differences in *B. buxtonensis* growth profiles may indicate different incorporation or degradation mechanisms for ISA and GA. Bacterial growth in the GA supplemented cultures was accompanied by the immobilisation of U(VI), however, further studies need to be conducted to understand the mechanism. The results imply that microorganisms may play various roles in decreasing the transport of radionuclides from a geological disposal facility, including the biodegradation of organic complexants, in addition to mediating bioaccumulation, biosorption, biomineralisation and bioreduction processes.

7.2 Introduction

Many countries are planning to dispose of intermediate- and some low-level radioactive wastes via cementitious geological disposal facilities (GDF), which will provide a multibarrier system against the transport of radionuclides to the surface (biosphere) through groundwater. In this concept, the surrounding geology and the cement backfilling of the wasteforms will provide the physical barrier (NDA, 2010), while the high pH environment produced from the leaching of cations from cement after resaturation of the facility with groundwater (Berner, 1992), will provide a chemical barrier in which radionuclide solubility is low.

These wasteforms are heterogeneous, and contain organic components, for example ion exchange resins, cellulosic materials and cement additives (NDA, 2014). There is concern that these organic polymers may facilitate the release of soluble radionuclide-complexants under the high pH, anaerobic conditions found in the GDF. Two polyhydroxy carboxylic acid complexants (isosaccharinic acid (ISA) and gluconic acid (GA)) are of particular concern, due to their ability to form stable complexes with a number of tri- and tetravalent actinides at high pH (Gaona *et al.*, 2008), which may potentially enhance their transport. Both molecules will be present in the GDF, as ISA is produced from the abiotic alkaline hydrolysis of cellulose (the main organic component of intermediate- and low level wastes (van Loon and Glaus, 1997; Glaus and van Loon, 2008; van Loon and Glaus, 1998)), and gluconic acid is used as a cement additive. These organic molecules may be used as electron donors by bacteria, coupling their oxidation to the reduction of a range of electron acceptors in the GDF, including Fe(III) from corroded steel canisters, nitrate in some wasteforms (e.g. raffinates) and sulphate that may be present in deep groundwaters (Duro *et al.*, 2014). In addition, the radionuclides that will be present in ILW, for example uranium (NDA, 2010), may also be used as terminal electron acceptors for the bacterial oxidation of organic molecules (Lovley *et al*., 1993).

Although the microbial degradation of gluconate has been demonstrated in a number of bacterial species, ISA biodegradation has received much less attention. Recent studies showed that bacterial consortia were able to utilise ISA for growth under various biogeochemical conditions, however, these studies were done at circumneutral pH (Maset *et al.*, 2006; Rout *et al.*, 2014). Previous studies have also shown that some bacterial isolates are able to degrade ISA under strictly aerobic conditions (Bailey, 1986; Strand *et al.*, 1984). These studies are relevant to near-surface (aerobic, circumneutral pH)

conditions rather than the high pH, anaerobic conditions that are expected to prevail in a GDF.

More recently, our group has shown that enrichment cultures supplemented by $Ca(\alpha\text{-ISA})_2$ as the sole electron donor, were able to support bacterial growth under various biogeochemical conditions at pH 10 (Bassil *et al.*, 2014). An isolate (*Bacillus buxtonensis* strain NB2006) that was able to degrade ISA and GA under similar conditions was subsequently isolated on solid media (Bassil and Lloyd, 2015). Here we compare the growth of this bacterial strain in the presence of ISA and GA under various biogeochemical conditions at high pH.

7.3 Materials and Methods

7.3.1 Isolation of bacterial strain

The bacterial strain that was used in this work was isolated from a nitrate-reducing culture that was grown on $Ca(\alpha\text{-ISA})_2$ as the sole electron donor (Bassil *et al.*, 2014; Bassil and Lloyd, 2015). The isolate was maintained in the same defined growth medium (Bassil *et al.*, 2014; Lovley *et al.*, 1993) under anaerobic conditions, supplemented with 5 mM sodium gluconate, and in the absence of any electron acceptor (fermentative conditions).

7.3.2 ISA Preparation and Ion Chromatography

$Ca(\alpha\text{-ISA})_2$ was prepared according to a protocol described previously (Bassil *et al.*, 2014; Vercammen *et al.*, 1999). The Na-ISA salt was prepared from $Ca(\alpha\text{-ISA})_2$ following previously reported procedures (Rai *et al.*, 2003). Analysis of the concentrations of a range of organic molecules by ion chromatography also followed methods from previous publications (Bassil *et al.*, 2014).

7.3.3 Preparation of Bacterial Cultures

Aerobic cultures were prepared in 150 ml shake flasks containing 10 ml medium supplemented with 5 mM NaISA or NaGA. Controls that were not supplemented with electron donors were also prepared, and all treatments were prepared in triplicate. The pH of the medium was adjusted to 10 using 10 M NaOH and the flasks were closed with a foam bung and then autoclaved. After cooling, a 1 % inoculum of strain NB2006 was added to each flask using aseptic techniques. The flasks were incubated in a shaker incubator at 20^{o}C with shaking at 130 rpm. Samples (1 ml) were taken using aseptic

techniques. The pH and OD_{600} of the samples were measured and the samples were frozen at -20^{o}C until the end of the experiment for ion chromatography analysis.

The anaerobic cultures were prepared in serum bottles containing 30 ml medium supplemented with 5 mM NaISA or NaGA as the electron donors, and 50 mM $NaNO_3$, or 10 mmol/L insoluble Fe(III) oxyhydroxide (Lovley and Phillips, 1986) as electron acceptors. In the case of the U(VI)-reducing cultures, 0.42 mM of filter sterilised (0.22 μm) $UO_2Cl_{2(aq)}$ (at pH 2.5) was added to the culture medium after autoclaving. Samples that were not supplemented with any electron acceptor were also prepared to study biodegradation under fermentative conditions. Controls that were not supplemented with electron donors were also prepared, and again all the treatments were prepared in triplicate. The pH of the cultures was adjusted to 10 using 10 M NaOH, and the bottles were stoppered with rubber butyl stoppers and then flushed with N_2 for 30 min and autoclaved. A 1 % inoculum of strain NB2006 was added, and the bottles were incubated at 20^{o}C. Samples (1 ml) were taken using anaerobic, aseptic techniques using a needle and a N_2 flushed syringe. The pH and OD_{600} of the samples under NO_3-reducing, and fermentative conditions were measured. Under Fe(III)- and U(VI)-reducing conditions, the pH and concentration of the electron acceptor species was measured using the ferrozine (Lovley and Phillips, 1987) and Bromo-PADAP (Johnson and Florence, 1971) colorimetric assays, respectively. Note that the U(VI)-reducing culture samples were centrifuged at 14,000 *g* for 5 min and the Bromo-PADAP assay was performed on the supernatant. The pellet was resuspended in 10 mM of argon flushed HCl and left in an anaerobic chamber overnight to leach surface-sorbed U(VI) (this did not completely disrupt the pellet). An equimolar amount of argon flushed NaOH was later added and the Bromo-PADAP assay performed on the resulting solution. The samples containing the supernatant were then frozen at -20^{o}C until the end of the experiment for ion chromatography analysis.

7.4 Results

Detailed comparison of *B. buxtonensis* cultures at pH 10 showed contrasting growth kinetics in the presence of GA or ISA as electron donors under the conditions tested. Under aerobic conditions, both substrates were degraded completely after 8 days in culture, concomitant with an increase in the OD_{600} of the samples, indicating bacterial growth (Figure 7.1). Although the ISA-containing cultures showed an earlier initial OD_{600} increase and ISA degradation (50% ISA degradation after 4 days of incubation), the GA-containing cultures showed a faster bacterial growth (0.07 h^{-1} and 0.03 h^{-1} in the GA- and ISA-containing cultures, respectively) and a higher OD_{600} after 5 days of incubation

(beginning of the stationary phase; 0.60 OD_{600} units, compared to 0.34 OD_{600} units in the ISA-containing cultures).

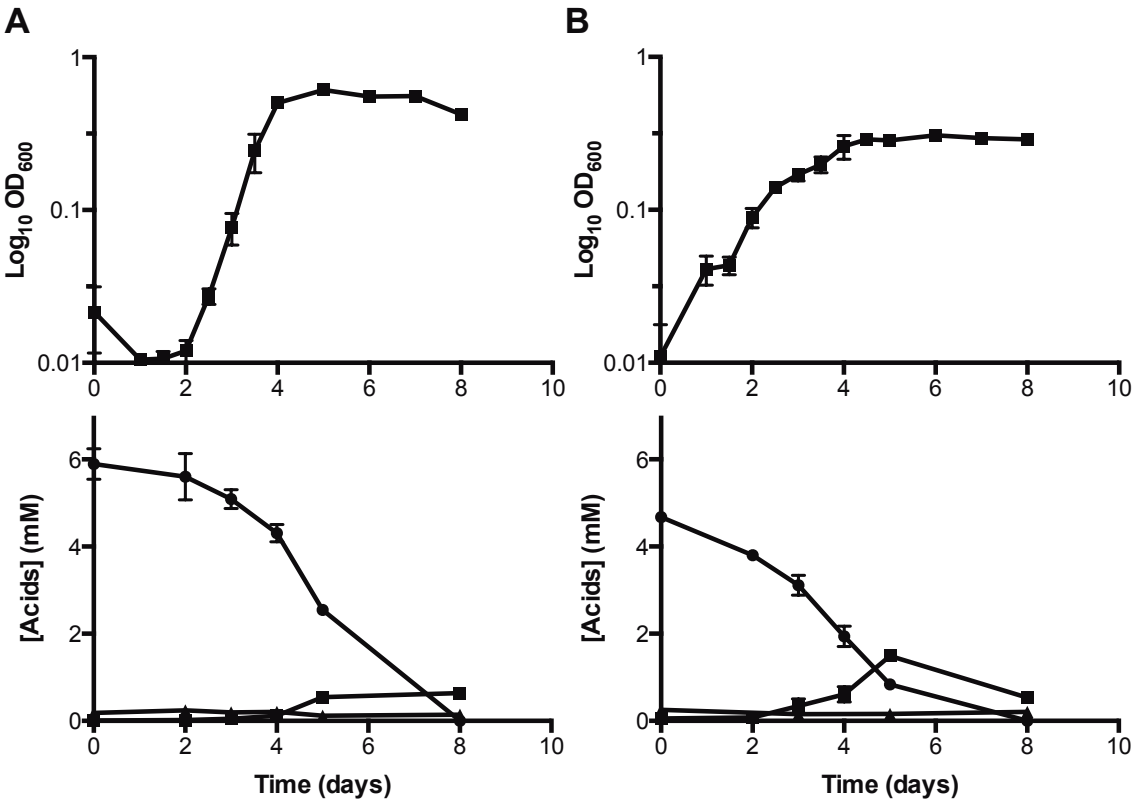

Figure 7.1: ISA and GA biodegradation by *B. buxtonensis* NB2006 under aerobic conditions and a starting pH of 10. (A) Samples containing GA as the electron donor. (B) Samples containing ISA as the electron donor. Upper panels show the OD_{600} of the samples (■). Lower panels show the concentrations of the added electron donor (GA or ISA, ●), acetate (■) and formate (▲) in mM.

Under denitrifying conditions, faster bacterial growth was observed in the presence of GA (0.08 h^{-1}) than with ISA (0.04 h^{-1}), although both systems reached similar OD_{600} values (about 0.7 OD_{600} units) at the late exponential phase of growth (Figure 7.2). Bacterial growth was accompanied by complete degradation of the electron donor, after 4 and 8 days in culture with GA and ISA, respectively. Acetate (2 and 3 mM in GA- and ISA-containing cultures, respectively) and formate (approximately 1 mM in both cultures) were produced, presumably as fermentation products. The degradation of the organic acids was coupled to the reduction of more than 70% of the added nitrate to nitrite after 8 days in culture.

B. buxtonensis cultures containing insoluble Fe(III) oxyhydroxide as a terminal electron acceptor, reduced about 30% of Fe(III) to Fe(II) (assessed by the ferrozine assay) over the experiment period, in the presence of GA or ISA as electron donors (Figure 7.3). Bacterial growth could not be estimated by changes in optical density in the presence of a mineral phase, and was not assessed. Complete degradation of GA was observed after 14 days, which was concomitant with the production of 6 and 3.5 mM of formate and acetate,

respectively. In contrast, incomplete degradation of ISA was observed after 45 days, and very little acetate and formate were produced.

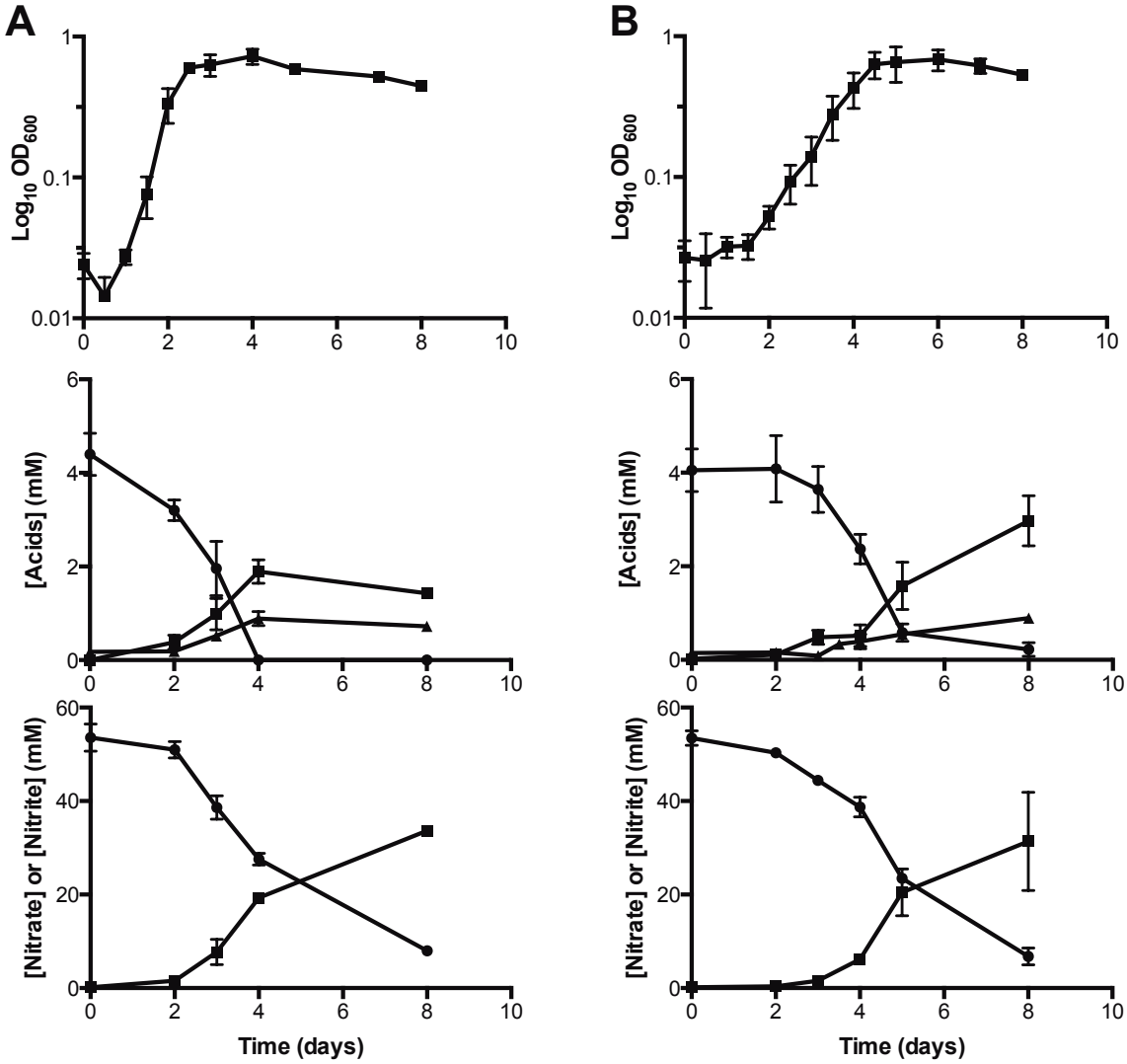

Figure 7.2: ISA and GA biodegradation by *B. buxtonensis* NB2006 under denitrifying conditions and a starting pH of 10. (A) Samples containing GA as the electron donor. (B) Samples containing ISA as the electron donor. Upper panels show the OD_{600} of the samples (■). Middle panels show the concentrations of the added electron donor (GA or ISA, ●), acetate (■) and formate (▲) in mM. Lower panels show the concentrations of nitrate (●) and nitrite (■) in mM.

Under fermentative conditions, in the absence of an added electron acceptor, an increase in OD_{600} was observed in the presence of GA (0.17 OD_{600} units at the late exponential phase), while only a slight increase was observed in the presence of ISA (0.06 OD_{600} units at the late exponential phase) (Figure 7.4). The increase in turbidity was accompanied by a complete degradation of GA and the production of 4 and 3 mM formate and acetate, respectively, after 14 days in culture. In contrast, only a slight degradation of the added ISA was observed (about 0.8 mM), and production of 0.5 and 0.2 mM acetate and formate, respectively.

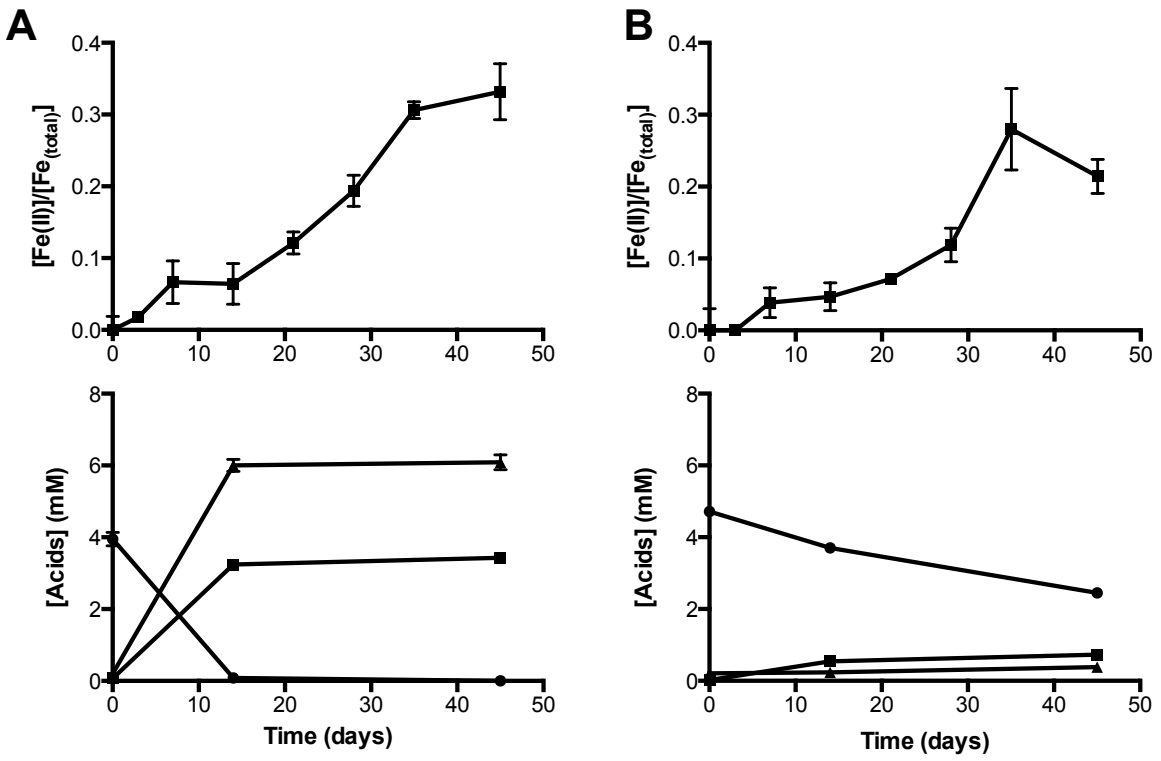

Figure 7.3: ISA and GA biodegradation by *B. buxtonensis* NB2006 under Fe(III)-reducing conditions and a starting pH of 10. (A) Samples containing GA as the electron donor. (B) Samples containing ISA as the electron donor. Upper panels show the ratio of Fe(II) produced to the added $Fe_{(total)}$ (■). Lower panels show the concentrations of the added electron donor (GA or ISA, ●), acetate (■) and formate (▲) in mM.

Under U(VI)-reducing conditions, growth of *B. buxtonensis* was implicated by an increase in the turbidity of the samples in the presence of GA only; there was no change in turbidity of the samples in the presence of ISA. Assessment of U(VI) concentration in these samples by the Bromo-PADAP spectrophotometric method, showed that (1) the soluble U(VI) concentration in the ISA containing bacterial cultures did not change over the course of the experiment; (2) the concentration of soluble U(VI) in the GA containing bacterial cultures decreased over time, and reached about 20% at the end of the experiment; and (3) a maximum of 6% of the added U(VI) was recovered after treating the bacterial pellets with 10 mM HCl (Figure 7.5). Furthermore, the decrease in the soluble U(VI) concentrations in the GA containing cultures, was accompanied by the almost complete degradation of GA after 14 days, and the production of about 3.8 and 2.2 mM formate and acetate, respectively. In contrast, only a slight decrease in ISA (about 1.2 mM), and a slight increase in acetate concentrations (about 0.31 mM) were observed.

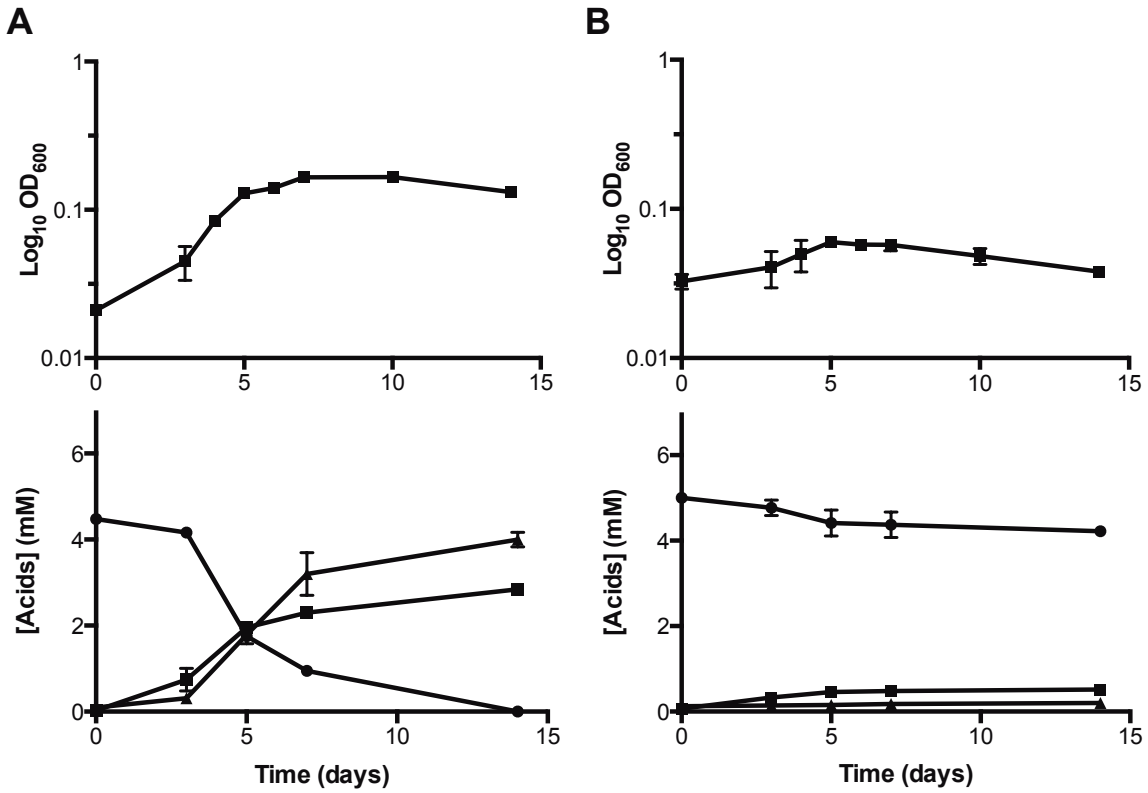

Figure 7.4: ISA and GA biodegradation by *B. buxtonensis* NB2006 in the absence of an electron acceptor (fermentation) and a starting pH of 10. (A) Samples containing GA as the electron donor. (B) Samples containing ISA as the electron donor. Upper panels show the OD_{600} of the samples (■). Lower panels show the concentrations of the added electron donor (GA or ISA, ●), acetate (■) and formate (▲) in mM.

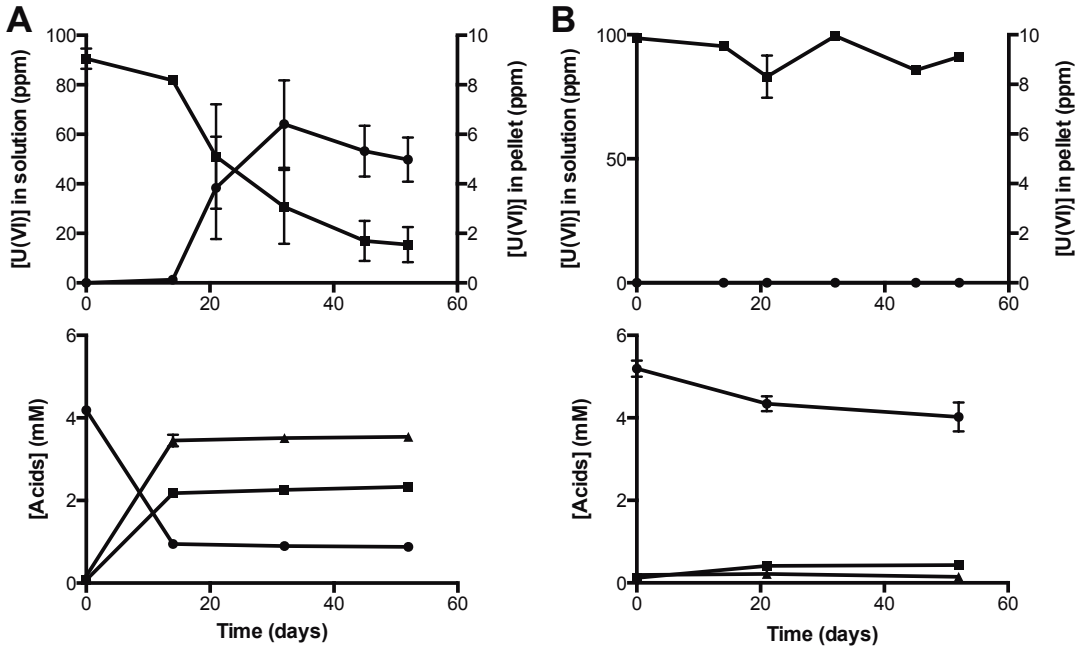

Figure 7.5: ISA and GA biodegradation by *B. buxtonensis* NB2006 with U(VI) added as an electron acceptor and a starting pH of 10. (A) Samples containing GA as the electron donor. (B) Samples containing ISA as the electron donor. Upper panels show the concntration of U(VI) in solution (■) and the concentration of U(VI) in the bacterial pellet (●), in parts per million. Lower panels show the concentrations of the added electron donor (GA or ISA, ●), acetate (■) and formate (▲) in mM.

7.5 Discussion

The GDF is expected to form a multibarrier system, minimising the transport of radioactive waste materials to the biosphere. Organic co-contaminants that will be present (for example GA) or formed (for example ISA) in the GDF challenge this radionuclide containment system (Askarieh *et al.*, 2000; Keith-Roach, 2008) as they have the potential to complex with and increase the solubility of a number of tri- and tetravalent actinides and lanthanides (Gaona *et al.*, 2008; Tits *et al.*, 2005), and could therefore lead to contamination of the surrounding geosphere. GA and ISA are polyhydroxy carboxylic acids with the molecular formulas $C_6H_{12}O_7$ and $C_6H_{12}O_6$, respectively, and are considered to have similar radionuclide-complexing properties (Gaona *et al.*, 2008).

The microbial degradation of the free or the complexed ligands found in or around the GDF, could play a role in minimising the transport of these radionuclides to the geosphere. Recent studies by our group, have shown that bacteria are able to degrade Ca(α-ISA)$_2$ in enrichment cultures prepared at pH 10, under various biogeochemical conditions (Bassil *et al.*, 2014). Furthermore, a novel bacterium (*B. buxtonensis* strain NB2006) was isolated from enrichment cultures and shown to be able to degrade ISA and GA, along with other electron donors under various conditions (Bassil and Lloyd, 2015).

B. buxtonensis showed complete degradation of GA and ISA under aerobic conditions, although the GA-containing systems showed more biomass production (Figure 7.1). Although similar amounts of biomass were observed in the two systems under denitrifying conditions, the rates of nitrate reduction and electron donor degradation were slower in the presence of ISA than with GA (Figure 7.2). In both systems, acetate and formate were produced from the degradation of the added electron donor. Fe(III) reduction was similar in the two growth regimes, however, complete degradation of GA was observed, and more acetate and formate were produced, which was in contrast with the results from the ISA-containing cultures (Figure 7.3). The main difference in the growth of this novel bacterium in the presence of GA or ISA was observed under fermentative and U(VI)-reducing conditions. Under fermentative conditions, *B. buxtonensis* showed significantly higher OD_{600} values in the presence of GA, as compared to ISA, which correlated with a complete fermentation of the electron donor and the production of acetate and formate (Figure 7.4). Under U(VI)-reducing conditions, no bacterial growth (assessed by a lack of turbidity in these samples) was implicated in the ISA-containing systems, which contrasted the GA-containing systems (data not shown). This was supported by an insignificant ISA degradation and acetate and formate production. A lack of bacterial growth may be linked

to the reduced growth of this bacterium under fermentative conditions, or to the formation of large complexes, involving more than one ISA molecule with the uranium species (a process not known to occur with GA (Warwick *et al.*, 2004; Gaona *et al.*, 2008)), which could prevent uptake of the complex into the bacterial cell. The GA-containing systems showed an almost complete degradation of GA after 14 days of incubation, which was coupled to the production of fermentation products, acetate and formate, and an increase in turbidity (Figure 7.5). After this initial period, GA degradation, and acetate and formate production stopped, however, a decrease in soluble U(VI) was observed over the course of the experiment. The uranium species that was used in these experiments is a soluble form of U(VI), which can be immobilised through (1) bioreduction, (2) biomineralisation, (3) bioaccumulation, or (4) biosorption (Newsome *et al.*, 2014). Although there was no indication of U(VI) reduction (no change in the colour of the media or the pellet which would be indicative of the formation of U(IV) as uraninite (Newsome *et al.*, 2014)) in these experiments, only a small fraction of the U(VI) was recovered from the bacterial pellet after overnight incubation with 10 mM HCl, in an attempt to leach surface-sorbed U(VI) species. Note that this procedure did not break the bacterial pellet after vigorous vortexing. This indicates that the mechanism of U(VI) immobilisation by *B. buxtonensis* is not dominated by biosorption onto the bacterial cell walls, and further experiments including X-ray diffraction, X-ray absorption spectroscopy and transmission electron microscopy need to be performed in order to identify the uranium species present in these samples.

Collectively, these and previous results (Bassil *et al.*, 2014; Bassil and Lloyd, 2015) indicate that alkaliphilic bacteria, similar to *B. buxtonensis* may be able to survive in the chemically disturbed zone surrounding the GDF. These bacteria may couple the degradation of free or complexed organic ligands to the reduction of electron acceptors that may be present in and around the GDF (Bassil *et al.*, 2014), and thereby mitigate the increased radionuclide transport to the biosphere. Furthermore, in the absence of suitable electron acceptors, these bacteria may be able to ferment organic material (note that ISA fermentation under the tested conditions was not definitive), and form insoluble forms of uranium that may become immobilised in the surrounding host-rock. These biogeochemical reactions, and other analogous processes involving, for example reductive immobilisation of Tc(VII) and Np(V) via enzymatic or Fe(II)-mediated mechanisms, require further study.

7.6 Acknowledgements

The authors would like to thank Prof. Kathrin Morris and Laura Newsome for their help with the U(VI) experiments. NMB would like to thank the CNRS-Lebanon for their financial support of this work. This work was supported by the BIGRAD consortium under the UK Natural Environmental Research Council, (NE/H007768/1). JRL acknowledges support from the Royal Society.

7.7 References

Askarieh M, Chambers A, Daniel F, FitzGerald P, Holtom G, Pilkington N, *et al.* (2000). The chemical and microbial degradation of cellulose in the near field of a repository for radioactive wastes. *Waste Manag* **20**:93–106.

Bailey M. (1986). Utilization of glucoisosaccharinic acid by a bacterial isolate unable to metabolize glucose. *Appl Microbiol Biotechnol* **1206**:493–498.

Bassil NM, Bryan N, Lloyd JR. (2014). Microbial degradation of isosaccharinic acid at high pH. *ISME J* **9**:310–320.

Bassil NM, Lloyd JR. (2015). *Bacillus buxtonensis* sp. nov., an alkaliphilic bacterium which can degrade isosaccharinic acid. (in preparation).

Berner UR. (1992). Evolution of pore water chemistry during degradation of cement in a radioactive waste repository environment. *Waste Manag* **12**:201–219.

Duro L, Domènech C, Grivé M, Roman-Ross G, Bruno J, Källström K. (2014). Assessment of the evolution of the redox conditions in a low and intermediate level nuclear waste repository (SFR1, Sweden). *Appl Geochemistry* **49**:192–205.

Gaona X, Montoya V, Colàs E, Grivé M, Duro L. (2008). Review of the complexation of tetravalent actinides by ISA and gluconate under alkaline to hyperalkaline conditions. *J Contam Hydrol* **102**:217–27.

Glaus MA, van Loon LR. (2008). Degradation of cellulose under alkaline conditions: New insights from a 12 years degradation study. *Environ Sci Technol* **42**:2906–2911.

Johnson DA, Florence TM. (1971). Spectrophotometric determination of uranium (VI) with 2-(5-bromo-2-pyridylazo)-5-diethylaminophenol. *Anal Chim Acta* **53**:73–79.

Keith-Roach MJ. (2008). The speciation, stability, solubility and biodegradation of organic co-contaminant radionuclide complexes: A review. *Sci Total Environ* **396**:1–11.

Lovley D, Phillips E. (1986). Availability of ferric iron for microbial reduction in bottom sediments of the freshwater tidal Potomac River. *Appl Environ Microbiol* **52**:751–757.

Lovley D, Phillips E. (1987). Rapid assay for microbially reducible ferric iron in aquatic sediments. *Appl Environ Microbiol* **53**:1536–1540.

Lovley DR, Roden EE, Phillips EJP, Woodward JC. (1993). Enzymatic iron and uranium reduction by sulfate-reducing bacteria. *Mar Geol* **113**:41–53.

Maset ER, Sidhu SH, Fisher A, Heydon A, Worsfold PJ, Cartwright AJ, *et al.* (2006). Effect of organic co-contaminants on technetium and rhenium speciation and solubility under reducing conditions. *Environ Sci Technol* **40**:5472–5477.

NDA. (2010). Geological disposal: An overview of the generic disposal system safety case. Nuclear Decommissioning Authority. NDA/RWMD/010 Moor Raw, Cumbria, UK.

NDA. (2014). Radioactive wastes in the UK : A summary of the 2013 inventory. Nuclear Decommissioning Authority. NDA/ST/STY (14) 0006, Moor Raw, Cumbria, UK.

Newsome L, Morris K, Lloyd JR. (2014). The biogeochemistry and bioremediation of uranium and other priority radionuclides. *Chem Geol* **363**:164–184.

Rai D, Hess NJ, Xia Y, Rao L, Cho HM, Moore RC, *et al.* (2003). Comprehensive thermodynamic model applicable to highly acidic to basic conditions for isosaccharinate reactions with Ca(II) and Np(IV). *J Solution Chem* **32**:665–689.

Rout SP, Radford J, Laws AP, Sweeney F, Elmekawy A, Gillie LJ, *et al.* (2014). Biodegradation of the alkaline cellulose degradation products generated during radioactive waste disposal. *PLoS One* **9**:e107433.

Strand S, Dykes J, Chiang V. (1984). Aerobic microbial degradation of glucoisosaccharinic acid. *Appl Environ Microbiol* **47**:268–271.

Tits J, Wieland E, Bradbury MH. (2005). The effect of isosaccharinic acid and gluconic acid on the retention of Eu(III), Am(III) and Th(IV) by calcite. *Appl Geochemistry* **20**:2082–2096.

Van Loon LR, Glaus MA. (1998). Experimental and theoretical studies on alkaline degradation of cellulose and its impact on the sorption of radionuclides. National Cooperative for the Disposal of Radioactive Waste, NAGRA NTB 97-04, Hardstrasse 73, CH-5430 Wettingen, Switzerland.

Van Loon LR, Glaus MA. (1997). Review of the kinetics of alkaline degradation of cellulose in view of its relevance for safety assessment of radioactive waste repositories. *J Environ Polym Degrad* **5**:97–109.

Vercammen K, Glaus MA, van Loon LR. (1999). Complexation of calcium by α-isosaccharinic acid under alkaline conditions. *Acta Chem Scand* **53**:241–246.

Warwick P, Evans N, Hall T, Vines S. (2004). Stability constants of uranium(IV)-α-isosaccharinic acid and gluconic acid complexes. *Radiochim Acta* **92**:897–902.

Chapter 8

Conclusions and Future Directions

8 Conclusion and Future Directions

8.1 Conclusions

8.1.1 Cellulose Degradation under Hyperalkaline Conditions

Previous studies had shown that alkaliphilic and anaerobic bacteria were able to degrade/hydrolyse cellulose and ferment the degradation products at pH ≤ 10 (Leschine, 1995; Lynd *et al.*, 2002; Zvereva *et al.*, 2006; Zhilina *et al.*, 2005; Zhilina and Zavarzin, 1994). Experiments performed in Chapter 4 showed that bacteria sampled from a legacy lime-kiln site, were able to survive in microcosms at a starting pH of ~12, and cause physical degradation of tissue paper that was added as the only carbon source. The degradation of cellulose in these microcosms was linked to enzymatic processes including fermentation reactions that produced acetate. These microcosms were dominated by bacteria belonging to the genus *Clostridium*, well known for their anaerobic, cellulolytic, and fermentative modes of growth. Interestingly, clostridia form recalcitrant endospores that enable them to survive when the environmental conditions are not favourable for growth (Zhilina *et al*., 2005). This mechanism may enable them (and other Firmicutes) to stay dormant in the waste material during the operational phase, and to survive the hyperalkaline conditions that are expected to dominate initially in the geological disposal facility (GDF). Furthermore, due to the inherent heterogeneity of intermediate-level waste (ILW), localised lower pH regions may develop inside the wasteforms. These lower pH niches may provide a microenvironment for cellulolytic, alkaliphilic bacteria (for example Clostridia) to germinate and start degrading the cellulosic material in these wastes (Askarieh *et al*., 2000). The extent of bacterial cellulose degradation under these conditions, and its effect on isosaccharinic acid (ISA) production is not yet clear. The results in Chapter 4 showed that there was no clear drop in the concentration of ISA in these microcosms over 2.5 years of incubation. However, these microcosms showed a stop in ISA production, which was linked to the removal of all of the cellulose as a precursor for ISA production, or to the drop in the pH of the microcosms, which prevented further hydrolysis of the remaining cellulose by alkali. These results may have profound impacts on the kinetics of cellulose degradation (note that the current accepted model predicts that the complete degradation of cellulose under GDF conditions is expected to take 1000-5000 years (Glaus and van Loon, 2008)), and the amount and duration of ISA production from the alkali hydrolysis of cellulose in the wastes. Furthermore, the bacterial degradation of cellulose was accompanied by the fermentation of degradation products into acetate and presumably CO_2, which caused acidification of the microcosms. The impact of these

processes on pH in the GDF are unknown, especially in the presence of high concentrations of $Ca(OH)_2$ that may buffer the pH, however, a drop in pH in the GDF may imply changes in radionuclide solubility that have to be accounted for in the safety case.

8.1.2 Bacterial Degradation of ISA and GA

Cellulose biodegradation at high pH and the prevention of ISA production may be a localised phenomenon, where a select number of bacterial species may colonise the heterogeneous ILW. On the other hand, the direct biodegradation of organic ligands like ISA and gluconic acid (GA) can be considered a more generalised phenomenon that could occur in the GDF or the chemically disturbed zone surrounding it, where conditions are favourable for growth of more diverse microbial consortia. In this respect, very few studies have looked into the bacterial degradation of ISA, and these were mainly conducted under aerobic conditions (Strand *et al.*, 1984; Bailey, 1986), which are not relevant to the conditions in the GDF and the surrounding chemically disturbed zone after closure. A more recent study showed that biogeochemical redox progression from aerobic to Fe(III) reduction is possible when a sediment is incubated in the presence of ISA (Maset *et al.*, 2006). These results were confirmed by a very recent study that showed that cellulose degradation products (which include α-ISA and β-ISA along with other short chain organic acids) could support biogeochemical redox progression from Fe(III) reduction to methanogenesis (Rout *et al.*, 2014). However, these two studies were conducted at circumneutral pH, which is not directly relevant to the GDF or the chemically disturbed zone where the pH would be ≥ 10 (Moyce *et al.*, 2014). The results presented in Chapter 5 showed for the first time that bacterial degradation of $Ca(\alpha\text{-ISA})_2$ is possible under anaerobic conditions at pH 10, in particular under denitrifying and Fe(III)-reducing conditions. These enrichment cultures also showed a decline in bacterial community biodiversity as the reduction potential of the electron acceptor decreased, and more specialised organisms dominated under anaerobic conditions. These results support previous studies that showed that bacterial growth at high pH becomes thermodynamically unfavourable as the reduction potential of terminal electron acceptors such as sulfate decreases (Rizoulis *et al.*, 2012). Collectively, these results imply that the bacterial diversity will drop as the bacteria reduce the different terminal electron acceptors that are present in or around the GDF, however, more studies need to be conducted in order to identify the limits to bacterial growth and survival under these conditions.

An ISA-degrading bacterial isolate was selected from the denitrifying culture and was identified as belonging to the same bacterial genus that completely dominated the Fe(III)-

reducing enrichment culture. This isolate was characterised in Chapter 6 as a novel species of the genus *Bacillus*, and was given the provisional name *Bacillus buxtonensis* strain NB2006. This strictly alkaliphilic, spore-forming bacterium can utilise a range of electron donors and acceptors for growth, including ISA and GA, which are expected to be present in the GDF.

The biodegradation of Ca^{2+} complexed ISA ($Ca(ISA)_2$) and free ISA (NaISA) in Chapters 5 and 6, respectively proved that some microorganisms have the machinery required for ISA biodegradation under conditions similar to those expected in the GDF or surrounding chemically disturbed zone. However, these studies did not look at the direct immobilisation of ligand complexed radionuclides, which was the focus of Chapter 8.

The studies that were conducted in Chapter 8 showed that *B. buxtonensis* was able to ferment GA in the presence of ~0.42 mM $UO_2Cl_{2(aq)}$, which led to an almost complete removal of U(VI) from solution. Overnight leaching of the bacterial pellets with 10 mM HCl (in an attempt to leach surface sorbed U(VI) from the biomass system) recovered only up to 6 % of the added U(VI), indicating that biosorption e.g. to the cell surface, is not the dominant mechanism for U(VI) immobilisation in the experiments. Note that no change in the colour of the solution or the pellets was observed, which would seem to rule out the formation of uraninite UO_2 as a U(VI) immobilisation mechanism although non-uraninite U(IV) cannot be ruled out using this visual indicator. Another additional mechanism for U(VI) immobilisation in these systems is its incorporation into the vegetative/spore cell wall through interactions with phosphorylated glycoproteins, which was demonstrated for a number of *Bacillus* species (Selenska-Pobell *et al*., 1999; Merroun *et al*., 2005). Also note that the added U(VI) remained in solution in the samples that contained ISA as the electron donor, which may be linked to the lower levels of fermentation of the ISA, as compared to GA by this bacterium, which indicates that different mechanisms are involved in the incorporation/degradation of these two molecules, especially when coordinated with uranium.

8.2 Future Directions

Microbial degradation of organics relevant to the GDF and under GDF-relevant conditions is a relatively new interdisciplinary field of exploration. Therefore, although significant insights into these processes were gained in this body of work, more questions arose and more work needs to be done.

The cellulose degradation studies conducted at pH ~12 in Chapter 4 suggested that microorganisms were involved in degradation of the cellulosic material, which caused a drop in pH and a cessation of ISA production. However, in a cement based GDF, the $Ca(OH)_2$ leachate will buffer a high pH, therefore it is important to identify the exact reason for the cessation of ISA production in these experiments. One method to resolve this would be to pass argon flushed water through cement/portlandite columns loaded with different cellulosic materials and a high pH sediment sample (similar to the one used in these studies), and analyse the effluents for ISA and other cellulose degradation products. This method should prevent significant falls in pH due to acetate or CO_2 accumulation, and would be representative of the cement filled ILW. In this respect, even further studies may be performed in underground research laboratories that are more representative of the bacterial communities that are likely to be present in a GDF. These studies should focus on identifying indigenous microbial communities that may be present in GDF host geology, and on the levels of heterogeneity in ILW and LLW, to identify poorly buffered zones where microbial activities may take hold.

Biodegradation of ISA in enrichments and pure cultures showed that bacteria were able to grow and degrade/ferment Ca^{2+} complexed ISA and free ISA under a range of biogeochemical conditions. However, the pure culture was unable to grow and degrade/ferment ISA in the presence of U(VI), although this was accomplished in the presence of GA and U(VI). This warrants the identification of the transporters involved in ISA and GA incorporation into the bacterial cells. Furthermore, only minor ISA fermentation (compared to GA fermentation) was observed in the absence of any electron acceptor, indicating that different enzymes and mechanisms are involved in the biodegradation of these ligands. Therefore, there is a need to identify the enzymes and pathways involved in the degradation/fermentation of these ligands. Next generation sequencing techniques for whole genome analysis will provide insights into the array of metabolic pathways that this bacterium can perform. Furthermore, transcriptomic and proteomic comparison of mRNAs and proteins extracted from pure cultures in the presence of ISA and GA, will provide valuable data on the transporters and enzymes involved in the degradation/fermentation of these ligands. These data are currently being acquired, and when coupled to metabolomic studies can also help identify the ISA and GA degradation pathways and products. The degradation/fermentation of GA in the U(VI)-containing samples was coupled to the immobilisation of U(VI) in the bacterial pellet, and various mechanisms were proposed, including bioreduction of the U(VI) (UO_2 formation is unlikely due to the lack of colour change), biomineralisation of U(VI) into insoluble

uranium containing minerals, bioaccumulation into the bacterial cells, and biosorption onto bacterial cell surfaces (this was shown to have a minor effect). Given these possible U(VI) immobilisation mechanisms, further studies, including X-ray diffraction, X-ray absorption spectroscopy, and transmission electron microscopy need to be performed on these pellets in order to identify the uranium species that are produces as a result of the biodegradation of the GA-U(VI) complexes by this novel bacterium.

The results and conclusions from these and further studies need to be modelled over long periods of time and varying redox and pH conditions, which the radionuclide-ligand complexes may be subjected to during the evolution of the GDF, or in worst-case scenarios where these complexes escape containment. More diverse microorganisms may be present under these conditions, and processes like sulphate reduction and methanogenesis may become favourable at these lower pH values. The latter is of particular concern to the GDF safety case, as it has the potential to increase the transport of ^{14}C-containing methane to the surface. These models may be used by implementers like the UK Radioactive Waste Management agency (RWM) and the French national radioactive waste management agency (ANDRA) to reduce undue pessimism in the long-term performance assessment evaluations of the GDF.

8.3 References

Askarieh M, Chambers A, Daniel F, FitzGerald P, Holtom G, Pilkington N, *et al.* (2000). The chemical and microbial degradation of cellulose in the near field of a repository for radioactive wastes. *Waste Manag* **20**:93–106.

Bailey M. (1986). Utilization of glucoisosaccharinic acid by a bacterial isolate unable to metabolize glucose. *Appl Microbiol Biotechnol* **1206**:493–498.

Glaus MA, van Loon LR. (2008). Degradation of cellulose under alkaline conditions: New insights from a 12 years degradation study. *Environ Sci Technol* **42**:2906–2911.

Leschine SB. (1995). Cellulose degradation in anaerobic environments. *Annu Rev Microbiol* **49**:399–426.

Lynd LR, Weimer PJ, van Zyl WH, Pretorius IS. (2002). Microbial cellulose utilization: Fundamentals and biotechnology. *Microbiol Mol Biol Rev* **66**:506–577.

Maset ER, Sidhu SH, Fisher A, Heydon A, Worsfold PJ, Cartwright AJ, *et al.* (2006). Effect of organic co-contaminants on technetium and rhenium speciation and solubility under reducing conditions. *Environ Sci Technol* **40**:5472–5477.

Merroun ML, Raff J, Rossberg A, Hennig C, Reich T, Selenska-Pobell S. (2005). Complexation of uranium by cells and S-layer sheets of *Bacillus sphaericus* JG-A12. *Appl Environ Microbiol* **71**:5532–5543.

Moyce EBA, Rochelle C, Morris K, Milodowski AE, Chen X, Thornton S, *et al.* (2014). Rock alteration in alkaline cement waters over 15 years and its relevance to the geological disposal of nuclear waste. *Appl Geochemistry* **50**:91–105.

Rizoulis A, Steele HM, Morris K, Lloyd JR. (2012). The potential impact of anaerobic microbial metabolism during the geological disposal of intermediate-level waste. *Mineral Mag* **76**:3261–3270.

Rout SP, Radford J, Laws AP, Sweeney F, Elmekawy A, Gillie LJ, *et al.* (2014). Biodegradation of the alkaline cellulose degradation products generated during radioactive waste disposal. *PLoS One* **9**:e107433.

Selenska-Pobell S, Panak P, Miteva V, Boudakov I, Bernhard G, Nitsche H. (1999). Selective accumulation of heavy metals by three indigenous *Bacillus* strains, *B. cereus*, *B. megaterium* and *B. sphaericus*, from drain waters of a uranium waste pile. *FEMS Microbiol Ecol* **29**:59–67.

Strand S, Dykes J, Chiang V. (1984). Aerobic microbial degradation of glucoisosaccharinic acid. *Appl Environ Microbiol* **47**:268–271.

Zhilina TN, Kevbrin VV, Tourova TP, Lysenko AM, Kostrikina NA, Zavarzin GA. (2005). *Clostridium alkalicellum* sp. nov., an obligately alkaliphilic cellulolytic bacterium from a soda lake in the Baikal region. *Microbiology* **74**:557–566.

Zhilina TN, Zavarzin GA. (1994). Alkaliphilic anaerobic community at pH 10. *Curr Microbiol* **29**:109–112.

Zvereva EA, Fedorova TV, Kevbrin VV, Zhilina TN, Rabinovich ML. (2006). Cellulase activity of a haloalkaliphilic anaerobic bacterium, strain Z-7026. *Extremophiles* **10**:53–60.

Appendices

Appendix 1

Images of *Bacillus buxtonensis* NB2006

Appendix 2

List of Conference Presentations and Awards

Appendix 3

Author's Contributions to Other Work

Appendix 1

A1. Images of *Bacillus buxtonensis* NB2006

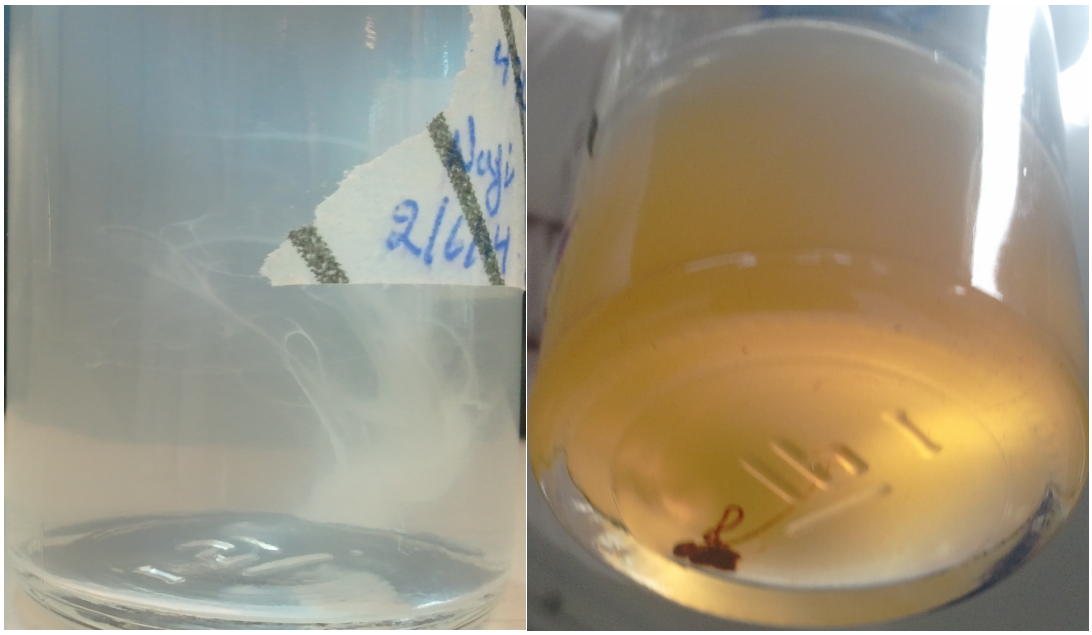

Figure A1.1: Biofilm formation in unshaken *B. buxtonensis* NB2006 cultures containing minimal media supplemented with gluconate and 25 mM nitrate (left) or 3 mmol/L Fe(III) oxyhydroxide (right).

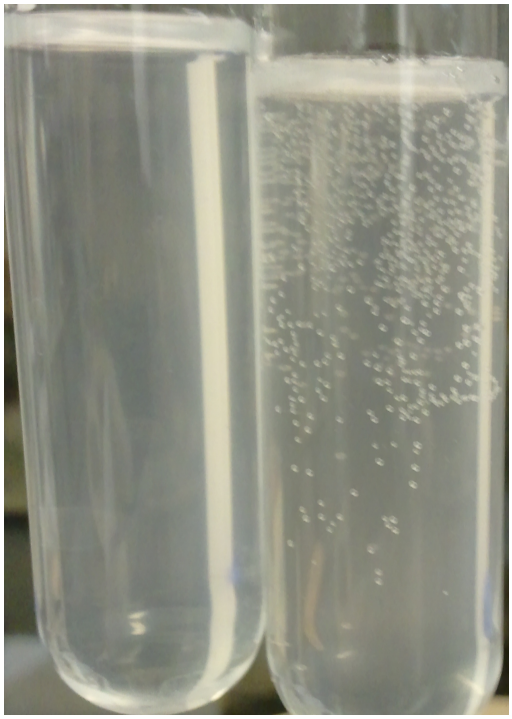

Figure A1.2: Catalase test of sample containing live (right) and autoclaved (left) *B. buxtonensis* NB2006 culture.

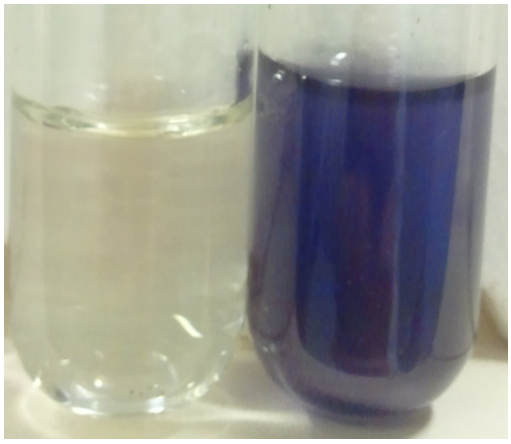

Figure A1.3: Oxidase test of sample containing live (right) and autoclaved (left) *B. buxtonensis* NB2006 culture.

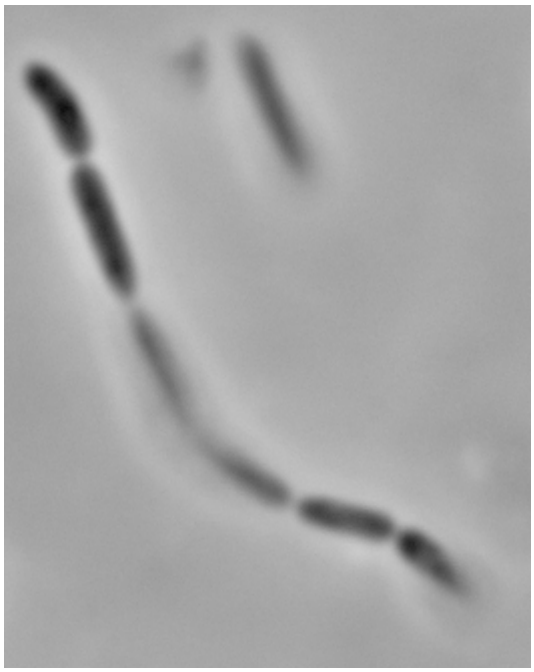

Figure A1.4: Wet mount micrograph showing *B. buxtonensis* NB2006 as a singlet and as a chain.

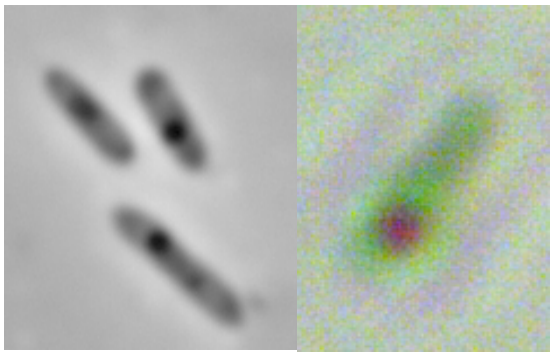

Figure A1.5: Micrographes of heat-fixed and endospore stained *B. buxtonensis* NB2006 slides.

Figure A1.6: Micrographs of heat-fixed *B. buxtonensis* NB2006 slides, stained with Gram stain.

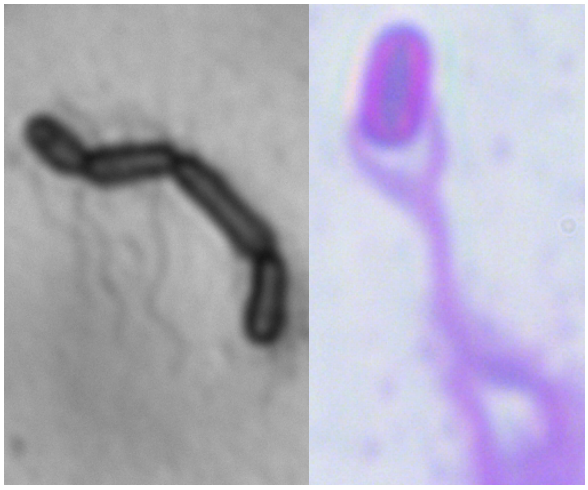

Figure A1.7: Micrographs of air-dried *B. buxtonensis* NB2006 slides, stained with flagellar staining.

Appendix 2

A2. List of Conference Presentations and Awards

A2.1. Poster Presentations

Microbial Degradation of Isosaccharinic Acid. **Bassil NM., Lloyd JR.** (2012). *Geomicrobiology and its Significance for Biosphere Processes conference.* University of Manchester, UK.

Cellulose Degradation in Intermediate Level Waste Repository. **Bassil NM., Lloyd JR.** (2012). *Williamson Research Centre Meeting on Environmental organic (geo)chemistry related research.* University of Manchester, UK.

ISA Biodegradation in an Intermediate and Low Level Waste Repository. **Bassil NM., Lloyd JR.** (2012). *The SEAES Postgraduate Research Conference 2012.* University of Manchester, UK.

Microbial degradation of ISA under high pH conditions representative of intermediate-level waste. **Bassil NM., Bryan N., Lloyd JR.** (2013). *14th International Conference on the Chemistry and Migration Behaviour of Actinides and Fission Products in the Geosphere (Migration conference 2013).* Brighton Conference Centre, UK.

Microbial degradation of ISA under high pH conditions representative of intermediate-level waste. **Bassil NM., Bryan N., Lloyd JR.** (2013). *The SEAES Postgraduate Research Conference 2013*. University of Manchester, UK.

A2.2. Oral Presentations

Microbial Utilisation of Cellulose and its Chemical Degradation Products in Intermediate Level Waste Repository. **Bassil NM., Lloyd JR.** (2012). *The 2nd Annual BIGRAD Meeting.* British Geological Survey, Nottingham, UK.

Microbial degradation of ISA under high pH conditions representative of intermediate level waste. **Bassil NM., Bryan N., Lloyd JR.** (2013). *The Environmental Mineralogy Group Research In Progress meeting.* University of Sheffield, UK.

Microbial degradation of ISA under high pH conditions representative of intermediate level waste. **Bassil NM., Bryan N., Lloyd JR.** (2013). *The 3rd Annual BIGRAD Meeting.* University of Sheffield, UK.

Microbial degradation of Isosaccharinic acid (ISA) under high pH conditions representative of an intermediate-level radioactive waste. **Bassil NM., Bryan N., Lloyd JR.** (2013). *The 1st Geo.Rep.Net Meeting.* University of Edinburgh, UK.

Microbial degradation of isosaccharinic acid under conditions representative of intermediate-level waste disposal. **Bassil NM., Bryan N., Lloyd JR.** (2014). *The IGDTP-Geodisposal 2014 Conference.* University of Manchester, UK.

A2.3. Awards

Bourses Doctorales du Conseil National de la Recherche Scientifique Libanais 2012-2013. PhD funding ($12,500 per annum for 2 years). National Scientific Research Council of Lebanon.

SEAES Postgraduate Research Student Best Outstanding Output Award for 2014. For the article "Microbial degradation of isosaccharinic acid at high pH" that was published in the ISME journal.

Manchester Doctoral College Best Outstanding Output Award 2015 (Faculty of Engineering and Physical Sciences). For the article "Microbial degradation of isosaccharinic acid at high pH" that was published in the ISME journal.

Appendix 3

A3. Author's Contributions to Other Work

The author assisted a new PhD student (Gina Kuippers) in the preparation of Ca(α-ISA)$_2$ and the preparation and sampling of microcosms and enrichment cultures. This work, which focuses on conditions representative of the far-field of a geological disposal facility, resulted in the production of a manuscript that has been submitted for review in the special issue of the Mineralogical Magazine on geological disposal of radioactive waste.

Microbial degradation of isosaccharinic acid under conditions representative for the far field of radioactive waste disposal facilities.

Gina Kuippers, Naji M Bassil, Christopher Boothman, Nicholas Bryan, Jonathan R. Lloyd